DESIGN AND CHARACTERISATION OF DENDRITIC MOLECULES

BY

GAURANG PUROHIT

BPharm, MRPharmS

A thesis submitted in partial fulfilment of the requirements for the degree of

DOCTOR OF PHILOSOPHY

of the

University of London

The School of Pharmacy

29/39 Brunswick Square

London WC1N 1AX

OCTOBER 2003

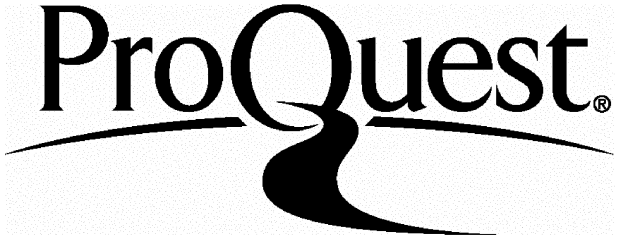

ACKNOWLEDGEMENTS

Many people have provided me with assistance, guidance and support during the time it has taken me to complete this PhD. The greatest and most enduring presence was that of my supervisor, Professor Alexander Florence. His guidance and patience has been both encouraging and motivating and his positive outlook has provided a source of endurance and inspiration. To compliment my supervisor, I was blessed with an ideal role model in Dr. Thiagarajan Sakthivel who taught me many skills, techniques and provided continuous guidance. He was always available and never too busy to help and assist. Without Prof. Florence, Dr. Sakthivel and the support of my family, this PhD would not have been possible.

I am very thankful to Dr. John Malkinson and Dr. Robert Falconer for their advice and guidance in the chemistry and synthetic aspects of this thesis, which has been crucial to my research. I must also give a special mention to Dr Colin James for molecular modelling assistance, Mr David McCarthy for his help with light and electron microscopy studies, and the mass spectrometry department for the analysis of my compounds.

The scientists and visiting scientists that I have had the pleasure to work with, in our department, have provided valuable insight and ideas to my methods of research. These include Dr. Vikas Jaitely, Dr. Nasir Hussain, Dr Parijat Kanaujia and Dr Shigeo Yanai.

I would also like to pay my gratitude to Behrooz Nasseri, Chandra Ramaswamy, Khuloud Al-Jamal, Baljit Rehal, Suzie Ribeiro and Parvinder Phul. They have been my fellow postgraduate research colleagues and have been the integral part to providing a wonderful atmosphere to work in. Funding from the Engineering and Physical Science Research Council (EPSRC) is also gratefully acknowledged.

Finally, I would like to dedicate this thesis to my late father Pramod Ambalal Purohit, who is my inspiration in life, and my wonderful wife, Jayna, who has been supportive and understanding throughout this period.

ABSTRACT

Dendritic molecules with highly versatile and synthetically controllable structures have been examined closely in the fields of drug delivery and targeting. This thesis focuses on the design and synthesis of a series of poly(lysine) dendritic molecules, and how their structural characteristics affect their physical and pharmaceutical properties. All molecules studied in this thesis were prepared using solid phase peptide synthesis.

Amphipathic dendrons having three lipidic (C_{14}) chains coupled to dendritic lysine head groups with 8, 16 or 32 free terminal amino groups were synthesised. Their interactions with charged and neutral liposomes were studied, and the interaction efficiency for all three dendrons was greater than 88%. The dendrimers produced cationic liposomes regardless of initial liposome charge and showed evidence of hydrophobic interactions with the liposome membranes. Membrane disruption of the liposomes was also seen with the highly cationic dendrons.

The interaction of the series of dendrons with albumin, was studied in the presence of NaCl, using dynamic dialysis and molecular modelling. Diffusion and membrane permeability studies (using cellulose membranes) were also performed. The stoichiometry of dendron: albumin interactions was found to be 1:1.5, 1:4 and 1:5 for the dendrons with 8, 16 and 32 amino groups, respectively. Calculation of shape factors showed that the dendrons had a more spherical confirmation with each generation of growth.

The synthetic approaches used to synthesise other dendrons as well as a novel didendron is detailed. Viscosity studies showed that a didendron with 128 terminal amino groups (2 x 64) had a dynamic viscosity greater than that of a single dendron with 128 terminal amino groups. A dendron with acetylated terminal groups was found to form unusual aggregates on the surfaces of glass slides.

Page No.

Acknowledgements ii

Abstract iii

List of Figures ix

List of Tables xiv

CHAPTER ONE : INTRODUCTION 1

1.1 What are dendrimers? 2

1.2 Components of a dendrimer 4

1.3 Synthetic methods 6

1.4 Different dendritic structures 8

1.4.1 Peptide dendrimers 12

1.4.2 Glycodendrimers 12

1.4.3 Metallodendrimers 13

1.5 Advantages and properties of dendrimers 15

1.6 Dendrimers as delivery agents and carriers 23

1.6.1 Physical entrapment of guest molecules 24

1.6.2 Dendrimer-drug conjugates 27

1.6.3 Dendrimers in gene delivery 29

1.6.4 Biocompatibility and toxicology of dendrimers 31

CHAPTER TWO : DESIGN AND SYNTHESIS OF DENDRITIC MOLECULES 37

2.1 Polyamino acid branching units 37

2.2 Solid phase peptide synthesis 38

2.3 A comparison of Boc and Fmoc chemistry 41

2.4 Peptide bond formation 42

2.5 Coupling reagents..... 43

2.6 Peptide chain assembly..... 44

2.7 Resin test to monitor efficiency of reactions..... 46

2.8 Boc resin cleavage and deprotection..... 47

2.8.1 HF cleavage..... 48

2.8.2 TMSOTf cleavage..... 48

2.9 Dendrimer and dendron synthesis..... 49

2.9.1 Lipophilic dendrons with polycationic surfaces..... 49

2.9.2 Polylysine dendrons with reactive glycine tail..... 51

2.9.3 Preparation of radiolabelled molecules..... 54

2.9.4 Mass spectrometry..... 54

2.9.5 High performance liquid chromatography (HPLC)..... 55

CHAPTER THREE: INTERACTION OF CATIONIC DENDRONS WITH LIPOSOMES **56**

3.1 INTRODUCTION..... 56

3.1.1 Liposomes..... 56

3.1.2 Interaction between dendritic structures and liposomes..... 59

3.2 MATERIALS AND METHODS..... 61

3.2.1 Synthesis of the cationic dendrons..... 61

3.2.2 Preparation of liposomes..... 61

3.2.3 Measurement of radioactivity..... 64

3.2.4 Measurement of vesicle size and zeta potential..... 65

3.2.5 Adsorption studies..... 65

3.2.6 Membrane disruption assay..... 67

3.2.7 Micrograph images..... 67

3.3 RESULTS AND DISCUSSION..... 68

3.3.1 Dendron entrapment/interaction during the DRV method..... 68

3.3.2 Adsorption studies..... 73

3.3.3 Membrane disruption assay..... 78

3.3.4 Membrane disruption model..... 82

3.4 CONCLUSION..... 85

CHAPTER FOUR : THE INTERACTION OF CATIONIC DENDRONS WITH ALBUMIN AND THEIR DIFFUSION THROUGH CELLULOSE MEMBRANES **86**

4.1 INTRODUCTION..... 86

4.1.1 Membrane permeability and diffusion..... 86

4.1.2 Passive diffusion in solution..... 87

4.1.3 Cellulose membranes..... 90

4.1.4 Interaction of molecules with albumin..... 91

4.2 MATERIALS AND METHODS..... 94

4.2.1 Synthesis of cationic dendrons..... 94

4.2.2 Dynamic dialysis..... 94

4.2.3 Diffusion studies..... 94

4.2.4 Dendron-albumin interaction studies..... 96

4.2.5 Apparent diffusion coefficient (D)..... 96

4.2.6 Apparent membrane partition coefficient (K)..... 97

4.2.7 Apparent membrane permeability coefficient (P)..... 97

4.2.8 Octanol-water partition coefficient (P_{ow})..... 98

4.2.9 Thermodynamics of diffusion..... 98

4.2.9 Molecular modelling and analysis..... 99

4.3 RESULTS AND DISCUSSION..... 100

4.3.1 Diffusion studies..... 100

4.3.2 Apparent membrane diffusion and permeability coefficients... 105

4.3.3 Membrane and octanol/water partition coefficients..... 108

4.3.4 Thermodynamics of diffusion..... 110

4.3.5 Dendron-albumin interaction studies..... 111

4.4 CONCLUSION..... 118

CHAPTER FIVE : THE SYNTHESIS AND PROPERTIES OF A NOVEL DIDENDRON **119**

5.1 INTRODUCTION..... 119

5.1.1 Multi-functionalised dendrimers..... 119

5.1.2 Viscosity of dendrimers..... 122

5.2 MATERIALS AND METHODS..... 123

5.2.1 Didendron synthesis on solid support..... 124

5.2.1.1 Core design (Part I)..... 124

5.2.1.2 Core design (Part II)..... 124

5.2.1.2 Core design (Part III)..... 125

5.2.2 Didendron synthesis by coupling dendrons in liquid phase..... 127

5.2.3 Dynamic viscosity measurements..... 127

5.2.3.1 Determining the viscosity..... 128

5.2.4 Molecular modelling and analysis..... 129

5.2.5 Self-assembling dendritic aggregates..... 129

5.2.6 Micrograph images..... 129

5.3 RESULTS AND DISCUSSION..... 130

5.3.1 Didendron synthesis..... 130

5.3.2 Viscosity studies..... 134

5.3.2.1 Dynamic viscosity..... 134

5.3.2.2 Intrinsic viscosity..... 137

5.3.3 Self-assembling dendritic aggregates..... 143

5.4 CONCLUSION..... 148

CHAPTER SIX : CONCLUSIONS AND FUTURE PERSPECTIVES 150

APPENDIX I..... 154

APPENDIX II..... 156

APPENDIX III..... 161

APPENDIX IV..... 163

APPENDIX V..... 164

APPENDIX VI..... 165

APPENDIX VII..... 166

PUBLICATIONS..... 167

REFERENCES..... 168

LIST OF FIGURES

Figure No.	Title of Figure	Page
Fig. 1.1	Diagrams of (a) Coniferous and deciduous trees with root systems, (b) fungal anatomy, and (c) giant interneuron of a cockroach.	3
Fig. 1.2	Molecular scale example of a dendrimer exhibiting a dense spherical structure of branching units.	4
Fig. 1.3	Fifth generation dendritic structure demonstrating the morphological and structural aspects that make them unique.	5
Fig. 1.4	Diagram showing how the generation of a dendritic molecule increases with each additional layer of branching units, where the core = G0.	6
Fig. 1.5	Schematic comparison of divergent and convergent synthesis methods.	8
Fig. 1.6a	A unimolecular micelle.	10
Fig. 1.6b	Newkome's dendrimer with internal binding units.	10
Fig. 1.7	Structures of a) PAMAM dendrimer; b) DAB-dendr-NH_2 dendrimer; c) Fréchet's dendron.	11
Fig. 1.8	Glycodendrimer motifs showing different positions in which the saccharide units can be placed within the framework.	13
Fig. 1.9	Dendrimer based on metal complexes developed by Campagna and co-workers.	14
Fig. 1.10	Dimensionally scaled comparison of a series of PAMAM dendrimers with a variety of proteins, a typical lipid-bilayer membrane and DNA.	16
Fig. 1.11	Environmental scanning electron microscopy image of Langmuir-Blodgett film, of amphiphilic dendrimers attached to a fourth generation PAMAM dendrimer core.	19

Figure No.	Title of Figure	Page
Fig. 1.12	Transmission electron micrograph of dendrisomes with membranes from 6 to 10 nm thick (left). Schematic representation of bilayer formation (right).	20
Fig. 1.13	Schematic representation of dendritic caged compounds and their expected functions.	25
Fig. 2.1	General scheme of solid phase peptide synthesis (SPPS).	39
Fig. 2.2	Resins for solid phase peptide synthesis; a) Boc-protected (4-carboxamidomethyl) benzyl ester resin; b) p-methylbenzhydrylamine resin.	40
Fig. 2.3	Protecting group strategies in SPPS for Fmoc and Boc chemistry.	42
Fig. 2.4	Structures of some of the coupling reagents used in peptide synthesis.	49
Fig. 2.5	Schematic diagram representing the synthetic route for molecules 1a-c.	52
Fig. 3.1	Different types of liposomes characterised according to size and number of lamellae.	57
Fig. 3.2	Transmission electron micrograph of a liposome showing the aqueous phase and the multi-lamella structure formed by the lipid bilayers.	60
Fig. 3.3	Schematic diagram of the 8, 16 and 32 amino group cationic dendrons which were studied.	62
Fig. 3.4	Molecular structures of the four lipids used to formulate the different liposomes.	63
Fig. 3.5	Dendron entrapment/interaction efficiency of neutral, anionic and cationic liposomes.	68
Fig. 3.6	Effect of dendron interaction on apparent vesicle diameters of liposomes.	69

Figure No.	Title of Figure	Page
Fig. 3.7a	Anionic liposomes in the absence of dendrons.	70
Fig. 3.7b	Anionic liposomes in the presence of the 32 amino group dendron.	70
Fig. 3.7c	Anionic liposomes in the presence of 32 amino group dendron after centrifugation and final resuspension of the vesicles during the DRV method.	71
Fig. 3.7d	Interaction of anionic liposomes and 32 amino group dendrons showing lipid bilayer membrane disruption and the formation of myelin figures.	71
Fig. 3.8	Effect of dendron interaction on zeta potential of liposomes.	72
Fig. 3.9	Adsorption of dendrons onto liposome surface after addition of dendrons with different numbers of amino groups, to liposome surfaces.	73
Fig. 3.10	Post-adsorption studies with anionic liposomes showing the average percentage of all three dendrons present (associated with the liposomes) and the corresponding zeta potentials.	77
Fig. 3.11	Structure of Riboflavin-5'-phosphate sodium salt dehydrate.	78
Fig. 3.12	Linear calibration plot for the standard solutions of riboflavin.	79
Fig. 3.13	Graph showing the percentage release of riboflavin from anionic liposomes over 24 h following the addition of dendrons after 30 min.	80
Fig. 3.14	a) The outer phospholipid layer of an anionic liposome formulated with DSPC and PG; b) The re-orientation of phospholipids following interaction with cationic dendrons.	83
Fig. 4.1	Membrane model showing how Fick's law can be applied.	88
Fig. 4.2	Molecular model of serum albumin showing the minimum dimensions required if placed in a box.	92
Fig. 4.3	Percentage diffusion of dendrons through the dialysis membrane in the absence of albumin and the percentage adsorption of the dendrons to membrane after 24 h at 25°C.	101

Figure No.	Title of Figure	Page
Fig. 4.4	Percentage diffusion of the three dendrons over 24 h at 25°C.	101
Fig. 4.5	Scanning electron micrographs of the cellulose membrane representing a) the complex fibrous structure and pores, and b) the membrane cross-section showing the thickness.	102
Fig. 4.6	Increase in percentage diffusion through the membrane over 24 h at 25°C, of the dendrons as NaCl concentration is increased.	104
Fig. 4.7	Decrease in percentage adsorption to the membrane after 24 h at 25°C, of the dendrons as NaCl concentration is increased.	104
Fig. 4.8	Membrane permeability and diffusion coefficients for the three dendrons which were calculated using the physical parameters of the cellulose membrane at 25°C.	106
Fig. 4.9	Graph showing how the Perrin or shape factor decreases with the number of amino groups.	107
Fig. 4.10	Graph showing the membrane partition coefficient values for the three dendrons at 25°C.	109
Fig. 4.11	Graph showing a linear correlation between membrane partition coefficient and log P_{ow} values.	109
Fig. 4.12	Arrhenius-like plot for the diffusion of the three dendrons, where the slopes of the lines are equal to the energy of activation for permeation.	110
Fig. 4.13	Scale molecular models of albumin in comparison with 8, 16 and 32 amino group dendrons.	111
Fig. 4.14	Diffusion profiles of dendrons with 8 amino groups and how various concentrations of albumin affects the average percentage of dendrons diffusing over 24 h at 25°C.	112
Fig. 4.15	Six different views of the albumin molecule showing the electrostatic potential on the molecular surface.	114
Fig. 4.16	Moles of dendrons interacting per mole of albumin at various molar ratios after 24 h at 25°C.	115

Figure No.	Title of Figure	Page
Fig. 5.1	Structural representation of a linear poly(ethylene glycol)-block-poly(L-lysine) dendrimer.	120
Fig. 5.2	Structural representation of a barbell-like triblock copolymer, poly(L-lysine) dendrimer- block -poly(ethylene glycol)- block -poly(L-lysine) dendrimer (PLLD-PEG-PLLD).	120
Fig. 5.3	Compound 1 representing di-(Boc)-2,3 diaminoproprionic acid attached to *p*MBHA resin.	126
Fig. 5.4	Compound 2 representing the final structure of the core.	126
Fig. 5.5	Diagrammatic representation of the structure of a didendron molecule, with 2 x 16 terminal lysine.	130
Fig. 5.6	Scale molecular wire models of the didendrons 3a-c.	132
Fig. 5.7	'Solvent accessible surface' models of didendrons 3a-c showing the *x/y* axis ratios for the three molecules.	133
Fig. 5.8	Dynamic viscosities (η) of didendrons 3a-c versus increasing didendron concentration at 25°C.	134
Fig. 5.9	Dynamic viscosities (η) of didendrons 3a-c versus increasing temperature(°C), with constant didendron concentrations.	135
Fig. 5.10	Comparison of dynamic viscosities (η) of molecules 2e, 2m and 3c of different concentrations at 25°C.	136
Fig. 5.11	Linear plot representing the Huggins-Kramer equation, $\eta_{red} = [\eta] + k^1 [\eta]^2 c$, to determine the intrinsic viscosity.	138
Fig. 5.12	Huggins-Kramer plot for didendrons 3a-c for viscosity measurements at 25°C.	140
Fig. 5.13	Intrinsic viscosity behaviour of polyether dendrimers and of polystyrene.	143
Fig. 5.14	Examples of molecular aggregates formed on a glass slide by a solution of dendrons 2d.	144
Fig. 5.15	Examples of molecular aggregates formed on a glass slide by a solution of dendrons 2h.	145
Fig. 5.16	Comparison of dynamic viscosities (η) of molecules 2d and 2h of different concentrations at 25°C.	146

LIST OF TABLES

Table No.	Title of Table	Page
Table 3.1	Physical characteristics of the three dendrons (1a-c) studied.	68
Table 3.2	Entrapment investigation results showing the amount of each dendron present and the resultant zeta potential for neutral, anionic and cationic liposomes.	75
Table 3.3	Adsorption investigation results showing the amount of each dendron present, and the resultant zeta potential for neutral, anionic and cationic liposomes.	75
Table 4.1	The physical properties of Spectra/Por 2 and 7 dialysis membranes used for the diffusion and albumin-interaction studies.	95
Table 4.2	Molecular weights, hydrodynamic radii and molar volumes of the three dendrons (1a-c) studied.	107
Table 4.3	The composition of amino acids in bovine serum albumin showing the number of each amino acid and their contribution to the formal charge.	113
Table 5.1	Summary of the three didendron molecules (3a-c) synthesised using Method C.	130
Table 5.2	Values for dynamic, relative, specific and reduced viscosities for didendrons 3a-c, at different concentrations in water at 25°C.	139

CHAPTER ONE

INTRODUCTION

A drug-delivery system is analogously, a vehicle-passenger concept in which a drug is attached to a carrier molecule or particle such as a polymer, antibody, hormone, liposome, noisome or a viral source. The pharmacokinetics and pharmacodynamics of the drug in such systems depends on the physicochemical and biological properties of the macromolecular carrier. Parameters such as site specificity, protection from degradation and minimization of side effects can be controlled by modifying the properties of the carrier, such as structural characteristics. An ideal drug carrier must possess the ability to remain associated with, and protect the load until it reaches the desired site of action, where the carrier can then release the drug. Many polymeric and branching drug-delivery systems have been developed over the years and new ones are still being investigated. Synthetic dendrimers and dendritic structures have the potential to possess many of the above-mentioned properties for an ideal drug-carrier system. Dendrimers are highly branched, globular, macromolecules of nanoscale dimensions, prepared by synthetic chemistry. Since the pioneering work of Tomalia *et al.* (1985) and Newkome *et al.* (1985) on dendrimer synthesis in the early 1980s, there has been much scope into dendritic technology and engineering by many research groups. There is a continuing effort to improve the efficiency and decrease the cost of harvesting these macromolecules, leading to potentially new applications and ideas. Continuing studies are also investigating the specific physical and chemical properties of dendrimers and, although some may say

that the science of dendrimers is still at an early stage, potential applications for dendrimers are now forthcoming. Dendritic molecules have surface functionality which can be modified to protect or provide access to internal cavities (Jansen *et al.*, 1994). These characteristics, along with possible water solubility, are some of the qualities that make them appealing for biomedical and drug-delivery applications (Esfand and Tomalia, 2001, Liu, M. and Fréchet, 1999).

1.1 What are dendrimers?

The term dendrimer is derived from *dendron*, the Greek word for tree, and the suffix *mer*, from the Greek word *meros*, denoting the smallest repeating structural unit (Dvornic and Tomalia, 1996). Dendrimers are defined as two or more dendrons that structurally radiate from a general, central core. In simple analogous terms, a dendrimer may be described as a tree, with the tree trunk and its branch crown corresponding to a single dendron. The root system corresponds to another dendron, with the entire tree structurally radiating from a general main trunk representing a didendron dendrimer (Tomalia *et al.*, 1990, Matthews *et al.*, 1998).

The formation of dendritic structures is perhaps one of the most continual and natural orientations observed on our planet (Tomalia *et al.*, 2000). Many examples of these patterns (Thompson, 1987) may be found in both non-biological systems (e.g., lightning patterns, snow crystals, tributary/erosion fractals), as well as in biological systems (e.g., tree branching/roots, plant/animal vasculatory systems, neurons) (Mizrahi *et al.*, 2000). In biological systems, these dendritic patterns can be discovered at dimensional length scales which can be calculated in metres (trees), millimetres/centimetres (fungi), or microns (neurons) as illustrated in Fig. 1.1 (Tomalia *et al.*, 2000). It is not completely apparent why nature emphasises on

examples of dendritic constructs. Tomalia *et al.* (2000) have suggested that evolution has played a major role in the optimisation of these structures to gain maximum efficiency and provide optimum conditions for survival.

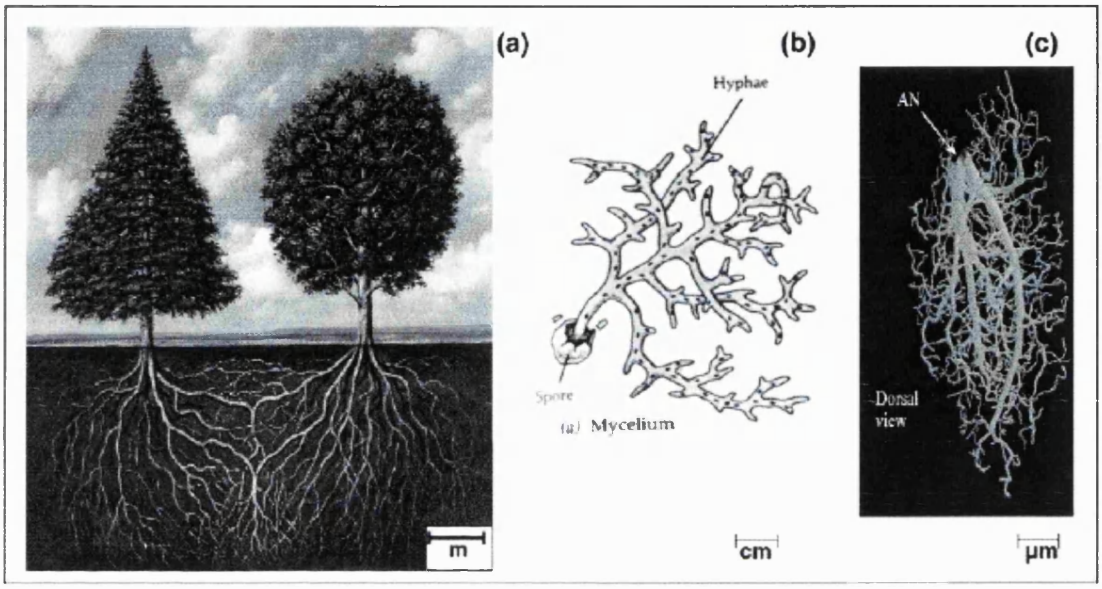

Fig. 1.1. a) *Coniferous and deciduous trees with root systems;* ***b)*** *fungal anatomy;* ***c)*** *giant interneuron of a cockroach. (from Tomalia et al. (2000) Pure Appl. Chem., 72, 2343–2358.)*

Dendrimers are nanoscale globular molecules that are made up of smaller molecules or units linked in a branched manner to produce a dense, spherical structure that can be described as spherical as shown in Fig.1.2. Since complete dendrimers have a symmetrical quasi-spherical or spherical topology, many dendrimers described in this thesis can be termed 'partial dendrimers' or 'dendrons' as they are asymmetrical fractions of a dendrimer.

1.2 Components of a dendrimer

Dendrimers are macromolecules with three discrete structural components which determine the potential applications of the molecules. The three components are a central core; surface functionalities; and branching units that link the two. The nature and size of the branching units determine volume which is created to form internal

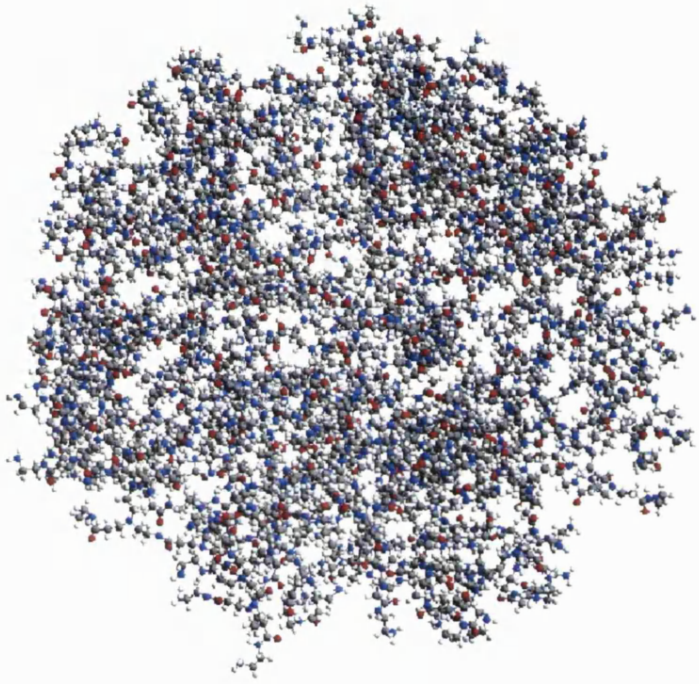

Fig. 1.2. *A molecular scale example of a dendrimer exhibiting a dense spherical structure of branching units (Ref: nano.med.umich.edu/dendrimers.html).*

cavities within the globular structure (Fig. 1.3). The term 'generation' is often referred to in dendrimer nomenclature on the basis that each layer of branching units added to the construct is known as a generation. Therefore the core of a dendrimer, without any branching units, is known as a 'zero generation' or 'G0' dendrimer. Each subsequent layer of branching units from the core is referred to as a generation. An example of this can be seen in Fig. 1.4. Molecular modelling of dendritic molecules can portray unusual appearances and their fascinating architectures can exhibit atypical characteristics as well. An interesting structural aspect of dendrimers

is the concept of the "starburst limit" (de Gennes and Hervet, 1983). It is considered that the number of monomer units in a dendrimer increases exponentially as a function of generation, while the sphere formed by their growth only increases with the cube of the generation. Based on this theory, it can therefore be concluded that, after a certain generation the dendrimer will stop growing as a consequence of limited space (de Gennes and Hervet, 1983).

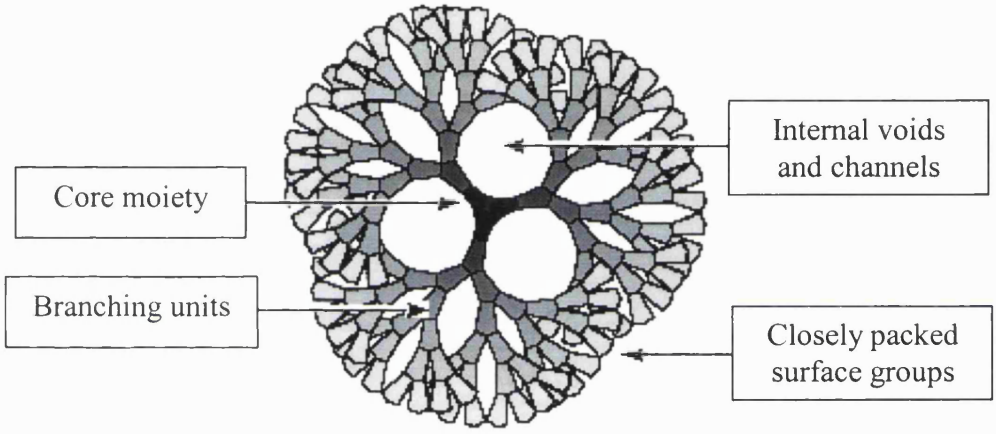

Fig. 1.3. *A fifth generation dendritic structure demonstrating the morphological and structural aspects that make them unique. (from Matthews et al. (1998) Prog. Polym. Sci., 23, 1-56.)*

With each generation of growth, there will consequently be an increase in branch density, which will have an effect on dendrimer structure. At higher generations, the peripheral branches are sterically crowded at the surface of dendritic molecules, causing them to orientate towards a more globular formation (Naylor *et al.*, 1989). The ends of the peripheral branches may lie either on the surface of the molecule, or fold towards the internal parts of the structure. The different orientations are often

determined by factors such as the solvent system in which the dendrimer is in, and the chemical properties of the units used to construct the dendrimer.

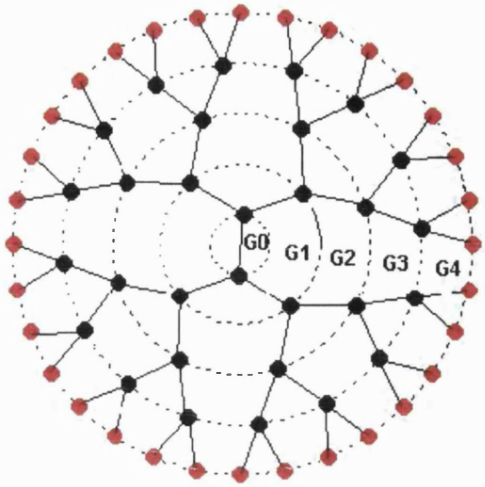

Fig. 1.4. *A diagram showing how the generation of a dendritic molecule increases with each additional layer of branching units, where the core = G0.*

1.3 Synthetic methods

Experimental details of synthesis of dendritic structures will be discussed in Chapter 2. Here we will summarise the major synthetic approaches developed for the preparation of dendrimers. The production of dendrimers and their derivatives is more directly related to organic synthetic chemistry rather than traditional polymer synthesis. Dendrimer formation requires a number of synthetic processes and procedures, including repetition of purification and characterisation.

Many dendrimers are referred to as 'peptide' dendrimers (Sadler and Tam, 2002). This term is used to describe dendrimers which incorporate peptide bonds into their structure, whether the bonds are in an amino acid core, the branching units, surface functional groups or as a combination of any of the three.

Generally two synthetic strategies are employed to construct peptide dendritic architechtures: the divergent and convergent approaches (Fig. 1.5). The divergent approach (Tomalia *et al.*, 1985, Newkome *et al.*, 1985) was used in early dendrimer synthesis, in which the dendrimer grows outwards from the core. Using a reactive core, attached to a solid support, subsequent generations can be grown in a stepwise manner. Speed is the main advantage of the divergent method and if a solid support is used, a multi-generation series can produced from the original reaction mixture. At the completion of a generation of growth, an amount can be removed from the reaction mixture and the remainder can be reacted to form the next subsequent generation. The convergent approach (Hawker and Fréchet, 1990, Miller *et al.*, 1992) is an alternative strategy and growth is initiated at what will be the surface of the desired molecule. The monomers or segments of the dendrimer are prepared separately and then attached to a suitable core molecule to form a complete dendrimer. The convergent approach requires less purification of the final product as only complete and pure intermediates are used to construct the dendrimers. However, convergent syntheses do have their disadvantages and this approach does not reduce the number of steps required to construct a large structure (Matthews *et al.*, 1998). When convergently attaching large dendritic segments to a core molecule, steric hindrance can pose problems for the segments trying to access the central core.

Although using the divergent or convergent method can affect the yield, other practical aspects of the chemistry can significantly alter the yield. These include the use and choice of solid supports and the methods of cleavage from the solid supports.

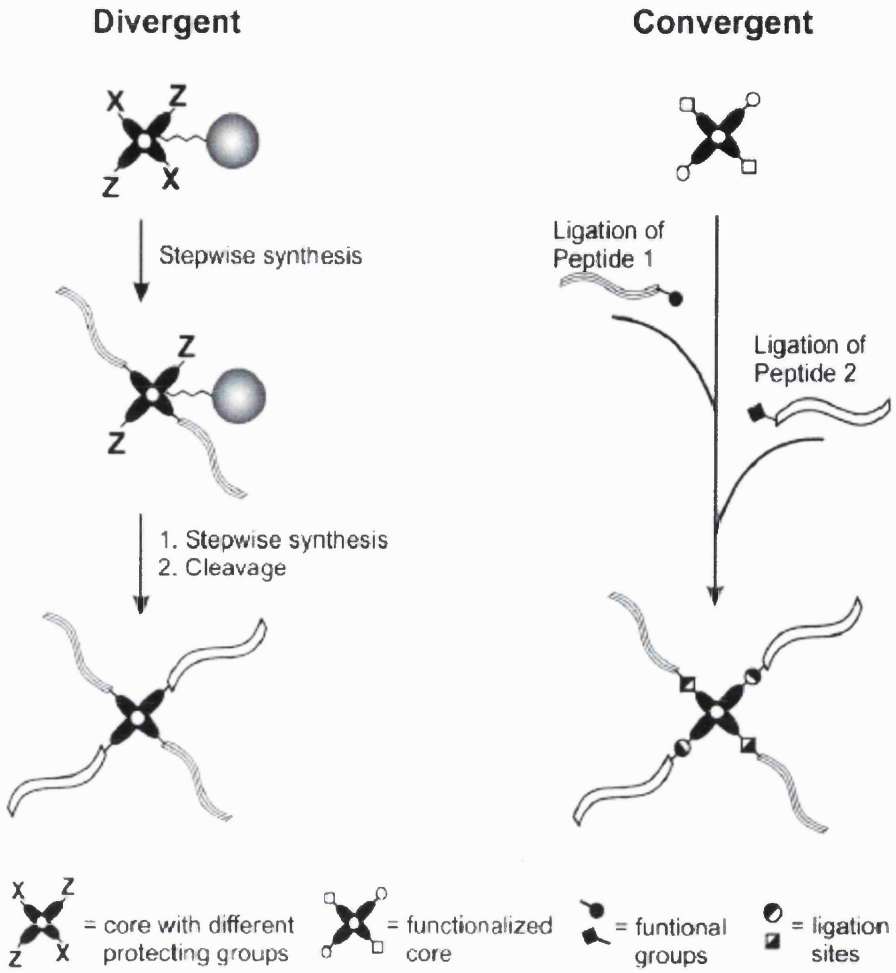

Fig. 1.5. *A schematic comparison of divergent and convergent synthesis methods. (from Sadler and Tam (2002) Rev. Mol. Biotechnology, 90, 195-229.)*

1.4 Different dendritic structures

Polymeric micelles provide a model for dendrimer design and construction. With polymeric micelles, the interior hydrophobic core can be used to entrap guest molecules, surrounded by a hydrophilic outer shell which makes the aggregate aqueously soluble. The stability of such polymeric aggregates are dependent upon a critical micelle concentration (CMC), and below a CMC, the aggregates will dissociate leading to the liberation of the guest molecules. To counter this problem, Newkome *et al.* (1991) have designed a dendritic unimolecular micelle (Fig. 1.6a) with a hydrophobic interior and hydrophilic surface functionality. These

unimolecular micelles exhibit greater stability due to covalent bonding. Newkome and co-workers demonstrated that the internal hydrophobic cavities of this unimolecular micelle were able to solubilise various hydrophobic guest molecules. Newkome's group has also prepared a series of dendritic molecules possessing internal heterocyclic loci (Newkome, 1996a) capable of specific binding of guest molecules (Fig. 1.6b). The unimolecular micelle was an early design of a dendritic covalently bound molecule which could act as a carrier.

A wide array of dendritic structures have been presented in the literatures: polyamidoamine (PAMAM), poly(propyl imine)(DAB-dendr-NH_2), polyethers, polyesters, poly(ester amides), poly(ether amides), polyalkanes, polyphenylenes, poly(phenylacetylenes), polysilanes, phosphorus dendrimers and others (Tomalia *et al.*, 1985, Liu, M. and Fréchet, 1999, Matthews *et al.*, 1998, Newkome *et al.*, 1996, Roovers and Comanita, 1999, Tomalia and Durst, 1993, Zeng and Zimmerman, 1997).

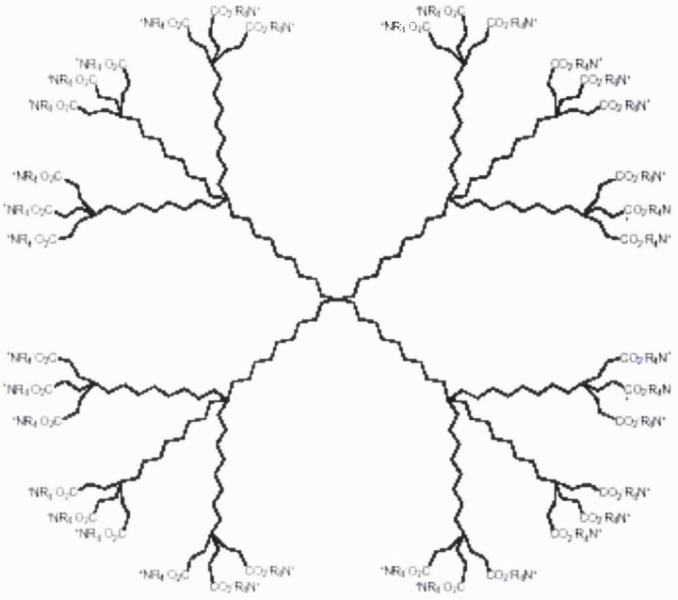

Fig. 1.6a. *A unimolecular micelle. (from Newkome et al. (1991) Angew. Chem. Int. Ed. Engl., 30, 1178-1180.)*

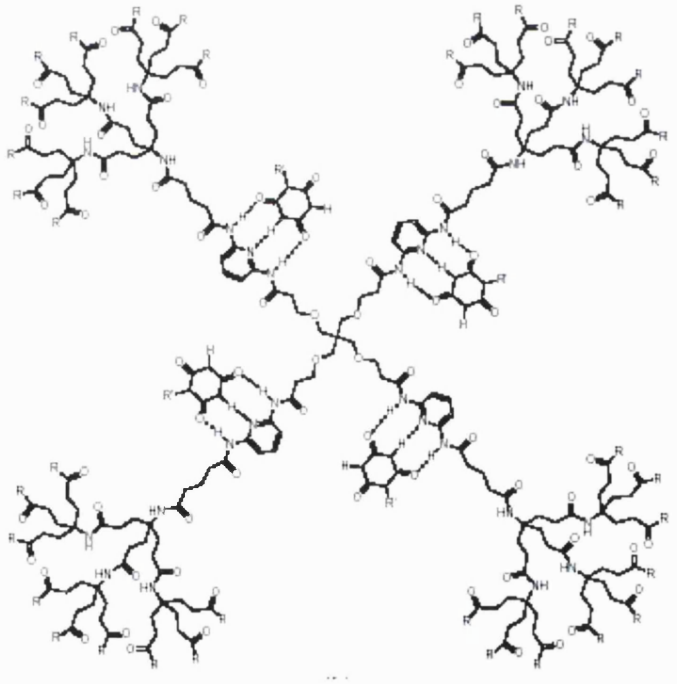

Fig. 1.6b. *Newkome's dendrimer with internal binding units. (from Newkome (1996) J. Heterocyclic Chem., 33, 1445-1460.)*

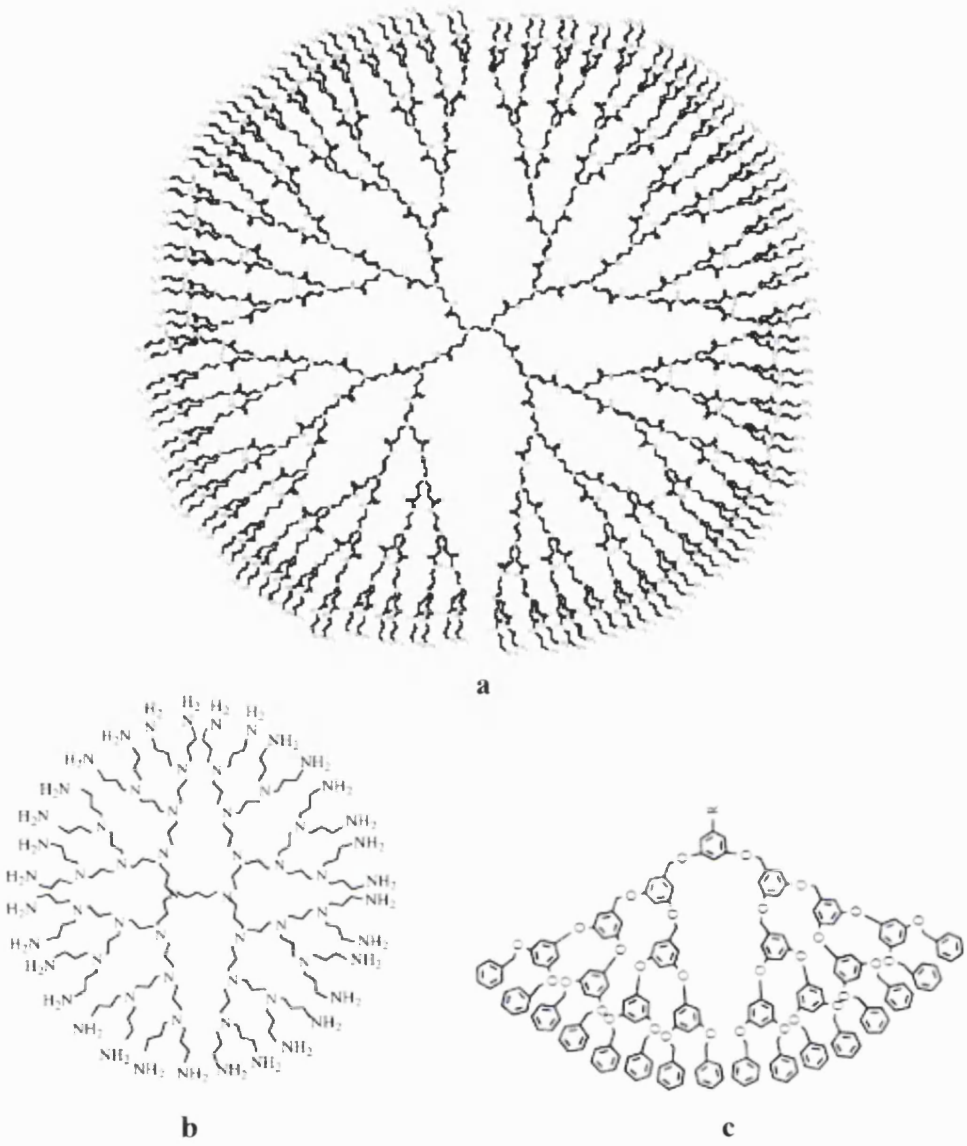

Fig. 1.7a) *PAMAM dendrimer;* ***b)*** *DAB-dendr-NH_2 dendrimer;* ***c)*** *Fréchet's dendron. (from Inoue (2000) Prog. Polym. Sci., 25, 453-571.)*

The prevalence of these covalently bound dendrimers, led to the design of more intricately structured dendrimers (Matthews *et al.*, 1998, Newkome *et al.*, 1996, Roovers and Comanita, 1999, Tomalia and Durst, 1993, Zeng and Zimmerman, 1997). Fig. 1.7a-c shows some of the typical examples used and how the various structures are presented in the literature (Inoue, 2000).

1.4.1 Peptide dendrimers

The potential applications of peptide dendrimers include antiviral and anticancer agents, vaccines and drug and gene delivery systems. The current progresses in peptide chemistry together with practical techniques, like solid-phase peptide synthesis, make amino acids favourable components for dendrimer synthesis. Perhaps the family of dendrimers most investigated is the polyamidoamine (PAMAM) dendrimer (Tomalia *et al.*, 1985). PAMAM dendrimers are synthesised by the divergent approach, starting with a functional amino core that is reacted with methyl acrylate by Michael addition reaction. Each amino group diverges with two branches to form a COOH-terminated dendrimer, which is called a 'half-generation' dendrimer. Subsequent amidation of the methyl ester with ethylene diamine gives a 'full generation' NH_2-terminated dendrimer. Michael addition and amidation steps can be repeated for each generation of growth required. Although this method is widely used, not all peptide dendrimers are constructed in this way.

1.4.2 Glycodendrimers

Another type of dendrimer which has been the focus of much recent work (Turnbull and Stoddart, 2002, Bezouška, 2002, Cloninger, 2002) is the 'glycodendrimer'. Glyco-dendrimers or -dendrons are dendritic molecules which incorporate carbohydrates into their architectures. The vast majority of glycodendrimers have saccharide residues on their outer surface, but glycodendrimers containing a sugar unit as the central core from which all branch points emanate as well as glycodendrimers with carbohydrates as the main dendrimer building blocks have also been described (Fig. 1.8). Biological applications have been the focus of glycodendrimer utilisation. Glycodendrimers with terminal carbohydrate molecules have been used to study protein–carbohydrate interactions that may give insight into

intercellular interactions. The affinities that lectins have for carbohydrates can be studied using a molecule which has the potential for multivalent interactions (Mammen *et al.*, 1998). Therefore dendrimers, with a large number of carbohydrate molecules attached to their surface, can provide suitable probes for studying protein–carbohydrate interactions. Dendrimers are also appealing because amino acids and carbohydrates can be incorporated into the architecture of a single molecule. Dendrimers may provide advantages in such studies, compared with other molecules (e.g. glycopolymers), because of their size and low polydispersity. Also, with glycodendrimers, the sizes of the molecules can be controlled by the choice of dendrimer generation. Examples of this include lactose-functionalized PAMAM dendrimers (Pavlov *et al.*, 2001) and the incorporation of the disaccharide, trehalose, into the core of a PAMAM dendrimer to increase the degree of branching at the core (Dubber and Lindhorst, 2001).

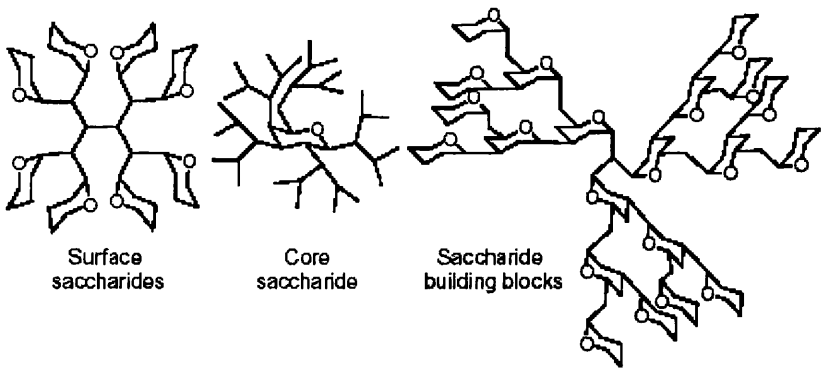

Fig. 1.8. *Glycodendrimer motifs showing different positions in which the saccharide units can be placed within the framework. (from Cloninger (2002) Current Opinion in Chemical Biology, 6, 1-7.)*

1.4.3 Metallodendrimers

The incorporation of metals into the architecture of dendrimers, either associated with the surface or the core provides a strategy for the design of an interesting sub-

class of dendrimers (Inoue, 2000). Using devised synthetic techniques, a variety of metallic molecules have been employed in the core, junction units, and the surface of dendritic structures. Dendrimers with metals as repeat units are constructed by a strategy called "complexes as metal/complexes as ligand", comprising of rigid organic molecules with two or three metal-binding sites, which provide supports for metal bridges to be placed. Campagna and colleagues (1995) studied the construction of dendrimers based on polypyridine-transition metal complexes (Fig. 1.9).

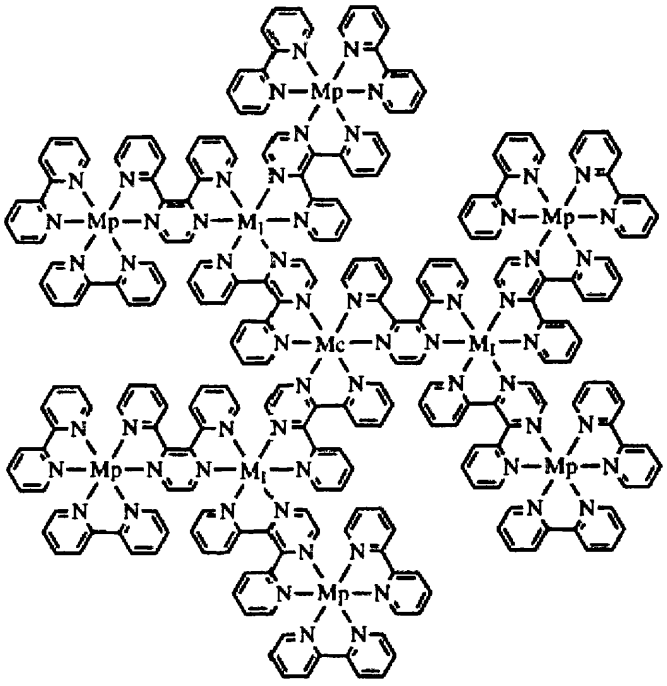

Fig. 1.9. *A dendrimer based on metal complexes developed by Campagna and co-workers. (from Campagna et al. (1995) Chem. Eur. J., 1, 211-221.)*

So far, metals such as Fe, Cu, Zn, Ni, Au, Co, Pd/Pt, Os/Ru, Rh, and Ge have been incorporated as branching units or at the periphery of dendrimers. Some of these metallodendrimers are widely studied as mimics of biological redox potential, sensors, catalysts, new materials for energy conversion, and organic semiconductors. Application details will be discussed further, later in this chapter.

1.5 Advantages and properties of dendrimers

The ability to accurately control size and architecture, is an appealing advantage of dendrimers. Fig. 1.10 shows how dendrimer size can be controlled by generation growth and how these sizes compare to biological structures and molecules. Dendrimer molecules can be grown to macro-dimensions with the ability to retain monodispersity. Therefore, dendrimers can possess the favourable properties of linear polymers with the exclusion of disadvantages such as a poor control of molecular shape or limited options for functionalisation (Esfand and Tomalia, 2001). A large variety of building blocks from organic, metalloorganic or inorganic chemistry have been employed for the construction of dendrimers, including biologically important molecules such as peptides or sugars, as discussed in section 1.4. Dendrimer research has explored many areas of the natural sciences to aid our understanding of different scientific problems. Currently, the roles of branched molecules are being investigated for technical and biochemical applications in catalysis, polymer science, bio-organic chemistry, biotechnology and medicine. Large dendrimers display properties different from linear polymers making them appealing candidates in areas of material science research.

Dendrimer architecture can be orientated to provide properties of unimolecular micelles or to possess cavities, which can accommodate guest molecules. Surface modification of dendrimers can also result in molecules which display catalytic properties (Reek *et al.*, 2002). Catalytic dendrimers can possess the properties of a homogenous catalyst including kinetic behaviour, activity and selectivity. They can be separated from the reaction mixture by utilising simple methods such as filtration. In general, it is the multivalent potential of dendritic molecules which make them well-suited for applications in biology, including diagnostic reagents, protein

mimetics, anti-cancer and anti-viral agents, vaccines as well as drug and gene delivery systems (Dennig and Duncan, 2002). The use of dendrimers in the fields of drug and gene delivery will be discussed later.

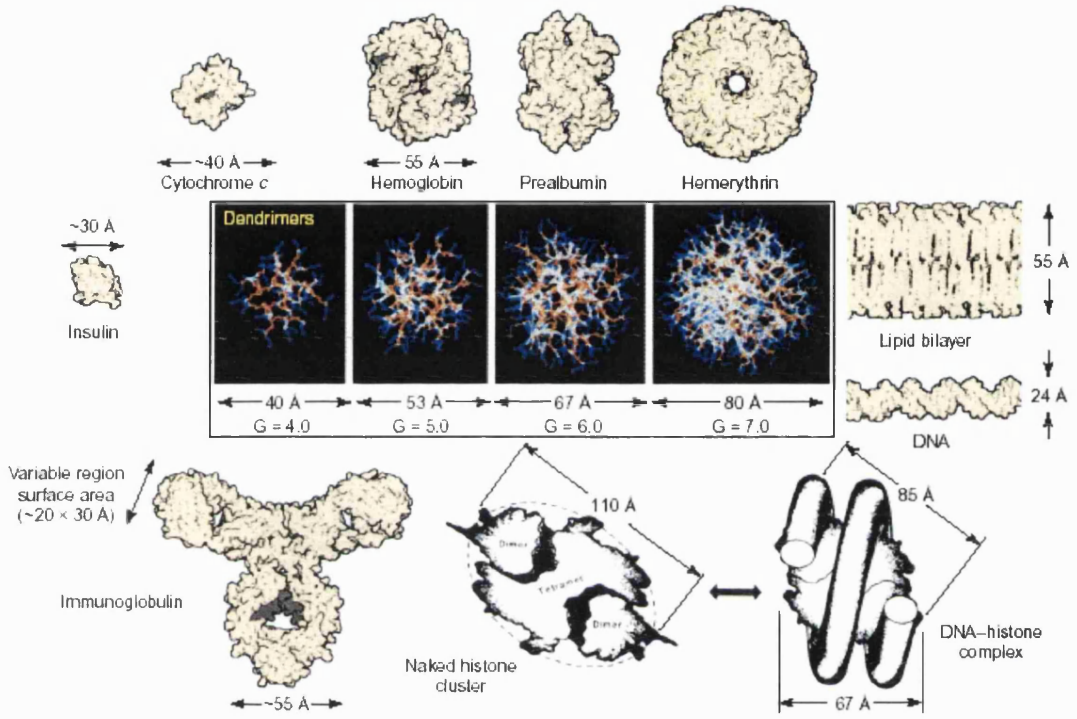

Fig. 1.10. *A dimensionally scaled comparison of a series of poly(amidoamine) (PAMAM) dendrimers (NH_3 core; G = 4–7) with a variety of proteins, a typical lipid-bilayer membrane and DNA, indicating the closely matched size and contours of important proteins and bioassemblies. (from Esfand and Tomalia (2001) Drug Discov. Today, 6, 427-436.)*

Dendrimers also display unique and unusual physical properties as a consequence of their topologies. One observation is the dependence of the intrinsic viscosity of dendrimers upon molecular weight (Fréchet *et al.*, 1994). It was observed that, the intrinsic viscosity of dendrimers began to decrease beyond a certain size threshold, a property not observed with linear polymers. This effect is believed to result from the lack of intermolecular entanglement of the high-generation globular molecules. The

viscosity of dendrimers is further discussed in Chapter 5. Comparisons between the solubility of dendrimers and their linear analogues have been studied (Fréchet, 1994). The solubility of a polyether dendrimer in tetrahydrofuran (THF) was found to be approximately 50 times that of its linear analogue, which indicates that shape has a pronounced effect on solubility.

Another property of dendrimers is their ability to self-assemble. Tomalia and Durst (1993), discussed the idea that dendrimers are ideal, well-defined functional building blocks for creating self-assembled nanostructures. Although the dreams of nanotechnologists have yet to be realised, dendrimers are already showing promise as exciting building blocks in the production of liquid crystals, monolayers and films. Examples of liquid-crystalline dendrimers, containing transition metal ions, have been described by Stebani *et al.* (1996). These compounds are derived from dendrimers built around a tris(2-aminoethyl)amine core – a moiety that binds a variety of transition metal ions.

With the construction of thin films and layers being the subject of much research interest, the structural properties of dendrimers – their uniform shapes, controllable surface functionalities and chemical stabilities – make them attractive building blocks for their assembly. Self-assembled dendrimer layers have been reported and the study of these materials is one of the most promising areas of applied dendrimer research at present. Multilayered thin films have been constructed on a Pt^{2+} - coated surface using a stepwise procedure (Watanabe and Regen, 1994). This process involves the functionalisation of a silicon wafer to produce an amino-terminated surface which is coated with Pt^{2+} ions. Immersing this material into a solution of various PAMAM dendrimers results in a monolayer that can be built upon by using a

repetitive process. Each cycle, in which either fourth- or sixth-generation PAMAM dendrimers is added, results in the addition of layers 40 Å and 70 Å thick, respectively. The Pt^{2+} coating adds 10 Å on to the surface and twelve repetitions of the cycle have been carried out, resulting in films up to 800 Å thick. In the absence of Pt^{2+}, no growth was observed. This indicated that the metal ions form inter-dendrimer metal-amine bonds between layers. Dendrimer molecules have also been incorporated into films on electrodes (Alonso *et al.*, 1995) and at air-water interfaces in the form of Langmuir films (Saville *et al.*, 1995). Sui *et al.* (2000) synthesised a new disk-shaped amphiphilic dendrimer by attaching sixty-four 12-hydroxydodecanoic acid chains to a fourth generation PAMAM dendrimer core. When the molecules were deposited on mica, at a surface pressure of 5mN/m, they observed Langmuir-Blodgett films (Fig. 1.11) It is possible to observe basically two types of different domains: rectangular and elliptical. Surface pressure and surface potential-area isotherm measurements showed that the dendrimer formed a stable monolayer at the air/water interface with a limiting molecular area of 160 $Å^2$/molecule. This small area relative to the huge size of the dendrimer suggested that the dendrimer molecules formed an edge-on disk-shaped structure at the air/water interface. Sakthivel *et al.* (1998) synthesised lipophilic polyamide dendrimers with 16 lipoamino acid branches which formed tubular supramolecular aggregates with a helical structure and dimensions in the long axis of 140-200 nm.

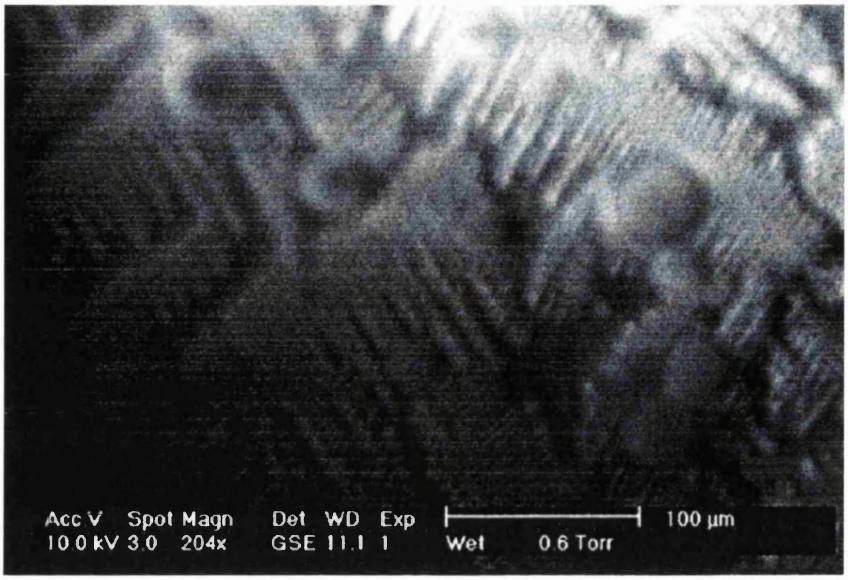

Fig. 1.11. *Environmental scanning electron microscopy image of Langmuir-Blodgett film, of disk-shaped amphiphilic dendrimers with sixty-four 12-hydroxydodecanoic acid chains attached to a fourth generation PAMAM dendrimer core, deposited on mica at surface pressure 5 mN/m. (from Sui et al. (2000) Langmuir, 16, 7847-7851.)*

Another recently discovered property of certain dendrimers is their ability to form vesicular structures. Al-Jamal and co-workers (2003), in our laboratories, studied a lysine dendron with lipidic character at all terminals of the molecule. The molecules were found to form higher order structures in aqueous media, which were termed "dendrisomes" (Fig. 1.12). Entrapment efficiency studies were also conducted using penicillin G. Gensch *et al.* (2001) formed giant vesicles in aqueous solutions with a fifth-generation poly(propylene imine) dendrimer decorated with palmitoyl- and azobenzene-containing alkyl groups. The vesicles were reported to have diameters ranging from 50 nm up to 20 µm with a "multilaminar onion-like structure". In collision experiments, the vesicles behaved like hard spheres, and merging was not observed.

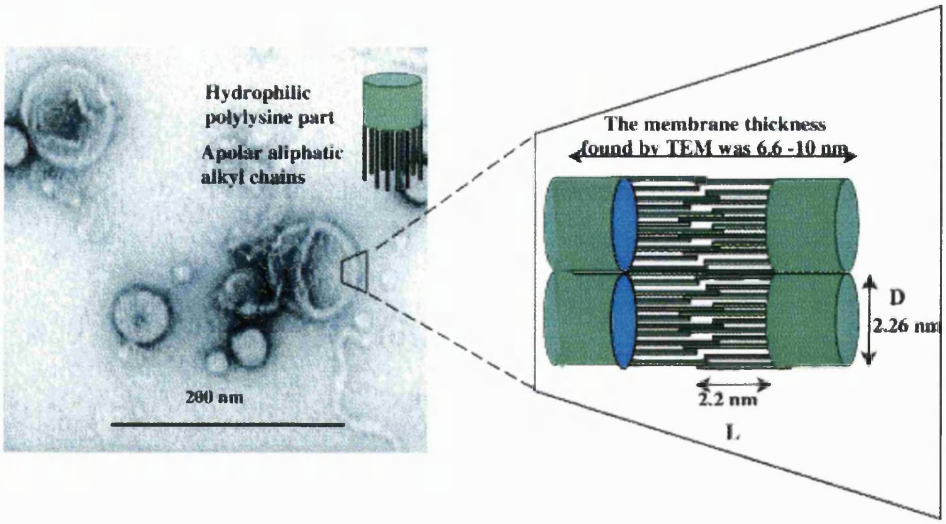

Fig. 1.12. *Transmission electron micrograph of dendrisomes with membranes from 6 to 10 nm thick (left). Schematic representation of bilayer formation (right). The diameter, D, was calculated from the molecular area found by surface pressure studies. The length of the alkyl chain, L, based on Corey–Pauling–Koltun (CPK) molecular modelling. (from Al-Jamal et al. (2003) Int. J. Pharm., 254, 33-36.)*

As a result of some of their unique physical properties, dendrimers have been used in a variety of analytical applications, including electrokinetic chromatography (EKC), ion-exchange displacement chromatography and immunoassays.

EKC is a class of separation technique which depends upon an electro-osmotic flow (Terabe *et al.*, 1985). Micelle-forming ionic surfactants, such as sodium dodecyl sulphate, sodium cholate or cetyltrimethylammonium bromide, are used as the counterflow electrolyte in EKC. Separation is dependent upon the electrolyte concentration, solvent strength, pH and temperature. These factors all have an effect on the heterogeneity of the dynamic micelles which are formed. Dendrimeric counterflow electrolytes have homogenicic properties such as their static, regular dimensions and uniform charge density, which facilitates (Muijselaar *et al.*, 1995, Kuzdzal *et al.*, 1994) high-performance separations using EKC. Another advantage

of employing dendrimers over their more commonly used counterparts is that selectivities appear to arise as a result of the characteristic molecular structures of both the surface and interior of the dendrimeric micelles. Therefore, EKC may also function as an assay for the guest binding properties of dendrimers.

Ion-exchange displacement chromatography is an efficient and cost-effective method for the large-scale purification of biomolecules. One of the requirements of this technique is the need of a displacer compound. A displacer compound is one which has a higher affinity for the stationary phase than any of the feed components. Most of the displacers which have been used to date are large polyelectrolytes and, because of their cost and regulatory constraints, they have not excited much interest from the biopharmaceutical industry. Polycationic pentaerythritol-based dendrimers (Jayaraman *et al.*, 1995) have been used as efficient displacers for proteins. Also, anion-exchange resins have been produced (Cherestes and Engel, 1994) by the covalent attachment of cationic dendrimers to a Merrifield resin. The use of dendrimers as standards in mass spectroscopy and gel permeation chromatography has also been proposed.

Highly effective immunoassays, based on antibodies covalently attached to fifth generation PAMAM dendrimers have been reported by Singh and co-workers (1994). The conjugates produced have unique properties such as high solubility, high charge density, high affinity and specificity, making them ideal candidates for immunoassays. Furthermore, the attachment of two antibodies to the same dendrimer resulted in a reagent which was specific for two analytes and the investigators observed no obvious effect on the biological binding activity.

Another alliance which is generating much interest is that of dendrimers and dyes. The combination of dendrimers with dye molecules has brought insight into new applications with scientific and industrial relevance. Various purposes include dyes as structural probes for dendrimers, dyes combined with dendrimers for capture and transfer of photon energy and extraction and encapsulation of dyes by dendrimers. When dyes are used as structural probes for dendrimers, dye molecules interact with some part of a dendrimer molecule, either end groups, branches or the core. The interaction leads to a change in the absorption or emission behaviour of the dye, which can give information on the structure of the dendrimer with its environment. Hawker *et al.* (1993) coupled the solvatochromic dye 4-(*N, N'*-dimethylamino)-1-nitrotoulene to the core of a poly(benzyl ether) dendrimer. In a solution of carbon tetrachloride the λ_{max} of the dye increased with higher dendrimer generation due to a shift of preferred interaction from dye-solvent to dye-dendrimer. Between generation 3 and 4 a marked discontinuity in the linear increase of λ_{max} was observed. The investigators explain this as, a transition in the dendrimer structure from a linear to a more globular configuration.

Dendrimers have been constructed with light-absorbing chromophore groups on the outside, which subsequently transfer the absorbed photon energy to a single laser dye located at the dendrimer's core. In this way a light harvesting system is obtained, which presents a strong analogy to the photosynthetic system of nature (Bar-Haim and Klafter, 1998). Gilat *et al.* (1999) were the first to report the practical synthesis of a dendrimer based light harvesting system using poly(benzyl ether) dendrimers. They used the laser dyes Coumarin-2 at the dendrimer's core and Coumarin-343 at the periphery. They showed that the molecule acted as a spectral energy concentrating system, with excellent absorption and emission characteristics. Junge

and McGrath (1997) developed a photoresponsive dendrimer, which reversibly changes its confirmation upon irradiation. By incorporation of an azobenzene chromophore in the core of a poly(benzyl ether) dendrimer, the molecule can change from an open structure with the core in the trans configuration to a closed structure with the core in the cis form.

This concept of the "dendritic box" was developed by Jansen *et al.* (1995). By constructing a dense, hydrogen-bonded shell around higher generations of poly(propylene imine) dendrimers in the presence of guest molecules, the guests can be trapped within the dendrimer. It was found that the shape of the dye molecule and the nature of the internal cavities, as well as the dendritic architecture determine the number of guest molecules that can be entrapped in this way (up to eight per dendrimer). Computer simulations of the entrapment process yielded the same results. Furthermore, mild hydrolysis can be used to partially remove the shell, resulting in the release of smaller molecules whilst retaining the larger ones.

1.6 Dendrimers as delivery agents and carriers

In the search for an ideal carrier system, dendrimers may have significant potential as discussed earlier with regard to their flexible physico-chemical properties. The utilisation of dendrimers as delivery vectors can potentially be envisaged in two ways: (a) molecules can be physically entrapped inside the dendritic cavities; and (b) molecules can be attached onto the surface directly or using linkers to form dendrimer-drug conjugates. The properties of an ideal macromolecular drug delivery or biomedical vector (Esfand and Tomalia, 2001) would include;

- Structural control over size and shape of drug or imaging-agent cargo-space.

- ❖ Biocompatible, non-toxic polymer/pendant functionality.
- ❖ Precise, nanoscale-container and/or scaffolding properties with high drug or imaging-agent capacity features.
- ❖ Well-defined scaffolding and/or surface modifiable functionality for cell-specific targeting moieties.
- ❖ Lack of immunogenicity.
- ❖ Appropriate cellular adhesion, endocytosis and intracellular trafficking to allow therapeutic delivery or imaging in the cytoplasm or nucleus.
- ❖ Acceptable bioelimination or biodegradation.
- ❖ Controlled or triggerable drug release.
- ❖ Molecular level isolation and protection of the drug against inactivation during transit to target cells.
- ❖ Minimal non-specific cellular and blood-protein binding properties.
- ❖ Ease of consistent, reproducible, clinical grade synthesis.

1.6.1. Physical entrapment of guest molecules

The internal cavity of an appropriately designed dendritic structure could be used for the entrapment of drugs with the possibility of subsequent controlled release. Jansen and co-workers (1994) reported that guest molecules such as Rose Bengal can be physically entrapped in the internal cavity of high generation poly(propylene imine) dendrimers by attaching amino acid derivatives to the terminal groups to form a shell (the dendritic box). However, the release of the encapsulated guest molecules could be achieved by selectively removing the shell either partially or completely using hydrolysis (Jansen *et al.*, 1995). Recently a similar strategy has been proposed by Watanabe and Iwamura (2003) using "sugar-ball" type caged compounds. They synthesised PAMAM and DAB dendrimers with 4–64 terminal caged compounds on

their surface. A "sugar-ball" is a glycodendrimer which has many sugar units in the peripheral region of the dendrimer. Glycodendrimers were used to entrap the bioactive compound (LeuLeuOMe) and the release of the compound was monitored upon irradiation. This concept led them to conclude that if the sugar ball-type caged compounds could be obtained, they should offer several benefits: (1) they can transport many bioactive compounds at a time in an inactive form; (2) they may be able to recognize cells due to the cluster effect of sugars attached to the dendrimer; (3) another bioactive compound or fluorophore can be accommodated by host–guest interaction between such molecules and the interior of the dendrimer. This concept is schematically depicted in Fig. 1.13. The amount of LeuLeuOMe released per molecule increased with the increase in the generation of dendrimers.

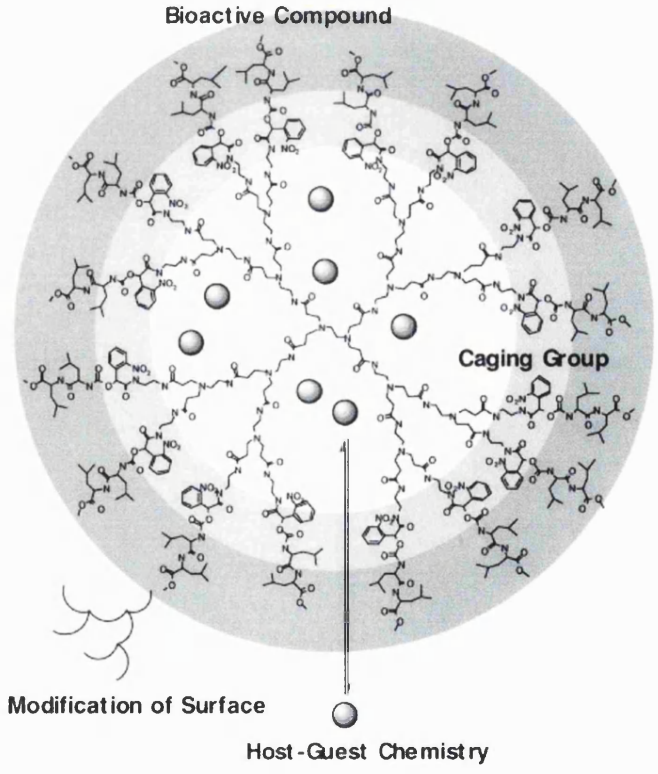

Fig. 1.13. *Schematic representation of dendritic caged compounds and their expected functions. (from Watanabe and Iwamura (2003) J. Photochem. Photobiol., A: Chem., 155, 57-62.)*

Encapsulation of guest molecules in dendrimers can also be accomplished using noncovalent chemical interactions (e.g. hydrogen bonding) between guest molecules and the internal dendritic architecture. Newkome *et al.* (1996) synthesised a dendrimer containing multiple hydrogen bonding sites at its core and evaluated the host–guest interactions using ^{1}H NMR. The third, and most easily implemented, strategy for the encapsulation of guest molecules in dendrimers makes use of hydrophobic interactions such as with the unimolecular micelle shown in Fig. 1.6a (Newkome *et al.*, 1991). The potential of dendritic unimolecular micelles in drug delivery systems, was investigated by Liu, M. *et al.* (2000) who prepared dendritic unimolecular micelles with a hydrophobic core surrounded by a hydrophilic shell. The monomer selected to build the dendritic cores was 4, 4-bis(4'-hydroxyphenyl) pentanol, providing flexibility to the dendritic structure while contributing to the encapsulating capacity of the molecule. Encapsulation was demonstrated by solubilising pyrene in aqueous solution. Entrapment of the model drug indomethacin in the dendritic micelles was achieved and preliminary in vitro release tests showed that sustained release characteristics were achieved.

The `dendritic box' is an impractical approach to drug delivery because of its limited capacity and the harsh conditions that are necessary to control release of the guest molecules. Further research into 'smart' materials may provide paths leading to an ideal 'dendritic box'. In contrast, designs involving the noncovalent binding of drug molecules inside the dendritic unimolecular micelles by hydrogen bonding or by hydrophobic interactions, appear attractive because of their simplicity (Liu, M. and Fréchet, 1999).

Other approaches have been used to engineer dendrimers with the ability to release drugs. To improve biocompatibility and solubility, PAMAM dendrimers with PEG grafts on the surface have been synthesized, and the encapsulation of anticancer drugs, including adriamycin and methotrexate, using these structures has been attempted (Kojima *et al.*, 2000). The ability to encapsulate the drugs in the dendritic core increases with increased generation and chain length of the attached PEG grafts. Though the drugs are released slowly from the matrix in low ionic strength aqueous solution, they are readily released in isotonic solutions. This suggests the need for further control of the drug release mechanism in these molecules. The pH-dependent change in the hydrodynamic radii of acid-terminated dendrimers has been investigated as a potential controlled-release system for encapsulated drugs from the interior hydrophobic areas of the dendrimer (Newkome *et al.*, 1993). Using this principle, Sideratou and co-workers (2000) have investigated the pH-dependent inclusion and release of pyrene in quarternized poly(propylene imine) dendrimers. The terminal quarternary ammonium salt not only enhances the water solubility of the dendrimer, but possess bactericidal, antifungal and antimicrobial properties. Pyrene is released when the internal tertiary amines are protonated between pH 4–2. This release within a narrower pH region suggests these materials are potential candidates for pH-sensitive controlled-release drug delivery applications.

1.6.2 Dendrimer-drug conjugates

Biologically active molecules, such as sugars (glycodendrimers) and antibodies (Roberts *et al.*, 1990) have been attached to the terminal end groups of dendrimeric molecules. Zanini and Roy (1997) synthesised a series of α-thiosialoside-conjugated dendrimers and studied their binding properties to a sialic acid-specific lectin from *Limax flavus*. Antibodies are useful in targeted drug therapy because of the

specificity of the antibody–antigen recognition process. When modifying the antibody molecule, to accomadate the association of a drug, it is important not to diminish or eliminate its biological activity. To counteract this potential problem, Roberts *et al.* (1990) have used PAMAM dendrimers as linkers to covalently attach porphyrin to chelated copper ions. The resulting PAMAM-antibody conjugate retained 90% of the immunoreactivity of the unmodified antibody. They have also investigated how the conjugation site of the porphyrin moiety affects immunoreactivity, and have reported 100% activity when the PAMAM dendrimer is conjugated to the heavy chain of the porphyrin unit.

In contrast, only a small number of groups have reported the conjugation of drug molecules to the periphery of dendrimers. The simplest way to construct dendrimer–drug conjugates is to couple drug molecules directly to the surface of the dendrimer. Due to its multivalent nature, one dendrimer molecule is able to associate with multiple drug molecules, and the number of drug molecules per conjugate can be controlled during the synthesis process. Malik and co-workers (1997) have prepared a PAMAM dendrimer–platinate conjugate and examined its antitumour activity; the conjugate showed antitumor activity in all of the tumour models tested, including a platinum-resistant tumour model. Milhem and co-workers (2001) developed G4 PAMAM-ibuprofen drug conjugates. They found that when the hydrophobic ibuprofen molecules (> 5) were coupled to the dendrimer surface, insoluble complexes were formed. Modification of this complex, using PEG, enabled an increase in the loading capacity of the dendrimer (32 ibuprofen molecules). The release of ibuprofen from these conjugates was studied. Zhuo *et al.* (1999) synthesised PAMAM dendrimers with a cyclic core, and attached 5-fluorouracil to the G4 and G5 dendrimers to form conjugates. Subsequent hydrolysis of the

conjugates in a phosphate buffer solution resulted in the release of free 5-fluorouracil.

An acetylated G5 PAMAM dendrimer labelled with fluorescein isothiocyanate, was conjugated (Patri *et al.*, 2002) to anti-PSMA (prostate-specific membrane antigen) antibody for targeting prostate cancer. This conjugate was shown to successfully target PSMA-positive LNCaP cell line with minimal loss of immunoreactivity, compared to the control molecule lacking the antibody.

Uppuluri *et al.*, (2000) prepared tectodendrimers with fluorescein cores to aid detection and folate moieties in the shell to facilitate targeting. The molecule was shown to successfully target hFR cell lines, displaying more efficiency than the single dendrimer having both agents on the surface of the molecule.

1.6.3 Dendrimers in gene delivery

Immunogenic adverse effects, associated with viral vectors in gene delivery, have actively directed research research groups in search of an effective non-viral vector. An ideal non-viral vector should protect DNA from enzymatic degradation and aid its delivery into the cell. The first published study, utilising dendrimers for this concept, was produced by Haensler and Szoka (1993). They reported that PAMAM dendrimers mediated the high-efficiency transfection of DNA into a variety of cultured mammalian cells, and that the transfection was a function of both the size of the complex and the dendrimer-DNA ratio. Transfection efficiency could be increased by covalent attachment of a water-soluble peptide to the dendrimer via a disulfide linkage. Because they form compact polycations under physiological conditions, PAMAM dendrimers, poly(propylene imine) dendrimers and partially

hydrolyzed PAMAM dendrimers have been used as DNA delivery systems (Gebhart and Kabanov, 2001, Sato *et al.*, 2001). The high cationic charge of the dendrimers condense the anionic DNA to form a complex. Scanning force microscopy data indicates that DNA wraps around the dendronised polymers (Gossl *et al.*, 2002). Tang and co-workers reported that 'fractured dendrimers', obtained by heat treatment of intact dendrimers in a variety of solvolytic solvents, enhanced the transfection activity dramatically (Tang *et al.*, 1996). They suggested that the increased transfection that followed the heating process was primarily the result of an increase in flexibility, which enabled the 'fractured dendrimers' to assume a compact shape when complexed with DNA and to swell when released from DNA. Another research group also reported the efficient transfer of genetic material using PAMAM dendrimers (Kukowska-Latallo *et al.*, 1996). PAMAM dendrimers functionalised with α-cyclodextrin showed luciferase gene expression about 100 times higher than for unfunctionalised PAMAM or for non-covalent mixtures of PAMAM and α-cyclodextrin (Arima *et al.*, 2001). Poly(ethylene glycol) functionalisation of G5 PAMAM dendrimers produced a 20-fold increase in transfection efficiency using plasmid DNA coding for a reporter protein β-galactosidase relative to partially degraded PAMAM dendrimers (Luo *et al.*, 2002). Choi *et al.* (1999) reported a novel linear-dendritic block copolymer that formed a water-soluble complex with plasmid DNA under physiological conditions. The complex was found to take a globular shape with a relatively narrow size distribution.

Toth *et al.* (1999) used cationic lipidic dendrimers with the presence of a sugar unit and a nuclear localisation signal peptide. The transfection activity of the products was assayed in vitro on Cos-7 (fibroblast) cells. The dendrimers displayed high transfection activity and the results indicated that the presence of more amino groups

on the surface of the dendrimers enhanced gene delivery. Ramaswamy *et al.* (2003), in our laboratories, studied the interaction of DNA with lysine dendrons with and without lipidic character in the core. They showed evidence of the formation of compact complexes which were termed 'dendriplexes'. The apparent diameters of the dendriplexes ranged from 60-70 nm for all dendrons used. The group confirmed the protection of the DNA component of these dendriplexes from nuclease degradation using DNase protection assays.

1.6.4 Biocompatibility and toxicology of dendrimers

The biocompatibility and toxicology of drug delivery vectors must be favourable, to successfully pursue potential applications. This is a growing area of dendrimer research. Malik *et al.* (2000) have investigated the relationship between structure and biocompatibility of PAMAM, poly(propyleneimine), poly(ethylene oxide) grafted carbosilane dendrimers with cationic (NH_2-terminated) and anionic (COONa-terminated) dendrimers *in vitro*. Their studies showed that cationic dendrimers were generally haemolytic and cytotoxic, at even relatively low concentrations. PAMAM dendrimers were found to be haemolytic, and the effect was more pronounced with an increase in dendrimers generation. The anionic dendrimers did not exhibit haemolysis or cytotoxicity with a range of cell lines, studied *in vitro*. They have further observed that PAMAM dendrimers of equivalent surface functionality were slightly less toxic than DAB (polypropylenimine) dendrimers with the same number of surface groups.

In an *in vitro* study, using an everted rat intestinal sac system, Wiwattanapatapee *et al.* (2000) have studied the effect of PAMAM dendrimer size, charge and concentration on uptake and transport across adult rat intestine. The results obtained

from this study showed that ^{125}I-labeled anionic dendrimers have decreased tissue deposition and fast serosal transfer rates. The larger anionic dendrimers (G5.5) displayed higher tissue accumulation compared with the smaller anionic molecules (G2.5 or G3.5). In contrast to this, cationic PAMAM dendrimers were associated with lower transport rates as the negatively charged cell membranes appeared to interact with the cationic dendrimer surface.

El-Sayed *et al.* (2002) investigated the influence of physiochemical parameters (such as size, molecular weight, molecular geometry, and number of surface amine groups) of PAMAM dendrimers, on their permeability across Caco-2 cell monolayers. The permeability of a series of PAMAM dendrimers, generations G0–G4, was investigated across Caco-2 cell monolayers in both the apical to basolateral (AB) and basolateral to apical (BA) directions. The influence of PAMAM dendrimers on the integrity, paracellular permeability, and viability of Caco-2 cell monolayers was also monitored by measuring the transepithelial electrical resistance (TEER), mannitol permeability, and leakage of lactate dehydrogenase (LDH) enzyme, respectively. G0, G1 and G2 demonstrated similar AB permeabilities, which were moderate several fold higher than the AB permeability of higher generations. The AB and BA permeability of G0–G4 typically increased with the increase in donor concentration and incubation time. TEER values decreased and mannitol permeability increased as a function of donor concentration, incubation time, and generation number. LDH results for G3 and G4 indicate that Caco-2 cell viability was reduced with increasing donor concentration, incubation time, and generation number. The appreciable permeability of G0–G2, coupled with their non-toxic effects on Caco-2 cells, lead the authors to suggest their potential as water-soluble polymeric drug carriers for controlled oral drug delivery.

The same group (El-Sayed *et al.*, 2001) have also investigated the influence of increase in size and molecular weight of fluorescent-labelled PAMAM dendrimers on the extravasation across microvascular endothelium and compared these molecules with corresponding linear poly(ethylene glycol) of similar molecular weight. They reported an exponential increase in the extravasation time with an increase in the molecular weight and size of PAMAM dendrimers, from G0-G4, which increased from 143.9 s to 422.7 s. Results showed that as the molecular diameter and size of the PAMAM dendrimer increases with generation, the viscous drag which is exerted on the molecule, together with its degree of exclusion from the endothelial pores increases, resulting in an increased extravasation time. Compared with PAMAM dendrimers, PEG molecules with a similar molecular weight took longer to extravasate across the endothelium into the interstitial tissue. A 6.0 kDa PEG had a higher extravasation time of 453.9 s compared with that of the G3 dendrimer of similar molecular weight (molecular weight 6909) with 203.8 s. This can be attributed to the larger hydrodynamic volume on the hydrated PEG chain because of the coiled conformation. Tajarobi *et al.* (2001) studied the permeability of a series of PAMAM dendrimers across a MDCK (Madin–Darby canine kidney) cell. The investigators labelled G0–G4 PAMAM dendrimers with FITC; and reported a permeability order of G4>>G1=G0>G3>G2. This suggested that migration through the vascular endothelium may be determined by a size threshold.

Florence and Hussain (2001) have reviewed the oral absorption of dendrimers with regard to the relationship between nanoparticle diameter and uptake from the gastrointestinal tract via normal enterocytes or M-cell pathways. Absorption of the dendrimer through both Peyer's patches and enterocytes was measured following administration of doses of lipidic lysine and ornithine dendrimers. The results

showed the preferential uptake of the dendrimer through Peyer's patches in the small intestine when calculated per gram tissue, although not in the large intestine. Corresponding figures for uptake through the enterocytes were lower. However in the large intestine, Peyer's patches appeared to play but a small role, with enterocytes showing higher levels of dendrimer localisation.

More recent work by Jevprasesphant *et al.* (2003 and 2003a) has focussed on surface modification of PAMAM dendrimers, to reduce cytotoxicity and enhance transepithelial transport. The investigators conjugated PEG 2000 and lauroyl chains (Jevprasesphant *et al.*, 2003) to the surface of G2-G4 cationic dendrimers. Using Caco-2 cells and a 3-(4,5-dimethythiazole-2-yl)-2,5-diphenyltetrazolium bromide (MTT) assay, the results showed that surface-conjugated dendrimers exhibited less cytotoxicity when compared to the unconjugated molecules. To quantitatively evaluate the cytotoxicity, IC_{50} values for mitochondrial dehydrogenase were determined. It was suggested that the lauroyl and PEG surface units shield the cationic charge, resulting in decreased cytotoxicity. Further work by the group (Jevprasesphant *et al.*, 2003a) concluded that PAMAM dendrimers with surface terminal lauroyl chloride groups had enhanced permeability through Caco-2 cell monolayers and that modified and unmodified PAMAM dendrimers have the potential to cross epithelial monolayers via paracellular and transcellular routes. To quantitatively evaluate permeation across the cell monolayer, the dendrimers were labelled fluorescein isothiocyanate (FITC). Their findings were consistent with those of Malik *et al.* (2000) showing increased cytotoxicity with increasing size and cationic charge. Fischer *et al.* (2003) conducted a comparative *in vitro* study to assess the cytotoxicity of different polycations, using LDH, MTT and haemolysis assays with different cell types. With regard to cytotoxicity, the polycations were ranked;

poly(ethylenimine) = poly(l-lysine) > poly(diallyl-dimethyl-ammonium chloride) > diethyl-aminoethyl-dextran > poly(vinyl pyridinium bromide) > PAMAM dendrimers > cationised albumin > native albumin. The studies showed that PAMAM dendrimers exhibited only moderate cytotoxic effects in comparison with the other polymers. The investigators stated that the important factors for cytotoxicity include the type of amino function, the charge density and the three-dimensional arrangement of the cationic residues. Shukla *et al.* (2003) prepared chromophorically labelled PEGylated, boronated G3 PAMAM dendrimers (PEG-BDEs) with and without conjugated folic acid. The purpose of the folic acid was to target folate receptors on cancer cells for *in vivo* studies and the role of PEG, was to reduce hepatic uptake. Biodistribution studies with folic acid-conjugated PEG-BDEs resulted in selective tumour uptake (6% of the injected dose per gram of tumour) but also high renal (63% of the injected dose per gram of kidney) and hepatic uptake (39% of the injected dose per gram of liver). *In vitro* evaluation of the folic acid conjugated molecule indicated folate receptor-mediated endocytosis.

There is a growing body of literature on the physico-chemical properties of dendrimeric structures. Such data is critical to the success of a delivery vector and in this thesis, some aspects of the physical properties, of the synthesised dendritic structures, will be discussed. The aim of the research was to study the physical properties of dendrons, synthesised in our laboratories, using *in vitro* studies to gain knowledge of pharamaceutical parameters. *In vivo* and toxicity studies, with the dendrons have not been discussed in this thesis but such studies have been conducted by other members of our research group. Chapter 2 will focus on the synthetic methods used to construct the dendritic molecules, the rationale behind their design, and the methods of characterisation. Chapter 3 introduces the topic of the interaction

of dendrons with liposomes, to give insight into how they might interact with biological membranes. This work uses liposomes with phospholipid membranes of positive, neutral and negative character to study the influence of charge on the interaction with cationic dendrons. In Chapter 4, the diffusion and other physical coefficients of dendrons are discussed, studied using a membrane dialysis technique. Studies of diffusion and permeability are paramount to understanding transport across cell membranes and transport within cells. This work was performed using porous fluid-filled cellulose membranes, and may provide insight into the extravasation properties of the dendrons. In this chapter, the interactions between dendrons and bovine serum albumin are also studied. The synthesis of a novel didendrons is discussed in Chapter 5. The shape of this series of three didendrons offers the opportunity to study the flow properties of the molecular species and the opportunity to compare with dendrons having the equivalent number of surface charge groups. The flow properties of nanoparticulate systems are important and can aid our understanding of dendron-solvent interactions, but flow is also an important feature of nano-carrier behaviour *in vivo*, for example, in microcapillaries.

CHAPTER TWO

DESIGN AND SYNTHESIS OF DENDRITIC MOLECULES

A series of dendritic structures were designed and synthesised as delivery vectors and with the potential to act as self-assembling systems in their own right. Dendrons of different compositions with terminal groups ranging from 8 to 128 were synthesised. Some were synthesised with cationic amino-terminals and others with neutral acetate- terminals. Certain dendrons were designed with the potential to be further reactive following completion of synthesis. Amphiphilic cationic dendrons with lipidic chains emanating from the core were also developed to ascertain the effect of the lipidic factor in membrane diffusion and interaction. The synthesis and design of a novel didendron structure will be discussed in Chapter 5.

2.1 Polyamino acid branching units

Amino acids form a relatively stable amide bond and this was the chosen method to connect the branches of all the dendritic structures investigated in the thesis. Although amide bonds of a peptide are subject to attack by specific enzymes, studies on amide bonds, -CONH- or –CONR-, as drug-matrix linkages determined that these 'unnatural' bonds were poorly cleaved in the absence of a 'spacer' bridging group. Ferruti (1986) concluded that when a spacer was present, the amide bonds were cleaved to a small extent inside lysosomes but were stable in the gastro-intestinal tract and the blood stream. The reactivity of the amide bond has limited the use of

this type of linkage in the prodrug approach to drug therapy. Studies on biodegradable polymers have shown that the relative rate of hydrolysis of labile bonds under neutral conditions is polycarbonate > polyester > polyurethane > polyorthoester > polyamide (Sanders, 1991). All dendritic structures studied in the present work have been constructed using lysine as the branching unit.

2.2 Solid phase peptide synthesis

Solid phase peptide synthesis (SPPS) is based on sequential addition of α-amino and side-chain protected amino acid residues to an insoluble polymeric support (Fig. 2.1). Solid phase peptide synthetic techniques were originally elaborated by Merrifield (1963). The techniques involve the cleavage of the peptide from the polymeric support, followed by purification. The polymeric supports (resins) available are the aminoacyl (4-carboxamidomethyl)benzyl ester resin (PAM) (Mitchell *et al.*, 1978), and the *p*-methylbenzhydrylamine (*p*MBHA) resin (Matsueda and Stewart, 1981). Both are derivatives of a suspension copolymer of styrene (1% w/w) divinylbenzene. Cleavage with a strong acid from the PAM resin results in a peptide with a free alpha-carboxyl group, while cleavage from the *p*MBHA resin yields a peptide with an alpha-carboxamide group (Fig. 2.2). Both PAM and *p*MBHA resins were used to synthesise the dendritic molecules.

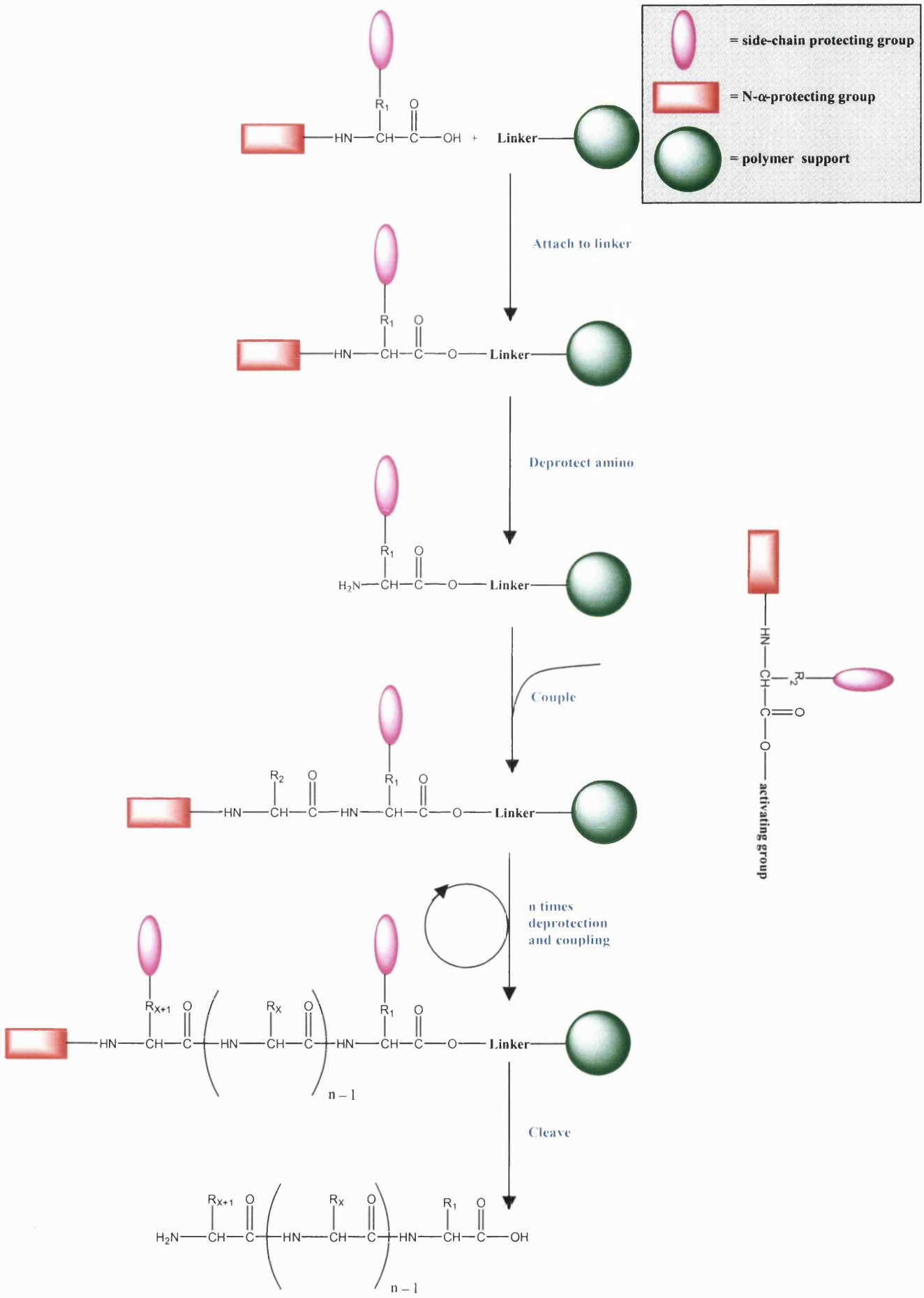

Fig. 2.1. *General scheme of solid phase peptide synthesis (SPPS).*

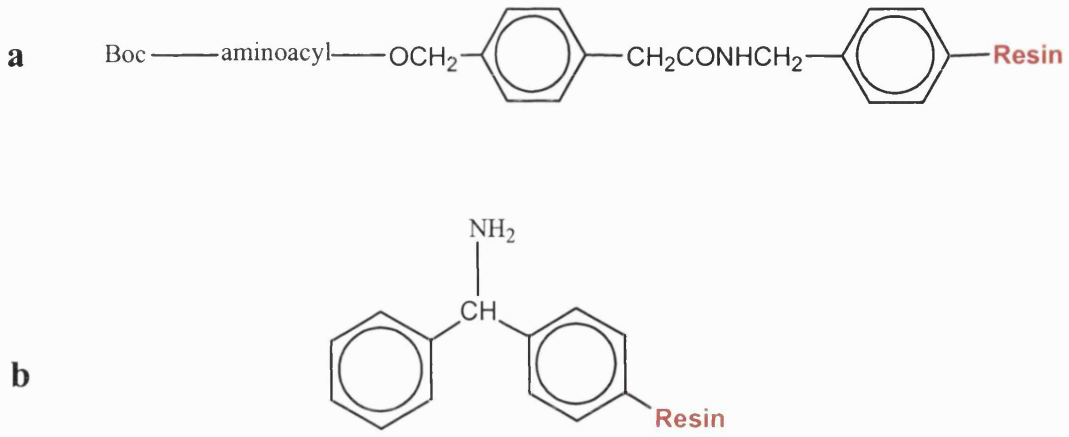

Fig. 2.2. *Resins for solid phase peptide synthesis;* ***a)*** *Boc-protected (4-carboxamidomethyl) benzyl ester resin;* ***b)*** *p-methylbenzhydrylamine resin.*

In solid phase peptide synthesis N-α-protection is provided by the acid-labile Boc group or the base-labile Fmoc group. Both protection groups will be discussed later in this chapter. After removal of this protecting group, the next protected amino acid is added using either a coupling reagent or a pre-activated protected amino acid derivative. The resulting peptide is attached to the resin, via a linker, through its C-terminus and may be cleaved to yield a peptide acid or amide, depending on the linking agent used. Side-chain protecting groups are often chosen so as to be cleaved simultaneously with detachment of the peptide from the resin.

Peptide synthesis can be carried out in a batch-wise or continuous flow manner. In the former technique, the peptidyl resin is contained in a filter reaction vessel and reagents added and removed under manual or computer control. In the continuous flow method, the resin is contained in a column through which reagents and solvents are pumped continuously, again under manual or automatic control. A range of manual, semi-automatic or automatic synthesisers are commercially available for

both batch-wise and continuous flow methods. Only the Fmoc strategy is fully compatible with the continuous flow method, which, depending on the instrument used, allows for real-time spectrophotometric monitoring of the progress of coupling and deprotection, although recently a similar method has been devised for Boc chemistry (Baru *et al.*, 1999)

2.3 A comparison of Boc and Fmoc chemistry

Cleavage of the Boc protecting group is achieved by trifluoroacetic acid (TFA) and the Fmoc protecting group by piperidine. Final cleavage of the peptidyl resin and side-chain deprotection requires strong acid, such as hydrogen fluoride (HF) or trifluoromethanesulfonic acid (TFMSA), in the case of Boc chemistry, and TFA in Fmoc chemistry.

The development of Fmoc SPPS arose out of concern that repetitive TFA acidolysis in Boc-group deprotection could lead to alteration of sensitive peptide bonds as well as acid catalysed side reactions. In Fmoc synthesis, the growing peptide is subjected to mild base treatment using piperidine during Fmoc-group deprotection and TFA is required only for the final cleavage and deprotection of the peptidyl resin (Fig. 2.3). By contrast, cleavage and deprotection in Boc chemistry requires the use of dangerous HF and expensive laboratory apparatus which is not always readily available to many researchers. All dendrons and dendrimers in the present work were synthesised using Boc chemistry.

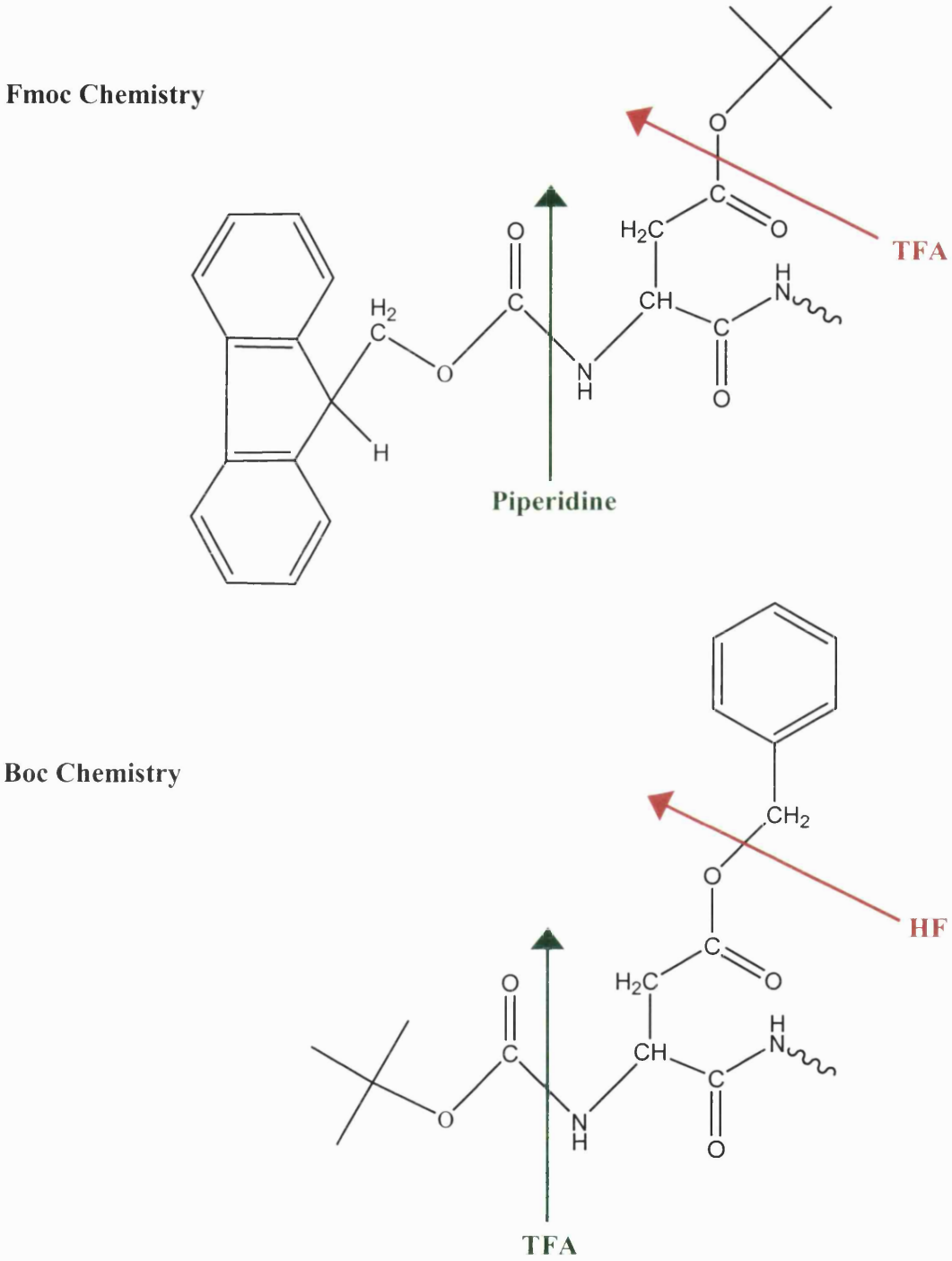

Fig. 2.3. *The protecting group strategies in SPPS for Fmoc and Boc chemistry.*

2.4 Peptide bond formation

The formation of an amide bond between two amino acids is an energy-requiring reaction. As carboxylic acids only react successfully with amines at elevated

temperatures, one of the groups that will produce the desired amide must be activated. Currently, activation of the carboxyl group remains the underlying principle of all coupling methods in use. Efficient and unambiguous peptide-bond formation requires chemical activation of the carboxyl component of the N-α-protected amino acid. Conversion of carboxylic acids to powerful acylating agents is achieved by substitution of the hydroxyl group for an electron withdrawing substituent which polarises the carbonyl group and renders its carbon atom sufficiently electrophilic to facilitate the nucleophilic attack by the amino group. A tetrahedral intermediate is formed and is stabilised by the elimination of the electron withdrawing substituent, which is usually a good leaving group.

The most widely used activating/coupling reagent is dicyclohexylcarbodiimide (DCC), introduced by Sheehan and Hess (1955), and it was chosen because of its simplicity and its appropriate choice for the apolar environment of polystyrene supports. Activation of the carbonyl group occurs through its addition to an N=C bond in the carbodiimide and it proceeds very rapidly. The principle limitation in using carbodiimides is the dehydration of asparagine and glutamine residues. The addition of 1-hydroxybenzotriazole (HOBt), (Bodanszky, 1984), to the reaction mixture will prevent dehydration and has the added benefit of acting as a catalyst (Mojsov *et al.*, 1980)

2.5 Coupling reagents

In situ activating reagents are widely accepted because they are easy to use, they give fast reactions, even between sterically hindered amino acids, and their use is generally free of side reactions. Most are based on phosphonium or aminium (formally known as uranium) salts which, in the presence of a tertiary base can

smoothly convert protected amino acids to a variety of activated species. The most commonly employed, benzotriazolyloxy-tris-(dimethylamino) phosphonium hexaflurophosphate (**BOP**); **PyBOP** (Martinez *et al.*, 1985); 2-(1H-Benzotriazole-1-yl)-1, 1, 3, 3-tetramethyluronium hexaflurophosphate (**HBTU**); and 2-(1H-Benzotriazole-1-yl)-1, 1, 3, 3-tetramethyluronium hexafluroborate (**TBTU**) (Knorr *et al.*, 1989) generate active HOBt esters, and these have found wide application in routine SPPS and solution synthesis for difficult couplings. Fig. 2.4 shows the chemical structures of the mentioned coupling reagents. Care must be taken when using aminium-based activation reagents. If an excess is used, relative to the carboxylic acid component, it can lead to capping of the amino terminus through guanidine formation (Gausepohl *et al.*, 1992). HBTU was chosen as the coupling reagent for the synthesis of all molecules in this thesis.

2.6 Peptide chain assembly

It is important to ensure that all solid phase supports are fully swollen before use (Merrifield, 1963). This is particularly important for polystyrene resins as their swelling properties vary widely from solvent to solvent. Once swollen in the appropriate solvent, the solid support provides an interpenetrating polymer network, within which synthesis occurs. Dichloromethane (DCM) and dimethylformamide (DMF) were used as the swelling solvents. The swollen bead provides pathways, via polymer chains randomly scattered throughout the interior of the bead, for chain assembly to occur. As the polymer is only lightly cross-linked, it is highly solvated and the covalently attached peptide chains are effectively in solution (Erickson and Merrifield, 1976).

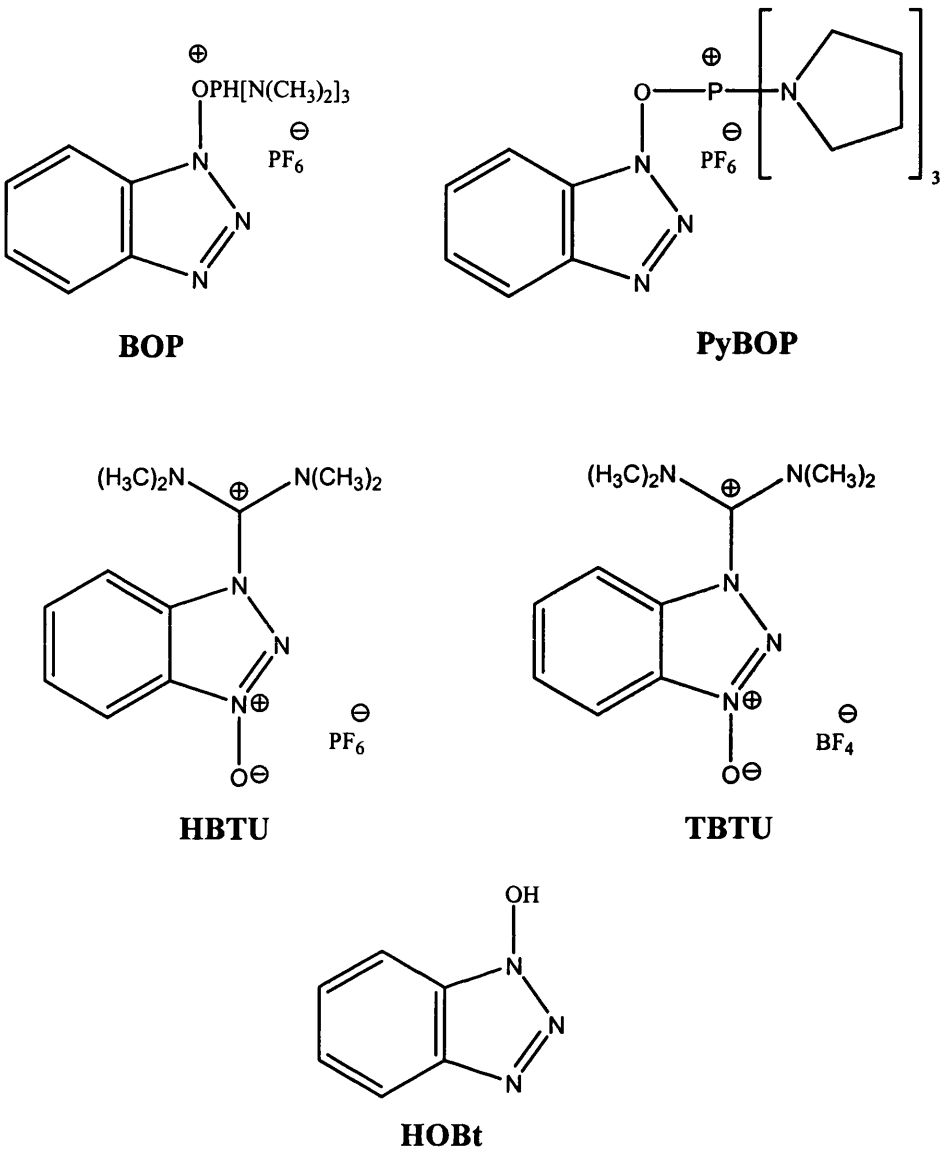

Fig. 2.4. Structures of some of the coupling reagents used in peptide synthesis.

Repetition of the following steps describes how the peptide chain is assembled prior to the final deprotection step. First the t-Boc protecting group is removed from the α-amino group of the resin-bound amino acid using 50-65% (v/v) TFA in DCM, this reaction is rapid ($t_{1/2}$ ~ 20 s) and goes essentially to completion within 15 min. The resulting trifluroacetate salt of the peptide resin is then neutralised with the hindered tertiary amine diisopropylethylamine (DIEA); the use of a highly purified tertiary amine helps minimise side reactions, especially those involving the aspartic acid side chain (Tam *et al.*, 1979).

2.7 Resin test to monitor efficiency of reactions

During the solid phase synthetic process purification is only achieved by filtration and washing of the resin-bound intermediates and therefore it is important to drive all reactions involved, in chain assembly, to completion. It is important to have accurate information of the progress at all steps of chain assembly so that the synthetic chemistry can be optimised. Monitoring the efficiency of chain assembly is of paramount importance to ensure the production of a molecule of high purity and known structure.

Resin tests are used to monitor the completion of reactions such as coupling or deprotection. The most widely used qualitative test for the presence or absence of free amino groups was devised by Kaiser (1970). This test, known as the 'Kaiser' or 'ninhydrin' test, is simple and quick; however it should be noted that some deprotected amino acids do not show the expected dark blue colour typical of free primary amino groups, (Fontenot *et al.*, 1991), (e.g. serine, asparagine, aspartic acid) and that proline, being a secondary amino acid, does not yield a positive reaction.
The following three solutions were prepared;

Solution 1: 19 g of liquefied phenol (99.5%) was dissolved, with the aid of heat, in 6 ml absolute ethanol.

Solution 2: 0.5 ml aqueous solution of potassium cyanide (0.001 M) was added to 24.5 ml pyridine (99%).

Solution 3: 1.25 g ninhydrin (99%) was dissolved in 25 ml ethanol (95%).

Following deprotection of the amines with TFA and washing with DMF, a small amount of the peptide-resin sample was washed five times with DCM/MeOH (50:50

ratios) and transferred to a small glass tube. Two drops of solution 1, four drops of solution 2 and two drops of solution 3 were added to the sample and the tube was placed in an oil bath at 100°C for 5 min. Next 5 ml 60% ethanol is added to the contents of the tube and a dark blue coloured solution indicates the presence of free primary amino groups. Following the coupling of Boc-protected amino acids, the sampling method is similar, but a clear solution as an end result indicates that all free amino groups have undergone coupling.

2.8 Boc resin cleavage and deprotection

The most popular reagent for cleavage of peptides from Boc-based resins is anhydrous HF. Of all the cleavage procedures, HF appears to be the most versatile and least harmful to a wide variety of peptides synthesised on Boc-based resins (Stewart and Young, 1984). The major drawback of this procedure remains its highly toxic and reactive nature which necessitates the use of expensive HF-resistant fume hoods and cleavage apparatus. Other strong acids such as TFMSA and trimethylsilyl trifluoromethanesulfonate (TMSOTf) can be used as alternatives to HF for cleavage from PAM and MBHA resins. Although less reactive than HF, it should be noted however, that both TFMSA and TMSOTf are extremely corrosive and great care must be taken when using either.

HF has many desirable characteristics for deprotection of synthetic peptides (Sakakibara, 1971), treatment with HF results in the generation of highly reactive carbonium species, since acidolysis proceeds by an S_N1 reaction mechanism (Tam *et al.*, 1983). To prevent the carbonium by-products alkylating side chains of the peptide, scavengers such as p-cresol, p-thiocresol and anisole are added to the reaction mixture to mop up these reactive species.

2.8.1 HF cleavage

The HF apparatus consists of a network of tubes with numerous taps which control and maintain the internal air pressure as well as the entry and exit of HF. The main components connected to the network of tubing are: the HF cylinder, a vacuum pump, a mercury manometer and a calcium oxide trap. The N-deprotected resin was dried, using a vacuum, and placed in the HF reaction vessel with an appropriate scavenger and a teflon coated stirrer bar. The vessel was attached to the HF apparatus and cooled using liquid nitrogen. Using the vacuum pump, the air pressure inside the apparatus was adjusted until a constant reading of 280-300 mmHg was obtained and the vacuum was sealed using the appropriate tap. The next step was to control the flow of HF into the reaction vessel by visually monitoring its collection (10ml per gram of resin). When a sufficient amount of HF was collected, its entry in to the vessel was cut off whilst monitoring the manometer to ensure there was no mercury suck-back. The reaction vessel was positioned in a beaker of ice water and left to stir using a magnetic stirrer for 60-90 min to cleave the resin from the molecule. Following cleavage of the resin, the apparatus was adjusted to allow the removal of traces of HF and left for 30 min. The crude dendritic peptide was isolated by precipitation using cold ether, dissolved in 90% acetic acid and lyophilised. HF cleavage was the method of choice for the cleavage of all molecules synthesised and discussed in the present work. The methods were devised by our research group to accommodate a clean and productive cleavage using the apparatus available.

2.8.2 TMSOTf cleavage

TMSOTf cleavage was tried as an alternative to HF (Yajima *et al.*, 1988). 1g of dried resin was placed in a round bottom flask containing a stirring bar. The flask was cooled to 0°C using an ice bath and to this the cooled cleavage mixture (1.95 ml

TMSOTf, 6.90 ml TFA, 1.2 ml m-cresol) was added. The temperature was maintained at 0°C for 2 h with constant mixing to cleave the resin. The resin was removed by filtration under reduced pressure and washed twice with clean TFA. The filtrates were combined and an 8-10 fold volume of cold ether was added drop-wise. The peptide was isolated and dissolved in 90% acetic acid and lyophilised. Although mass spectrometry showed the presence of the desired molecule, this method was abandoned as HF cleavage produced a more crude and higher yielding molecule.

2.9 Dendrimer and dendron synthesis

For the synthesis of all the dendritic compounds mentioned, a procedure using 3 times excess reagent for each coupling step has been used to ensure completion of each reaction. The excess amounts have been calculated according to the molar capacities of the resins used. The HBTU solution, used for the synthesis of all compounds, contained 19.5 g HBTU in 100 ml DMF and the ninhydrin test was used to monitor each coupling and deprotection step. The sources for all chemicals and reagents used can be found in Appendix 1.

2.9.1 Lipophilic dendrons with polycationic surfaces

METHOD A

We designed and synthesised lipid-lysine dendrons with polycationic and neutral surfaces. Such lipid-lysine dendrons were originally designed and synthesised, in our laboratories, by Sakthivel *et al.* (1998). Three lipidic chains were attached on solid support (*p*MBHA resin, capacity = 0.67 mmol/g) using α-aminotetradecanoic acid and glycine was used as a spacer between the solid support and lysine building blocks. The subsequent generations were built using lysine units which were Boc-protected at both α- and ϵ-amino functions, Boc-Lys (Boc)-OH, resulting in two

couplings per lysine unit. The first level of coupling produced two terminal amino groups; the 2nd, 3rd, 4th and 5th levels of coupling produced 4, 8, 16 and 32 terminal amino groups respectively. Some of the dendrons had their free terminal amino groups acetylated to produce the range of molecules **1a-f** (see Appendices 2 and 3 for characterisation data).

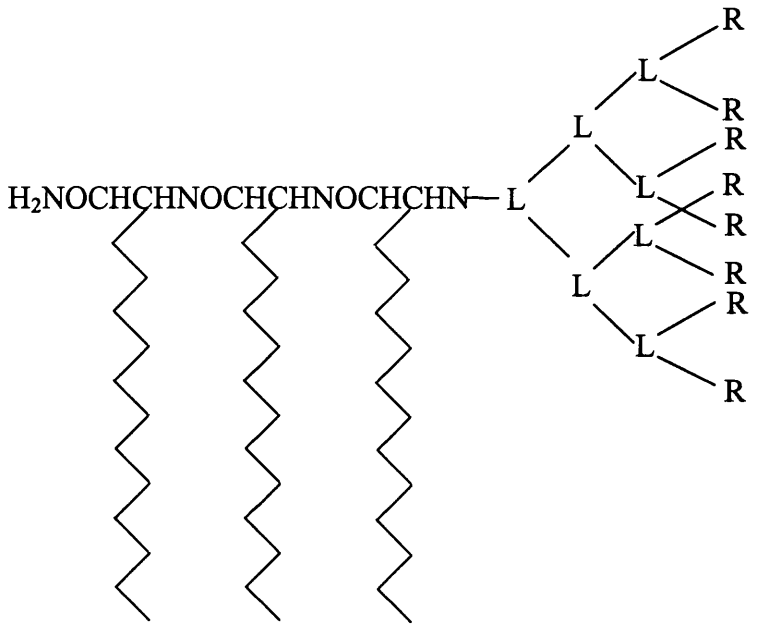

MOLECULE	R	TERMINAL GROUPS	M_R
1a	NH_2	8	1588
1b	L-$(NH_2)_2$	16	2612
1c	L-[L-$(NH_2)_2$]$_2$	32	4660
1d	$NHCOCH_3$	8	1924
1e	L-$(NHCOCH_3)_2$	16	3284
1f	L-[L-$(NHCOCH_3)_2$]$_2$	32	6004

The range of lipophilic dendrons synthesised, where L = lysine.

All couplings were performed using HBTU and DIEA (the molar quantities used were doubled for each generation of growth with Boc-Lys (Boc)-OH) and acetylation was completed using the same reagents and ethyl acetate. After cleavage (1g resin peptide, 10 ml HF, 1.5 h at -5°C) from the resin, the dendrons were isolated and dissolved in 90% acetic acid and lyophilised. The presence of the desired molecules was confirmed by mass spectroscopy (Appendix 2). The compounds were purified

by reverse-phase high performance liquid chromatography (RP-HPLC) using acetonitrile and water as solvents. If acetic acid was detected, compounds were solubilised in excess water and lyophilised further. All six compounds were obtained in yields greater than 80% and were water-soluble (see Appendix 6). A schematic diagram outlining the synthesis of molecules 1a-c is shown in Fig. 2.5.

2.9.2 Polylysine dendrons with reactive glycine tail

METHOD B

We designed and synthesised polylysine dendrons, incorporating glycine tails of varying length, with polycationic and neutral surfaces. The glycine chains, of 2 to 5 molecules were attached on solid support (Boc-Gly-PAM resin, capacity = 0.76 mmol/g). PAM resin was used as cleavage of the solid support would leave a COOH group at the end of the tail. The remainder of the dendrons were built using lysine building blocks. The subsequent generations were built using lysine units which were Boc-protected at both α- and ε-amino functions, Boc-Lys (Boc)-OH, resulting in two couplings per lysine unit. The first level of coupling produced two terminal amino groups; the 2^{nd}, 3^{rd}, 4^{th}, 5^{th}, 6^{th} and 7^{th} levels of coupling produced 4, 8, 16, 32, 64 and 128 terminal amino groups respectively. Some of the dendrons had their free terminal amino groups acetylated to produce the range of molecules **2a-n** (see Appendices 2 and 3 for characterisation data).

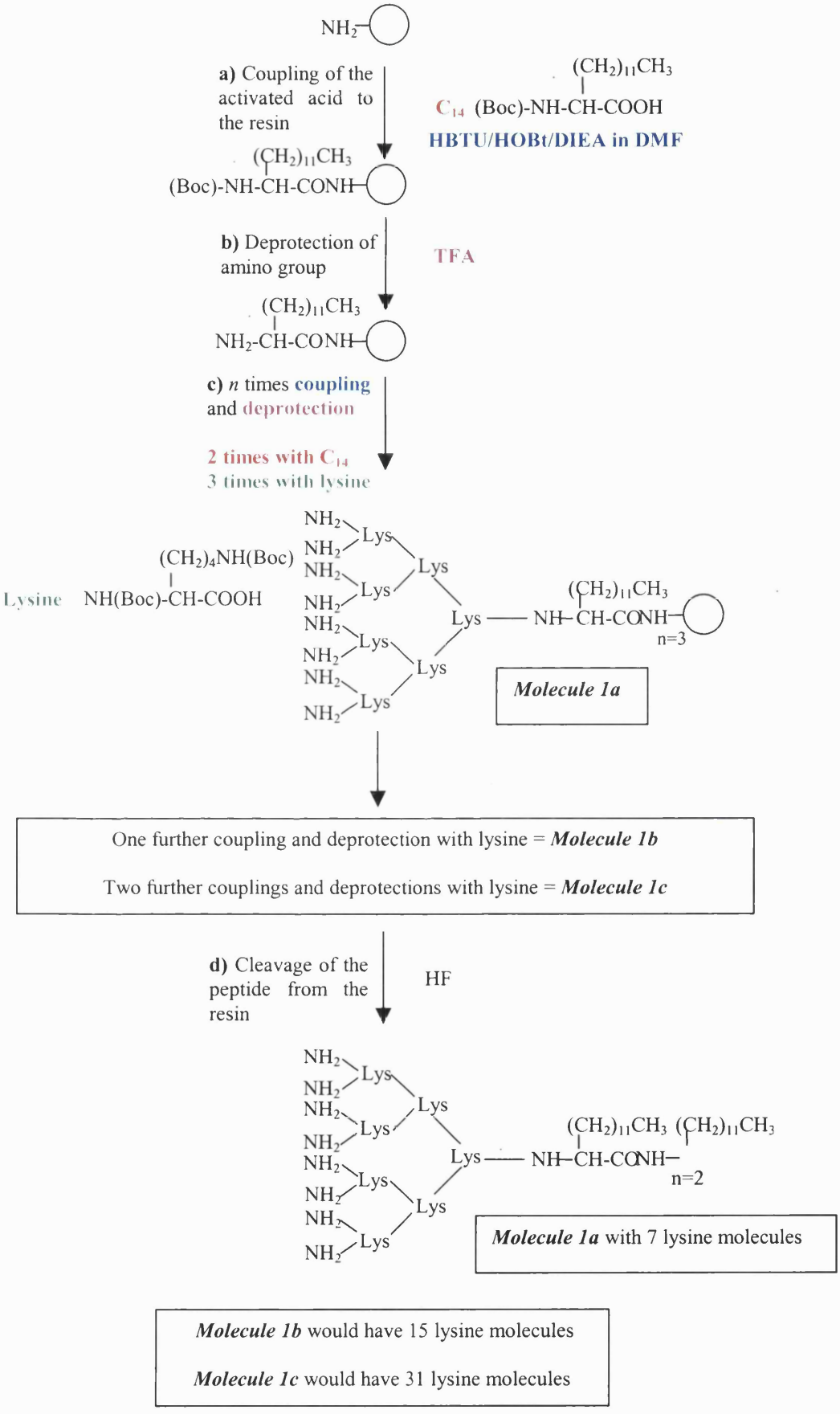

Fig. 2.5. *Schematic diagram representing the synthetic route for molecules 1a-c.*

All couplings were performed using HBTU and DIEA (the molar quantities used were doubled for each generation of growth with Boc-Lys (Boc)-OH) and acetylation was completed using the same reagents and ethyl acetate. After cleavage (1g resin peptide, 10 ml HF, 1.5 h at -5°C) from the resin, the dendrons were isolated and dissolved in 50% acetic acid and lyophilised. The presence of the desired molecules was confirmed by mass spectroscopy. The compounds were purified by reverse-phase high performance liquid chromatography (RP-HPLC) using acetonitrile and water as solvents. All fourteen compounds were obtained in yields greater than 71%. When synthesis of compounds with more than 5 glycine molecules in the tail was attempted, the resin beads aggregated and resulted in poor coupling efficiency. Molecules 2a-2m were water soluble, molecule 2n showed limited solubility (see Appendix 6).

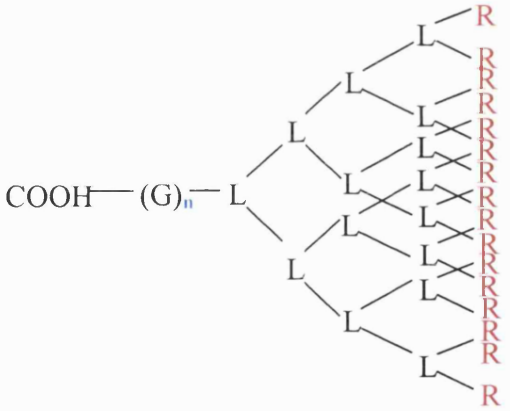

MOLECULE	N	R	TERMINAL GROUPS	M_R
2a	2	NH_2	16	2052
2b	2	$NHCOCH_3$	16	2724
2c	2	L-$(NH_2)_2$	32	4100
2d	2	L-$(NHCOCH_3)_2$	32	5444
2e	2	L-[L-$(NH_2)_2]_2$	64	8196
2f	2	L-[L-$(NHCOCH_3)_2]_2$	64	10884
2g	3	L-$(NH_2)_2$	32	4157
2h	3	L-$(NHCOCH_3)_2$	32	5501
2i	3	L-[L-$(NH_2)_2]_2$	64	8253
2j	3	L-[L-$(NHCOCH_3)_2]_2$	64	10941
2k	5	NH_2	16	2223
2l	5	$NHCOCH_3$	16	2895
2m	5	L-(L-[L-$(NH_2)_2]_2)_2$	128	16559
2n	5	L-(L-[L-$(NHCOCH_3)_2]_2)_2$	128	21935

The range of glycine-tailed dendrons synthesised, where L = lysine and G = glycine.

2.9.3 Preparation of radiolabelled molecules

To enable the quantification of dendrons in liposome interaction/adsorption studies (Chapter 3) and for diffusion/albumin-interaction studies (Chapter 4), some molecules were radiolabelled with tritium. Tritiated L-lysine, (4,5-^{3}H) was purchased from Moravek Biochemicals, California, USA. The lysine was obtained as an aqueous solution of 5.0 mCi/5 ml (3.7 μg/ml, 37 MBq/ml) had to be Boc-protected. 2g of lysine was mixed with radiolabelled (hot) lysine (2.5 ml) to give a total of 13.7 mmol. This was suspended in a 2:3 mixture of *tert*-butyl alcohol/water (50 ml) and 8 M aqueous NaOH was added drop-wise to adjust the pH=13. Di-*tert*-butyl dicarbonate (10 g, 45.8 mmol) in *tert*-butyl alcohol (20 ml) was added at room temperature. The pH value was adjusted to 11-12 and the reaction mixture was stirred overnight. Next the reaction mixture was diluted with water (25 ml) and solid citric acid was added to adjust the pH=3. The oil was then extracted with ethyl acetate (3 x 75 ml). After drying (anhydrous $MgSO_4$), the organic layer was evaporated. The residue was triturated with cold acetonitrile and the product was filtered and dried to yield 2.349 g Boc-Lys (Boc)-OH (M_r = 346.4). During the synthesis of radiolabelled compounds hot Boc-Lys (Boc)-OH was mixed with cold Boc-Lys (Boc)-OH to bulk up reaction constituents.

2.9.4 Mass spectrometry

Mass spectra were run on a VG analytical ZAB-SE instrument, using the fast-atom bombardment (FAB) technique. 20 kV Cs^+ ion bombardment was used, with 2 μl of an appropriate matrix consisting of solution of either 3-nitrobenzyl alcohol in methanol, or thioglycerol with NaI in methanol. Mass spectra were also run on a Kratos Analytical Kompact MALDI 3 Matrix Assisted Laser Desorption Time of

Flight Mass Spectrometer operating in linear mode using a 337 nm laser. Mass spectra data is shown in Appendix 2.

2.9.5 High performance liquid chromatography (HPLC)

HPLC equipment consisted of an Applied Biosystems 400 Solvent Delivery System and an Applied Biosystems 1480 injector Mixer (Applied Biosystems, Cheshire, UK). Solvent gradients (0 min = 100% water → 20 min = 100% acetonitrile) were affected by two microprocessor-controlled Gilson 302 single piston pumps. Compounds were detected with an Applied Biosystems Programmable Absorbance Detector and chromatographs were recorded with LKB 2210 single channel chart recorder (Pharmacia Biotech Ltd, Herts, UK). All solvents were of HPLC grade and filtered under vacuum through a 25 μm filter, prior to column application. Analytical separations were carried out using a Beckman Ultrasphere Octyl column (5 μm, 4.6 mm x 250 mm) with a guard column (5 μm, 4.6 mm x 45 mm), obtained from Beckman Instruments, Bucks, UK. Semipreparative separations were carried out using a C_{18} Hypersil ODS column (10 μm, 10 mm x 250 mm) obtained from FSA Chromatography, Leicestershire, UK. Preparative separations were carried out using TSK-Gel preparative C_{18} column (20 mm x 300 mm) obtained from HPLC Technology, Macclesfield, UK. The C_{18} column is very hydrophobic, resulting in the elution of more hydrophilic molecules first. HPLC data is shown in Appendix 3.

CHAPTER THREE

INTERACTION OF CATIONIC DENDRONS WITH LIPOSOMES

3.1 INTRODUCTION

3.1.1 Liposomes

Liposomes, or phospholipid vesicles, are self-assembled colloidal particles that occur naturally and can be prepared synthetically (Gregoriadis and Ryman, 1972), as shown by Bangham and his co-workers (1965) in the mid-1960s. Liposomes are composed of biocompatible and biodegradable material, and they consist of an aqueous volume entrapped by one or more bilayers of natural and/or synthetic lipids (Fig. 3.1). Molecules with widely varying lipophilicities can be encapsulated in liposomes, either in the phospholipid bilayer, in the entrapped aqueous volume or at the bilayer interface. Fig. 3.1 also represents how liposomes can be classified on the basis of their size and number of bilayers. Liposome size can vary from very small (0.025 μm) to large (5 μm) vesicles and may have single or multiple bilayer membranes. They can be placed into one of three categories: (i) multilamellar vesicles (MLV); (ii) large unilamellar vesicles (LUV); and (iii) small unilamellar vesicles (SUV).

At first, they were used to study biological membranes; several practical applications, most notably in drug delivery, emerged in the 1970s (Lasic and Papahadjopoulos, 1995). Today, they are a very useful model, reagent and tool in various scientific disciplines, including mathematics and theoretical physics

(topology of two-dimensional surfaces floating in a three dimensional continuum), biophysics (properties of cell membranes and channels), chemistry (catalysis, energy conversion, photosynthesis), colloid science (stability, thermodynamics of finite systems), biochemistry (function of membrane proteins) and biology (excretion, cell function, trafficking and signalling, gene delivery and function) (Lasic and Papahadjopoulos, 1995).

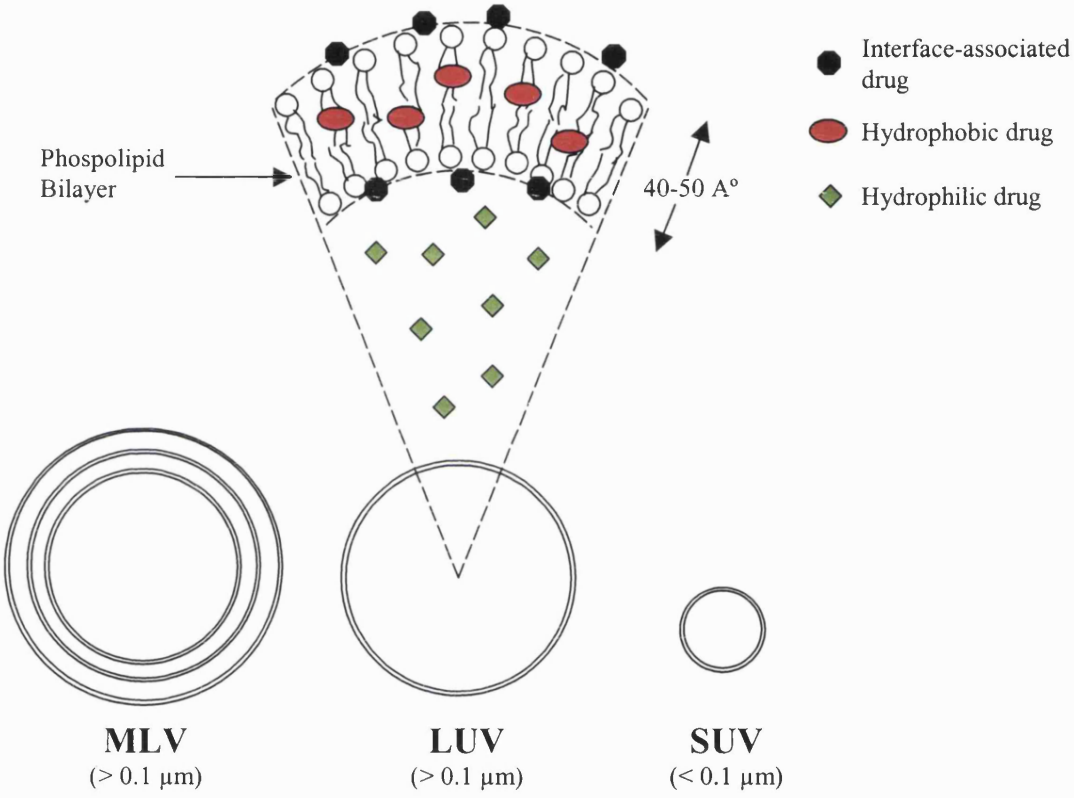

Fig. 3.1. *The different types of liposomes characterised according to size and number of lamellae.*

On the applied side, several products rely on their colloidal, chemical, microencapsulating and surface properties; these products range from drug-dosage forms (antifungals, cytotoxic agents, vaccines), cosmetic formulations (skin-care products, shampoos) to diagnostics and various uses in the food industry. However, it seems that drug-delivery applications are now the most widely investigated area of their practical applications (Duncan, 1997). Liposomes offer several advantages over

other delivery systems including biocompatibility, capacity for self-assembly, and a wide range of physical properties that can be modified to control their biological properties. Liposomes were introduced as drug-delivery vehicles in the 1970s. Early results were, however, rather disappointing, owing mainly to their colloidal and biological instability, and their inefficient and unstable encapsulation of drug molecules. Their utility was improved following basic research that increased our understanding of their stability and interaction characteristics (Lasic and Papahadjopoulos, 1995). In parallel, several pharmaceutical enterprises were founded that survived the decline in the commercial appreciation of liposomes in the 1980s and early 1990s and, eventually, achieved commercial successes in gaining regulatory approvals while others are well into clinical development in several countries.

Liposome preparations in current use have improved physical properties to enhance their therapeutic benefits. Thus, formulation parameters including lipid composition, vesicle size (Gabizon *et al.*, 1990), lipid membrane fluidity (Banno *et al.*, 1986), surface charge (Lee *et al.*, 1992), cholesterol content (Gregoriadis and Davis, 1979), and steric stabilisation (Emanuel *et al.*, 1996, Mori *et al.*, 1991), have been optimised to extend the therapeutic index of liposomal drugs over that of the corresponding conventional formulations. While these approaches have resulted in therapeutic gains, further improvements are desirable and could lead to additional clinical advantages. Site-directing moieties and ligands incorporated into the liposome membrane surface therefore have been investigated intensely in an effort to enhance further the selectivity of liposomal drug delivery.

3.1.2 Interaction between dendritic structures and liposomes

Until recently the interaction between dendrimers or dendrons and vesicular structures has not been investigated. The ability to control the permeability of biological membranes is an area of great current interest. There is much focus on the use of carriers which facilitate the transport of DNA and pharmaceutical compounds into target cells. Dendritic polymers have been shown to function effectively as transfection agents in tissue-culture cells. These include poly(amidoamine) (PAMAM) dendrimers, which have been studied for DNA transfection (Kukowska-Latallo *et al.*, 1996, 1998, Tang *et al.*, 1996), and also cationic dendrons with lipid character (Sakthivel *et al.*, 1998). The interaction of cationic dendritic molecules with the lipid bilayer membrane may be an important step in the transfection process, particularly since the plasma membranes of mammalian cells carry a net negative charge. Moreover, at some point in the transfection process a lipid bilayer membrane either the plasma membrane or an endosomal membrane must be breached. The mechanisms by which polymeric transfection agents cause this membrane disruption are not understood, but may involve interactions with anionic lipids, nonbilayer lipids, and/or osmotropic effects (Haensler and Szoka, 1993). Fukushima et al. (1981) studied the binding of amphiphilic peptides to unilamellar vesicles and Zhang and Smith (2000) investigated the interaction between PAMAM dendrimers and anionic vesicles.

In this chapter, the discussion will focus on studies involving the interaction of cationic dendrons with lipid character and free amine groups, and charged and neutral liposomes. The compositions of the vesicles used do not mimic biological bilayer membranes but are used to investigate the effects that dendron interactions may have. These dendrons, although soluble in water, have three lipidic chains to

improve transmembrane transport potential. They can be either entrapped inside the aqueous phase of the liposomes, entrapped in the lipid bilayer, adsorbed onto the surface or co-exist between two of the phases mentioned (Fig. 3.2).

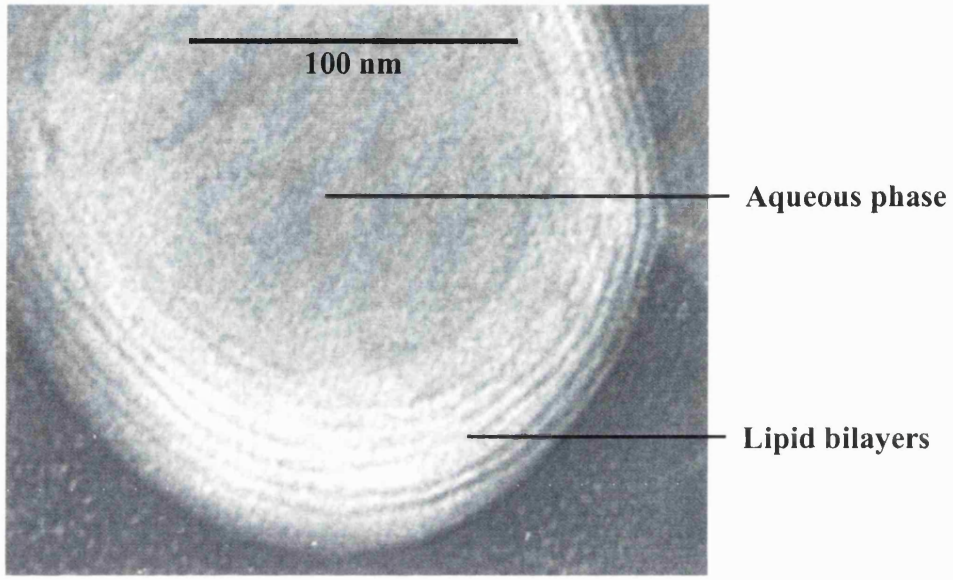

Fig. 3.2. *A transmission electron micrograph of a liposome showing the aqueous phase and the multi-lamella structure formed by the lipid bilayers.*

3.2 MATERIALS AND METHODS

3.2.1 Synthesis of the cationic dendrons

The amphipathic dendrons having three lipidic 14-carbon chains coupled to dendritic lysine head groups with 8, 16 or 32 free terminal amino groups (Fig. 3.3) were synthesised by solid phase peptide synthesis. This series of dendrons were radiolabelled with tritium and were water-soluble. The methods are described in detail in Chapter 2 (**1a-c**).

3.2.2 Preparation of liposomes

The lipids used for the preparation of liposomes were obtained from Sigma Chemical Company, UK. The four lipids (Fig. 3.4) were distearoyl phosphatidylcholine (DSPC), cholesterol (CHOL), phosphatidylglycerol (PG), and dimethylaminoethyl carbamate cholesterol (DC-CHOL). Liposomes with different compositions containing DSPC/CHOL (ratio 1:1 which were neutral), DSPC/CHOL/PG (ratio 1:1:0.1 which were negatively charged), and DSPC/CHOL/DC-CHOL (ratio 1:1:0.1 which were positively charged), were prepared according to the dehydration-rehydration vesicle (DRV) method (Gregoriadis, 1998). Regarding the composition ratios above with respect to the method outlined below; 1=32 μmol and 0.1=3.2 μmol.

The lipid compositions were dissolved in chloroform and the chloroform was evaporated using a rotary evaporator at 37°C (Buchi Rotavapor-R). The lipid film was flushed with N_2, hydrated and left at 25°C for 2 h to produce a milky suspension of MLVs. This suspension was sonicated using a titanium probe (Sanyo Soniprep 150 Sonicator) to produce an opaque to clear suspension of SUVs. This was obtained using four sonication cycles, each lasting 30 s with 30-s rest intervals in between.

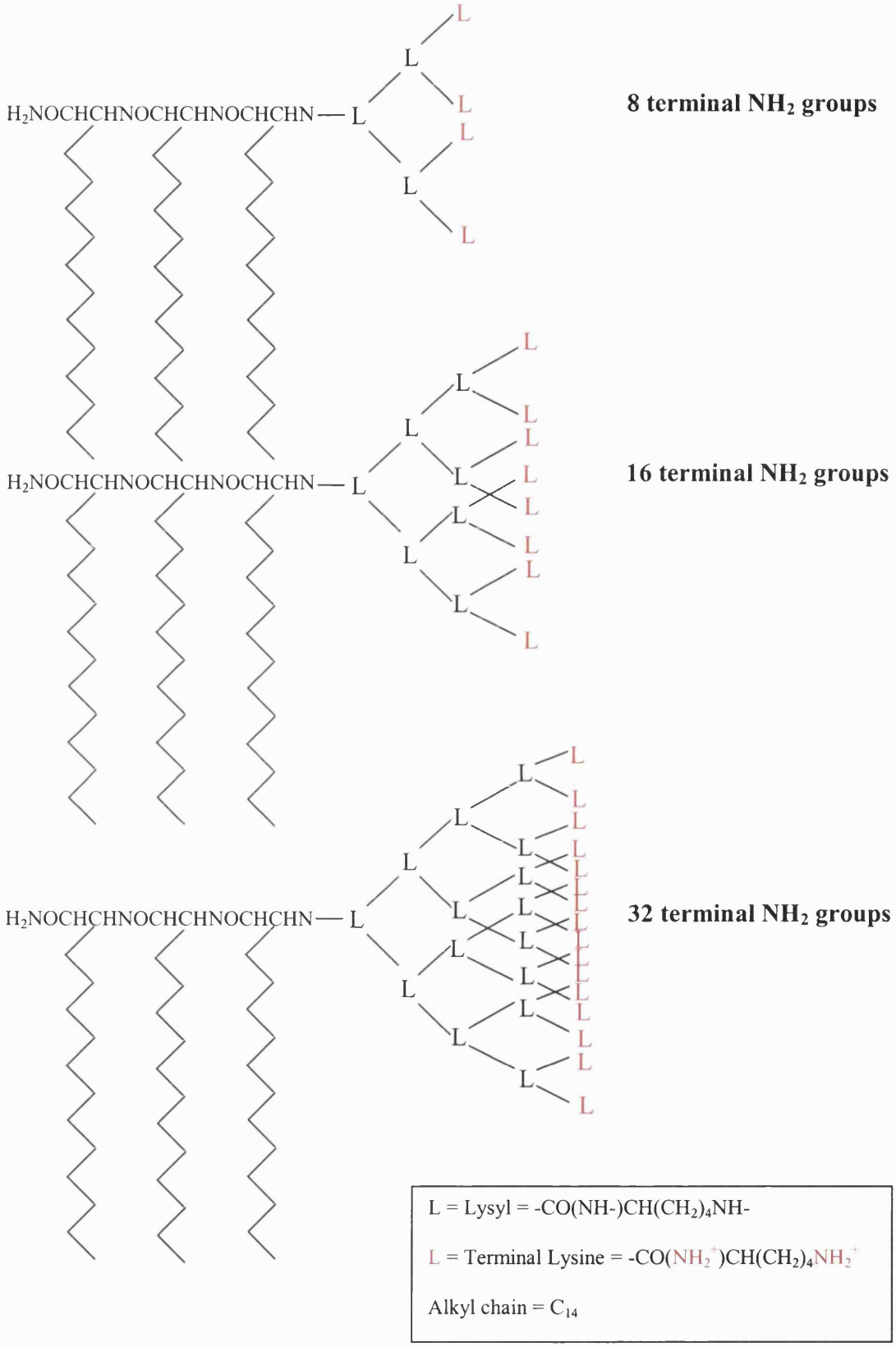

Fig. 3.3. *Schematic diagram of the 8, 16 and 32 amino group cationic dendrons which were studied.*

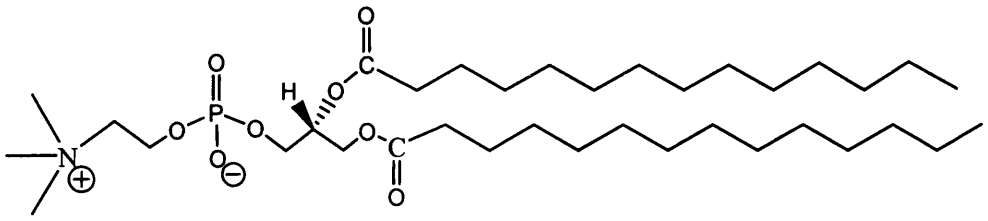

Distearoyl phosphatidylcholine (DSPC)

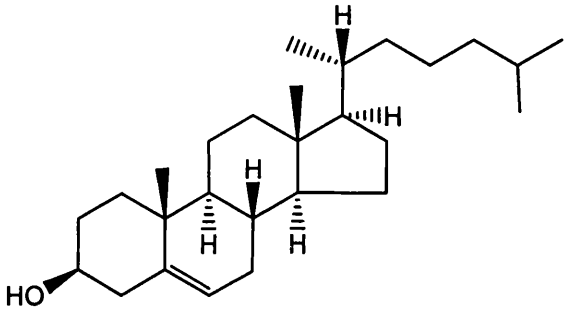

Cholesterol (CHOL)

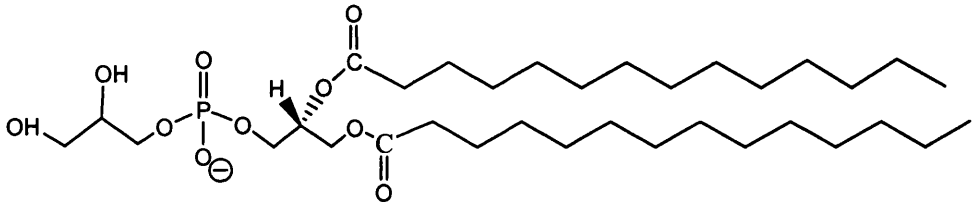

Phosphatidylglycerol (PG) (anionic)

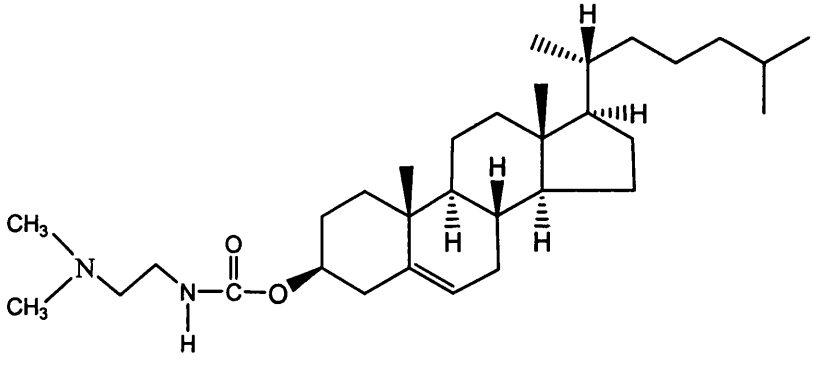

Dimethylaminoethyl carbamate cholesterol (DC-CHOL) (cationic)

Fig. 3.4. Molecular structures of the four lipids used to formulate the different liposomes.

The SUV suspension was left at 25°C for 2 h and then centrifuged at 2500 x *g* for 10min (Heraeus Sepatech Megafuge 1.0), to remove any large foreign matter (probe particles). An aqueous solution containing 2mg of radiolabelled dendron was added (the addition of dendron was omitted for the preparation of control liposomes). This mixture was frozen and freeze-dried (Edwards Micro Modulyo Freeze Dryer) for 24h to yield an amorphous powder. Following the freeze-drying process the powder was rehydrated; 0.1 ml H_2O was added and swirled vigorously to ensure complete dissolution of the powder and left to stand at 25°C for 30 min; this process was repeated with 0.1 ml H_2O and, 30 min later, with 0.8 ml phosphate buffer solution (PBS, pH 7.4) and allowed to stand for a further 30 min to yield DRVs. The DRV suspension was centrifuged at 25,000 rpm for 30 min at 4°C, (Sorvall Combi Plus Ultracentrifuge). The pellet obtained (dendron-containing DRV) was suspended in PBS and centrifuged again to remove the remainder of non-entrapped/interacted dendron. The final pellet was suspended in 3 ml PBS and used for further studies. Radioactivity was measured using a scintillation counter to determine the encapsulation efficiency of the DRVs. Radioactivity of dendron-containing solutions, which were discarded, was also measured to account for loss of dendrons during experimental procedures.

3.2.3 Measurement of radioactivity

All dendrons were radiolabelled with tritium (^3H) (see section 2.10.3). For each individual sample, 100 µl was placed in a scintillation tube and made up to 5 ml with Wallac OptiPhase HiSafe scintillation cocktail and placed in a Beckman LS 6500 multi-purpose scintillation counter. Counting continued for 3 min, each sample was measured three times, to calculate CPM.

3.2.4 Measurement of vesicle size and zeta potential

The vesicle size of DRVs was measured using a Mastersizer X (Malvern Instruments, Malvern, UK) using a magnetically stirred sample holder, with He-Ne laser. The apparent diameters of SUVs (<1 μm) were measured using the Zetasizer 3000 (Malvern Instruments, Malvern, UK). Samples were transferred to a cuvette and placed in a cell. To measure zeta potential 20 μl was diluted to 10 ml with double deionised water. Samples were placed and analysed immediately in the Zetasizer 3000 with He-Ne laser; the angle of measurement was 90 degrees. Five repeat measurements were carried out at 30 s intervals.

3.2.5 Adsorption studies

To determine the amount of dendron associated with the surface of liposomes, dendron-free liposomes were prepared using the DRV method. The process, which was carried out for all three liposome formulations, is described in detail in Scheme 3.1.

For these studies, the dendrons were added to pre-formed DRV liposomes to evaluate dendron interaction with the outer membranes of the liposomes. The changes in zeta potential and size of the liposomes were also measured and could be correlated with the number of terminal amine groups of the dendrons. The total amount of radioactivity of the dendron solutions (0.33 mg) was measured before addition to the 1 ml DRV suspensions for all three liposome formulations. During the final step in Scheme 3.1 (centrifugation of each sample twice at 25,000 rpm, 30 min, 4°C), dendrons not associated with the liposome membranes were collected in the supernatant and quantified.

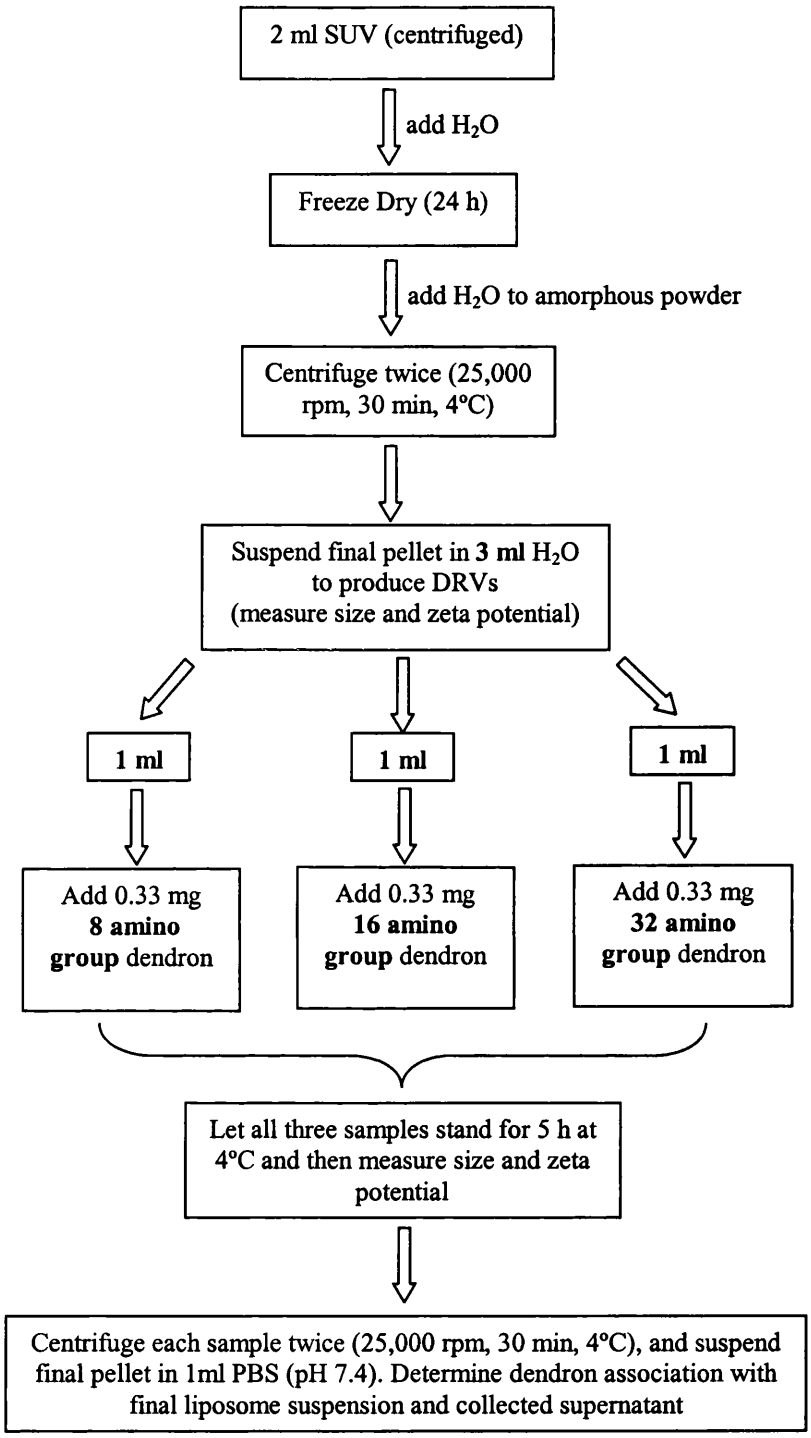

Scheme 3.1. *The process carried out for each liposome formulation to determine the extent of dendron adsorption to the liposomes.*

3.2.6 Membrane disruption assay

Riboflavin-5'-phosphate sodium salt dehydrate (riboflavin), was obtained from Avocado Research Chemicals. 2 mg riboflavin was entrapped in liposomes using the DRV method as above using all three liposome formulations. The liposomes were sonicated to produce SUVs with an average diameter 500 nm. Due to the photosensitivity and thermosensitivity of riboflavin, all samples containing riboflavin were foil wrapped and kept cold (4°C). The three dendrons were added in solution, to the various liposome samples and the release of riboflavin was monitored over 24 h in the dark at 25°C. Control liposomes were also prepared. Entrapment and release of riboflavin was determined using a fluorimetric assay. Riboflavin, in the aqueous phase, was measured fluorimetrically at excitation and emission wavelengths 445 and 520 nm respectively (Loukas *et al.*, 1995, 1995a), using a Perkin Elmer LS-3 fluorescence spectrometer. Emission intensities were determined for standard riboflavin solutions and a calibration plot was constructed. The emission intensity corresponding to 100% release was determined by the addition of Triton X-100 (Sigma Chemical Co.).

3.2.7 Micrograph images

Light micrographs were taken using the Nikon Microphot-FXA light microscope which was attached to a Sony UP-860CE video graphic printer. Cryo-Transmission electron microscopy (TEM) was performed using a Philips 201L transmission electron microscope at 100 kV with a 1% aqueous phosphotungstic stain (see Appendix 5).

3.3 RESULTS AND DISCUSSION

Note: In the respective figures, the distribution of data values is represented by showing a single data point, representing the **mean** *value of the data, and the error bars represent the overall* **distribution** *of the data.*

The structures (confirmed by mass spectrometry; Appendix 2) of the dendrons with 8 to 32 amino groups are given in Fig. 3.3. Table 3.1 summarises some characteristics of the three dendrons studied, where the apparent hydrodynamic diameters were calculated using molecular simulation software (Quanta 96 and CHARMm).

Table 3.1. *Showing some physical characteristics of the three dendrons studied.*

Number of Amino Groups	Apparent Diameter (nm)	Molecular Weight
8	2.1	1588
16	2.4	2612
32	2.8	4660

3.3.1 Dendron entrapment/interaction during the DRV method

The entrapment/interaction efficiency of the three dendrons studied ranged from 88% to 98% (Fig 3.5). The interaction studies carried out between dendrons and liposomes were performed with neutral, anionic and cationic liposomes.

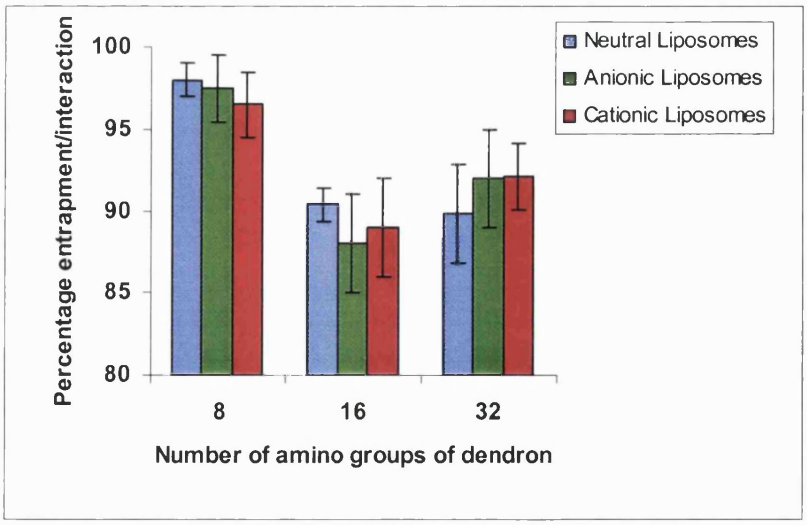

Fig. 3.5. *Dendron entrapment/interaction efficiency of neutral, anionic and cationic liposomes, expressed as a percentage of the total amount of dendron added, as a function also of the dendron structure.*

The smallest dendron, with 8 amino groups, showed the highest percentage of entrapment/interaction with all three liposome formulations (96-98%). Anionic liposomes formulated with DSPC/CHOL/PG showed large increases in apparent diameter with increasing number of amino groups of the dendrons used (see Fig. 3.6).

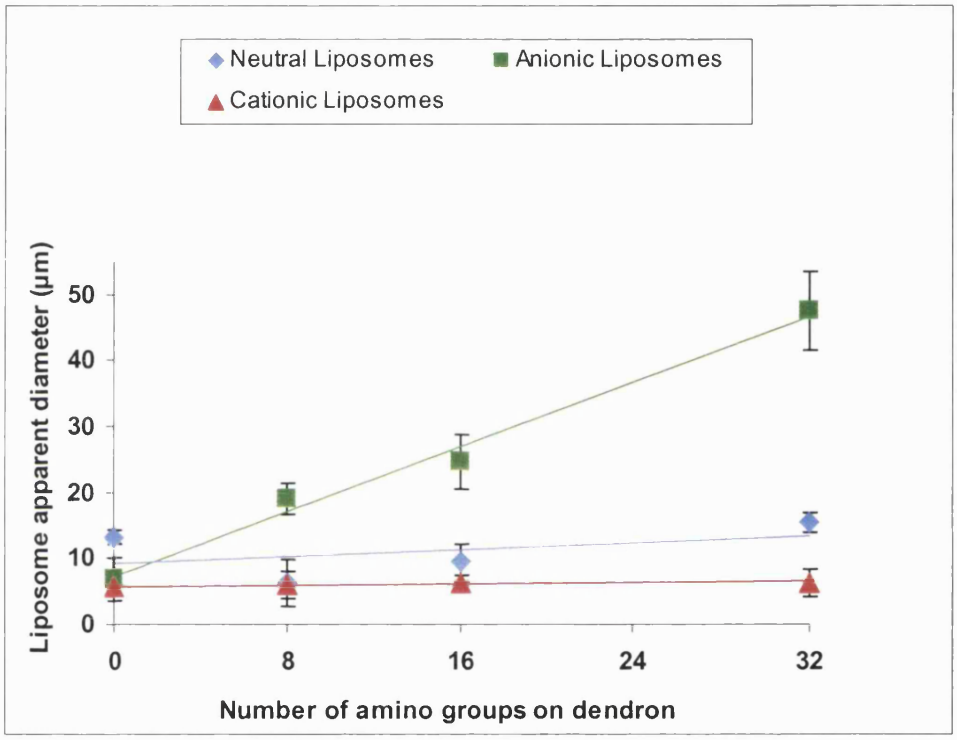

Fig. 3.6. *Effect of dendron interaction on apparent vesicle diameters of liposomes.*

Fig. 3.6 represents the apparent vesicle diameter of the resuspended pellet following centrifugation to remove non-interacted/entrapped dendron. The sizes of the cationic and neutral liposomes remained approximately constant for all three dendrons used. Although this was not the case with anionic liposomes, where increasing dendron size, produced an increase in apparent vesicle diameter. The approximate sizes (apparent diameters) of the structures formed, from anionic vesicles, by 8, 16 and 32 amino dendrons were 19, 24 and 47 µm, respectively. The following

photomicrographs show the structures that were formed before and after centrifugation of dendron-entrapping anionic liposomes

.

The photomicrographs (Fig. 3.7a-c) show anionic liposomes, with and without 32 amino group dendron present. Figures 3.7a and 3.7b show anionic liposomes in the absence of and presence of dendrons, respectively, and there is no significant change in size or shape. Figure 3.7c shows the formation of large vesicular structures (average apparent diameter of 47.4 μm) following centrifugation of dendron-entrapping anionic liposomes.

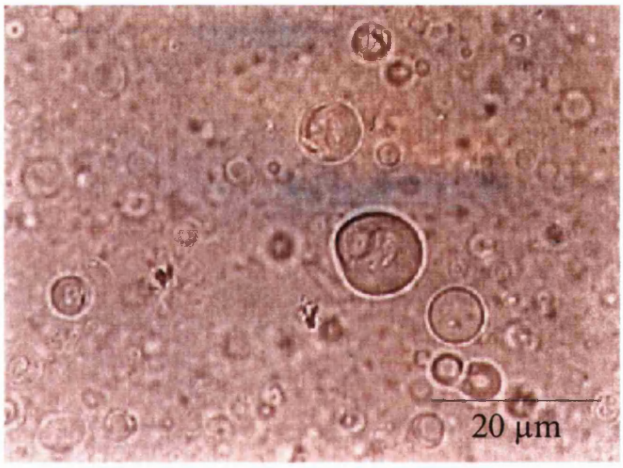

Fig. 3.7a. *Anionic liposomes in the absence of dendrons.*

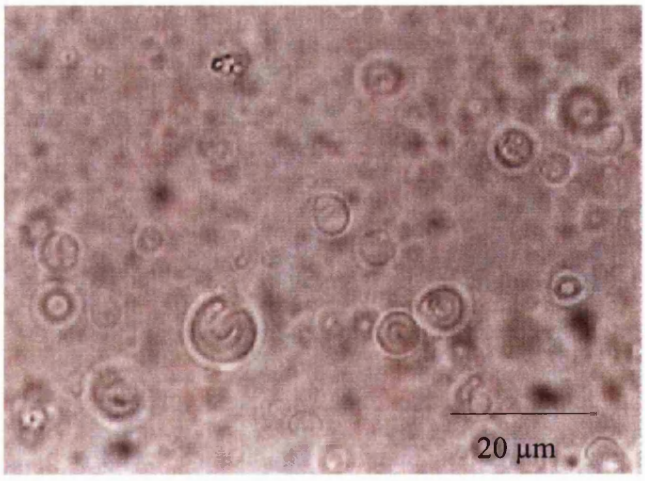

Fig. 3.7b. *Anionic liposomes in the presence of the 32 amino group dendron.*

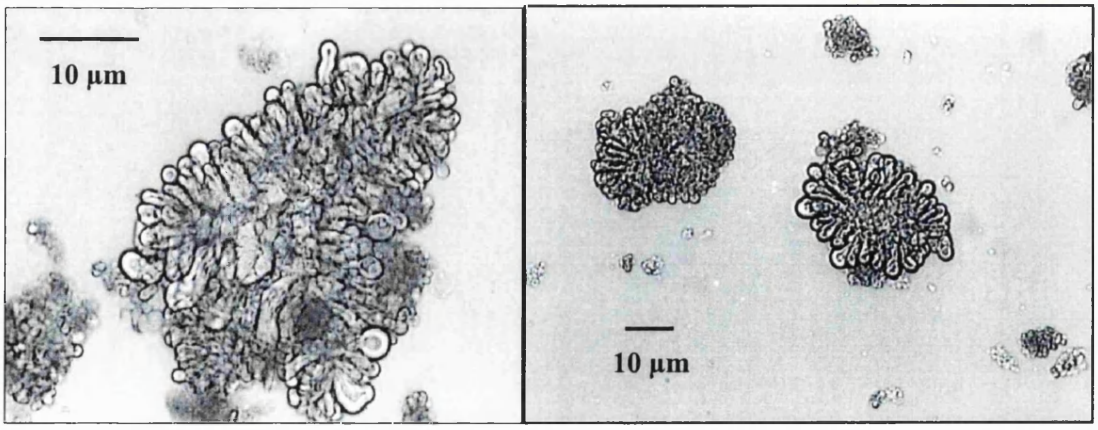

Fig. 3.7c. *Anionic liposomes in the presence of 32 amino group dendron after centrifugation and final resuspension of the vesicles during the DRV method.*

When these abnormal large structures are viewed more closely (Fig. 3.7d), evidence of myelin figures can be seen. This suggests that the amphiphilic dendrons disrupt the anionic bilayers of the liposomes through a solubilisation effect with a surfactant-like action. The membrane disruption increases as the cationic charge of the dendrons increases.

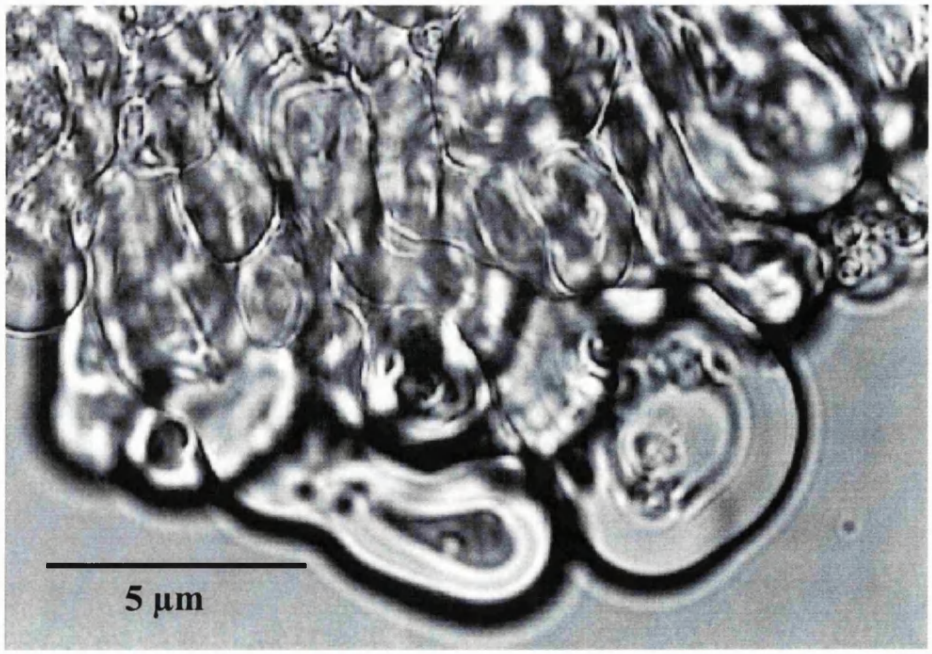

Fig. 3.7d. *Interaction of anionic liposomes and 32 amino group dendrons showing lipid bilayer membrane disruption and the formation of myelin figures.*

Although Fig. 3.7d shows disruption and disorientation of the lipidic bilayers, the anionic membranes maintained their integrity and there was no leakage of entrapped dendrons.

The effect of the cationic dendrons on the zeta potential of the liposomes is given in Fig. 3.8. The zeta potentials of the control liposomes (without additive) were approximately -40 mV for the anionic liposomes and 25 mV for the cationic liposomes. When the cationic dendrons are present, all three formulations of liposomes produced positively charged species ranging from 35 mV to 61 mV. This showed that, during the entrapment procedure, the dendrons associated with the liposome bilayers regardless of liposome charge. As the dendrons are only a few nanometers in size, they are approximately equivalent to the thickness of the aqueous space between two liposomal bilayers. They can therefore be encapsulated in this aqueous space.

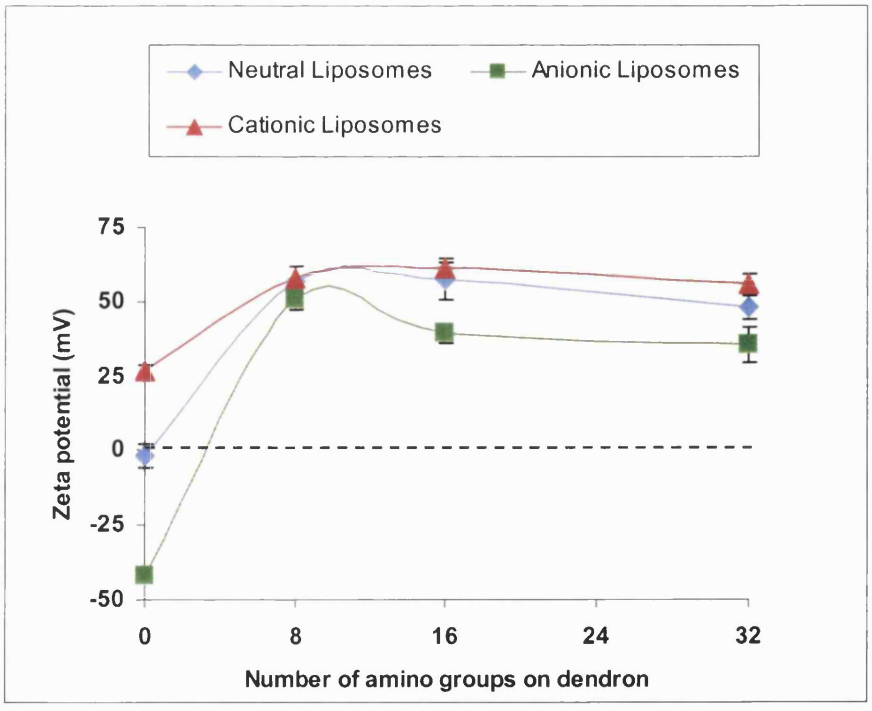

Fig. 3.8. *Effect of dendron interaction on zeta potential of liposomes.*

The dendrons also have lipidic character which may improve their ability to incorporate in to the lipidic bilayer itself. To investigate the mode of interaction further, adsorption studies were performed.

3.3.2 Adsorption studies

The effect of adsorption of dendrons to preformed liposomes is given in Fig. 3.9, indicating that dendron adsorption is clearly dependent on head size and not charge on the liposome.

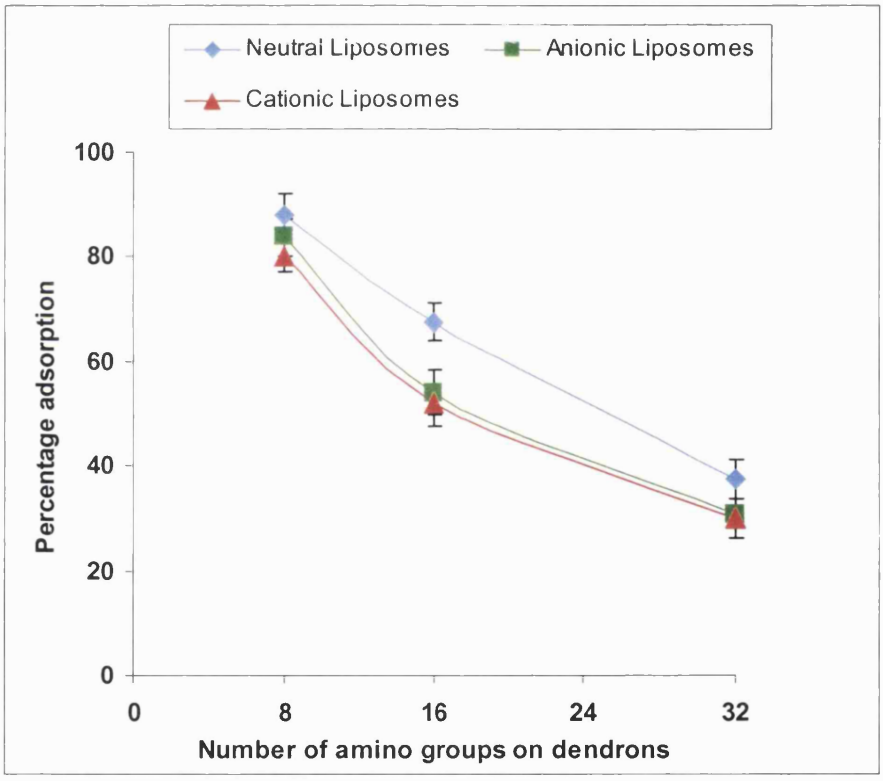

Fig. 3.9. *Adsorption of dendrons onto liposome surface after addition of dendrons with different numbers of amino groups, to liposome surfaces.*

To help clarify the discussion, the terms 'entrapping investigation' and 'entrapping liposomes' refers to liposomes which had dendrons incorporated into their structure. The terms 'adsorption investigation' and 'adsorbing liposomes' refers to preformed liposomes which had dendrons added onto their surface.

Tables 3.2 and 3.3 show the amount of dendron present and the resultant zeta potential for both entrapment, and adsorption investigations respectively for the liposome formulations used. The amount of dendron adsorbed decreases with increasing dendron head size. This ranges from approximately 80% adsorption for compound with 8 amino groups to approximately 30% adsorption for 32 amino groups; this trend is evident for all three liposome formulations. The zeta potential of the adsorbing liposomes is similar (between 56 mV and 68 mV). This order of effect can not be seen with the entrapping liposomes. With regard to greater interaction of the dendrons with liposomes, zeta potentials are similar or lower (between 35 mV and 58 mV) than that of the adsorbing liposomes. This suggests that there is a degree of interaction in the interior of the liposomes. The adsorption studies show that the dendrons saturate the surface of the liposomes and that lower amounts of the larger dendrons are required to produce similar zeta potentials compared to the smaller dendrons. Although cationic, these dendrons do not show preference for anionic liposomes and adsorb to all liposomes similarly, suggesting hydrophobic interaction.

***Table 3.2**; Entrapment investigation results showing the amount of each dendron present and the resultant zeta potential for neutral (DSPC/CHOL), anionic (DSPC/CHOL/PG) and cationic (DSPC/CHOL/DC-CHOL) liposomes.*

Initial Charge of Liposome	Number of amino groups on dendron	Molecular weight of dendron	% of dendron interacting/entrapped	Average Zeta Potential (mV)
Neutral	8	1588	98.01	56
	16	2612	90.36	57
	32	4660	89.83	48
Anionic	8	1588	97.50	51
	16	2612	88.04	39
	32	4660	93.99	35
Cationic	8	1588	96.47	58
	16	2612	88.97	61
	32	4660	95.09	56

***Table 3.3**; Adsorption investigation results showing the amount of each dendron present, and the resultant zeta potential for neutral (DSPC/CHOL), anionic (DSPC/CHOL/PG), and cationic (DSPC/CHOL/DC-CHOL) liposomes.*

Initial Charge of Liposome	Number of amino groups on dendron	Molecular weight of dendron	% of dendron adsorbed onto liposome surface	Average Zeta Potential (mV)
Neutral	8	1588	87.95	68
	16	2612	67.54	68
	32	4660	37.46	67
Anionic	8	1588	83.71	63
	16	2612	53.99	60
	32	4660	30.89	61
Cationic	8	1588	80.23	56
	16	2612	52.13	58
	32	4660	30.10	61

With the adsorption studies, centrifugation to remove non-adsorbed dendrons did not produce large vesicular structures following resuspension of the pellets. The entrapment studies showed large increases in size and shape after centrifugation of anionic liposomes but this was not evident during the adsorption studies. This suggests that the dendrons are not being incorporated into the bilayer structure after being allowed to stand for 5 h at 4°C. The samples were then allowed to stand at 25°C and centrifuged every 2 h to detect any loss of adsorbing dendrons or changes in the zeta potentials of the liposomes.

Neutral and cationic liposome samples did not show any significant changes, but interesting results were seen with anionic liposome samples. Fig. 3.10 shows the results obtained for post-adsorption studies with anionic liposomes. The dashed lines represent the amounts of 8, 16 and 32 amino dendrons present up to 8 h after the initial adsorption studies. Centrifugation at 2 h intervals did not show decreases in the amounts of dendrons present, showing that all three dendrons remained associated with the anionic liposomes. Although the amounts of dendrons remained constant there were significant changes in the zeta potentials of these anionic liposomes. Dendrons with 8 amino groups did not show significant changes in zeta potential but those with 32 amino groups produced a decrease in zeta potential of the anionic liposomes from 61 mV to 46 mV. With regard to 16 amino group dendrons, the zeta potential decreased from 60 mV to 56 mV. This shows that although the dendrons are present, they are associating with the anionic liposomes away from the surface. This suggests that the adsorbing dendrons are breaching the liposomal bilayer and internalising themselves. This is more evident as the number of amino groups of the dendrons increase.

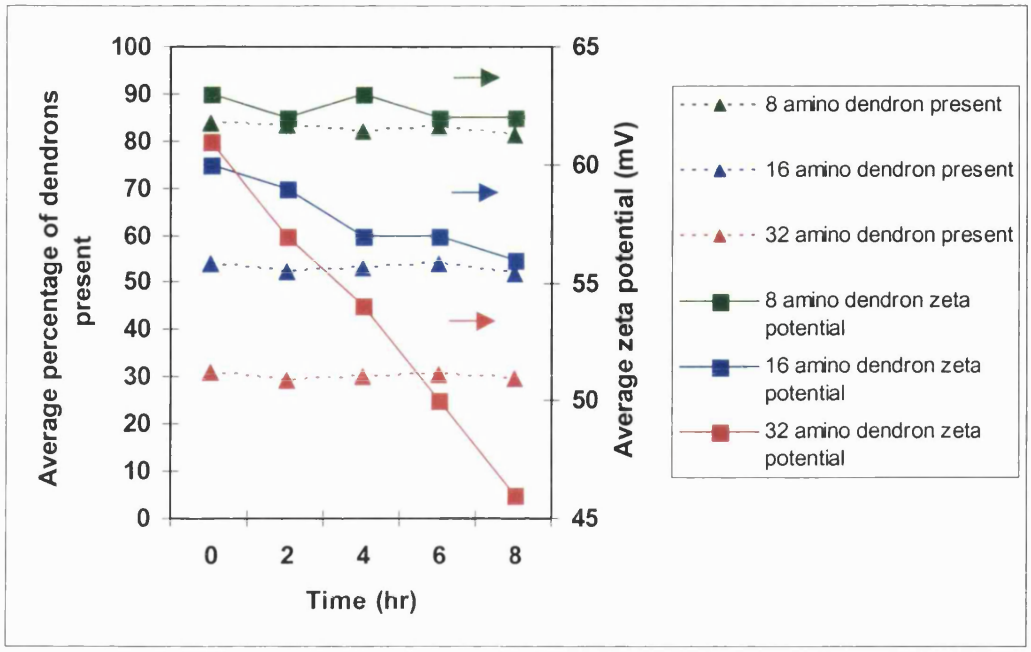

Fig. 3.10. *Post-adsorption studies with anionic liposomes showing the average percentage of all three dendrons present (associated with the liposomes) and the corresponding zeta potentials.*

When post-adsorption samples were kept for 24 h at 4°C, the amounts of dendrons remained constant and there were not changes in zeta potential. This can be explained by the nature of the phospholipids used. Bilayers of liposomes can be in a "fluid" or "rigid" state at ambient temperature (T_a) (Gregoriadis, 1998). The fluid state is achieved with phospholipids that have a gel-liquid crystalline transition temperature (T_c) below the T_a. The value for T_c is the temperature at which the fatty acid chains melt. Therefore at 4°C DSPC is in the rigid state and prevents the dendrons from accessing the lipid bilayer.

3.3.3. Membrane disruption assay

Riboflavin (Fig. 3.11) was entrapped in the aqueous compartments of neutral, anionic and cationic liposomes. The encapsulation efficiency ranged from 63% to 68% and was determined using a fluorimetric assay. The charge of the liposomes did not effect the encapsulation of riboflavin.

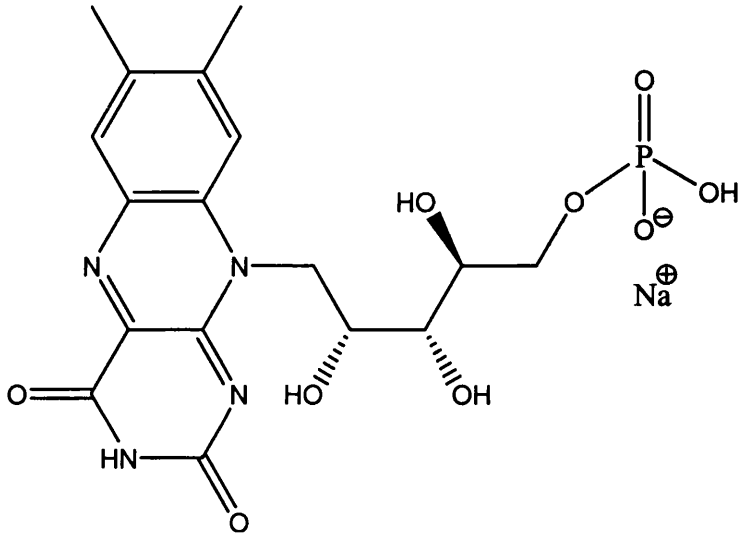

Fig. 3.11. *The chemical structure of Riboflavin-5'-phosphate sodium salt dehydrate.*

Fig. 3.12 shows a calibration plot of the emission intensities obtained from standard riboflavin solutions. The standard solutions of riboflavin only produced a linear plot up to a concentration of 1.00 μg/ml. During the study, all samples requiring fluorimetric analysis were diluted by a factor of 1000 and the concentration values obtained from the calibration plot were multiplied by 1000 to determine the actual concentration of riboflavin in the sample.

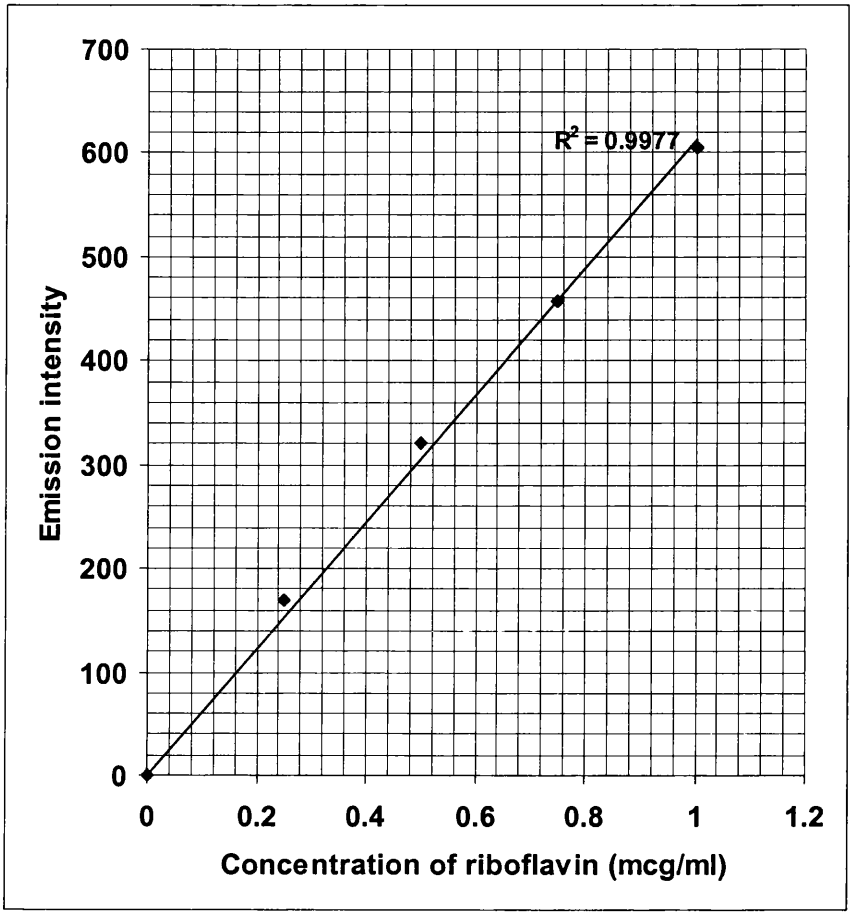

Fig. 3.12. The linear calibration plot for the standard solutions of riboflavin.

The cationic dendrons with 8, 16 and 32 amino groups were added to neutral, anionic and cationic SUV suspensions which had encapsulated riboflavin. As a control, SUVs containing riboflavin and made from all three liposome formulations were kept free from dendrons. The aim of the study was to investigate whether the addition of dendrons resulted in the release of riboflavin from the liposomes. The release of riboflavin was calculated as a percentage. The value for 100% release was determined by the addition of Triton X-100 to the SUV suspensions after 30 min and the dendrons were also added after 30 min. The SUV suspensions were centrifuged at certain time-points and riboflavin collected in the supernatant was determined as the "free" or released riboflavin.

The addition of dendrons to neutral and cationic SUV suspensions produced results which were not significantly different from those obtained with control liposomes (not shown). When the dendrons interacted with anionic SUVs, there was significant release of riboflavin over a 24 h period as can be seen in Fig. 3.13.

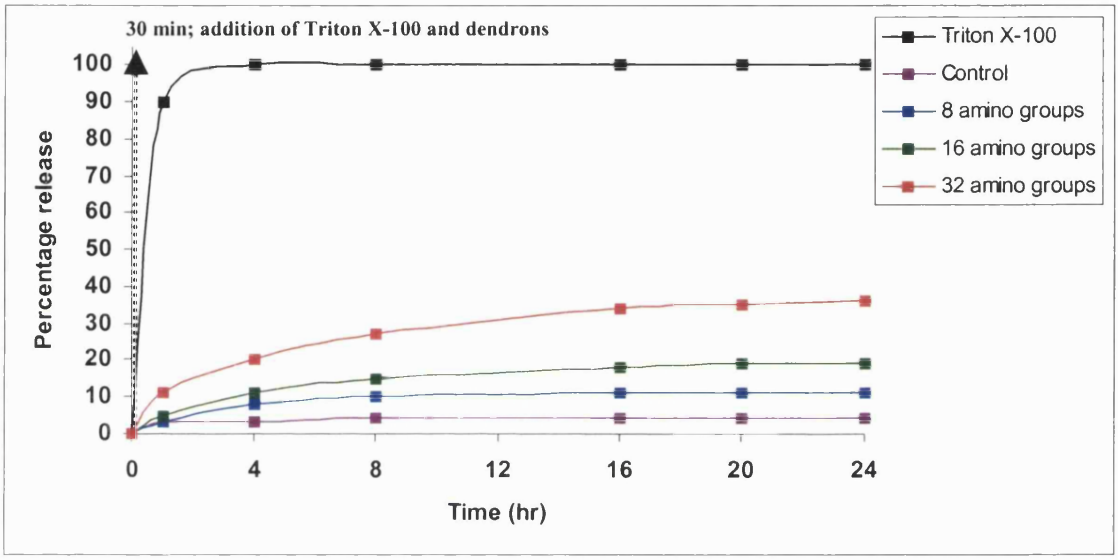

Fig 3.13. *A graph showing the percentage release of riboflavin from anionic liposomes over 24 h following the addition of 8, 16 and 32 amino group dendrons after 30 min.*

The percentage release of riboflavin, after 24 h, produced by the control liposomes was 4% and remained constant. The addition of dendrons caused an increase in riboflavin release, this being more evident as the number of dendron amino groups increased. The percentage of riboflavin released resulting from the addition of 8, 16 and 32 amino group dendrons was 11%, 19% and 36% respectively. This trend was only noticeable with anionic vesicles and is further evidence that cationic dendrons disrupt anionic lipidic bilayers.

Polycationic peptides such as poly-lysine are known to bind tightly to anionic vesicles and promote vesicle-vesicle interaction (Zhang and Smith, 2000). The final outcomes of such interactions may be aggregation, vesicle leakage or mixing of lipidic bilayer constituents but they are dependent upon the composition and size of the vesicles. Zhang and Smith (2000) also studied membrane disruption using PAMAM dendrimers and found that the high-generation species were unusually effective at disrupting anionic vesicles. They specifically stated that G6 (256 amino groups) and G7 (512 amino groups) induced large amounts of lipid mixing and leakage of aqueous contents. This study also concluded that smaller dendrimers, below G4 (64 amino groups) were not significantly effective. Our study shows that dendrons with 32 amino groups can induce membrane disruption. The novel dendrons which we have studied can not be directly compared to PAMAM dendrimers which do not have lipidic character. The lipidic alkyl chains aid the interaction of the dendrons with the lipidic bilayer of the anionic vesicles. Another important factor is that these dendrons are not quasi-spherical like PAMAM dendrimers, thus having the ability to interact with the vesicle membranes at different angles and with different orientations (i.e. contact with the liposome membrane could be via the core, branched periphery or a combination of both). The amphiphilic nature of the dendrons allows interaction via their amino head groups, lipidic chains or a combination of both. The dendron/dendrimer-vesicle interaction is largely dependent on the vesicle membrane composition (Ottaviani *et al.*, 1998). Dendritic molecules disrupt different types of anionic vesicles and although other anionic vesicle compositions were not studied there is evidence of varying results (Ottaviani *et al.*, 1998). This variation may provide evidence of membrane selectivity which can explain differences in transfection efficiencies and cell toxicities observed with different cell lines (Tang *et al.*, 1996, Loup *et al.*, 1999). Zhang and Smith (2000)

concluded that PAMAM dendrimers did not internalise in to the anionic liposomes using certain assays involving quenching probes but they did not rule out the possibility. The adsorption studies (see Fig. 3.10) suggest that dendrons may breach the anionic bilayer and enter the aqueous compartments of the liposomes but this requires further investigation. It is important to note that PAMAM dendrimers are up to four times the size of the dendrons studied

3.3.4. Membrane disruption model

The results obtained from entrapment/interaction studies, adsorption studies and the membrane disruption assay show that dendrons induce changes to anionic vesicle membranes. These changes are more pronounced as the cationic charge of the dendrons increases. Although it is not a definitive answer, the following model is a possible explanation as to why anionic membrane disruption is induced by the dendrons.

During the entrapment/interaction studies large anionic vesicular structures (Fig. 3.7c-d) were produced following centrifugation to remove non-entrapped dendrons. Before the centrifugation step, dendrons were already incorporated within the liposomes in both the aqueous and lipidic phases. During centrifugation, the liposomes were subjected to very high packing stresses which enhanced the mixing of the lipids and lipidic dendrons. The combination of these packing stresses and electrostatic forces produced large anionic vesicular structures when resuspended. The evidence of myelin figures in Fig. 3.7d is not due to a simple detergent effect as these abnormal structures are not produced during the other studies with anionic vesicles and dendrons.

To understand how the dendrons breach the bilayers of the anionic vesicles, resulting in their entry in to liposomes or the release of entrapped riboflavin, it is important to consider the phospholipids involved. In this study, the zwitterionic DSPC and the anionic PG were used. As can be seen in Fig. 3.4 both phospholipids are similar in structure and only differ in their polar head groups. Fig. 3.14a-b represents a possible membrane disruption model. The model is a representation of the outer phospholipid layer of an anionic bilayer produced by DSPC and PG in the "fluid" state.

Fig. 3.14a

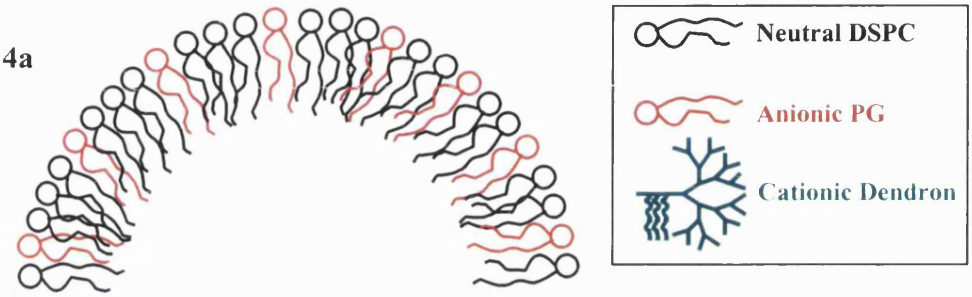

Fig. 3.14b

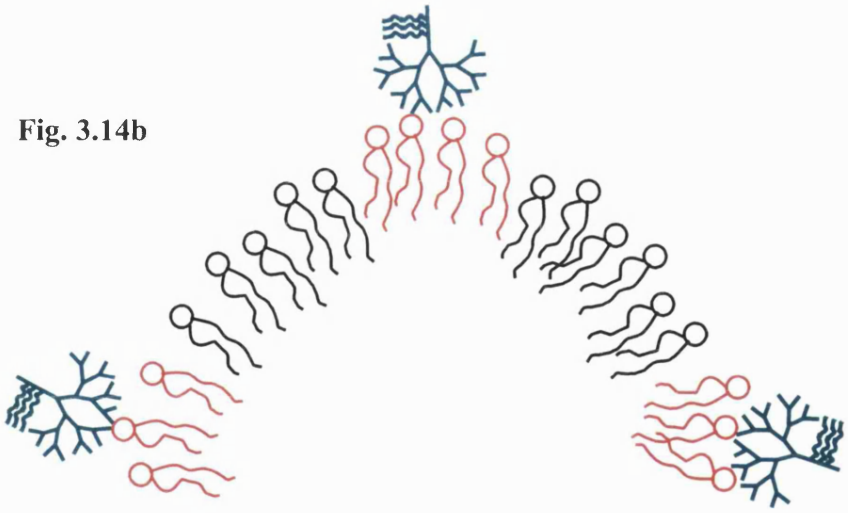

Fig. 3.14. a) *The outer phospholipid layer of an anionic liposome formulated with DSPC and PG;* ***b)*** *The re-orientation of phospholipids following interaction with cationic dendrons.*

As shown by the adsorption studies, the initial interaction of dendrons onto the liposome surface is similar, regardless of the liposomal membrane charge. This

model is suggesting what may happen when a highly cationic dendron interacts with a anionic liposomal membrane over a period of time.

Fig 3.14a shows an even distribution of DSPC and PG in the phospholipid layer which is in a "fluid" state. Fig 3.14b represents the effects on the phospholipid layer following the addition of highly cationic dendrons. In the "fluid" state the phospholipids have sufficient mobility to re-orientate their positions in the phospholipid layer. The dendrons disorder lipid orientation by electrostatically attracting the PG molecules to the liposome surface at the point of dendron contact. This is not an immediate process as the lipids have to re-assemble. Ensuring that the lipids are kept above the gel-liquid crystalline transition temperature (T_c), they will self-assemble to form a bilayer again. It is during these disordered 'windows of opportunity' that dendrons can breach the liposomal bilayer and entrapped molecules can escape. The greater the cationic charge possessed by the dendrons, the greater their ability to cause disruption. Another important factor to consider is that dendrons are branched and the surface amino groups are not densely packed. High generation PAMAM dendrimers have a densely packed spherical surface, which may not be properly hydrated for steric reasons. Dendrons with less amino groups are not sterically hindered and phospholipid molecules can interact within the branched structure of the dendrons.

3.4. CONCLUSION

The studies show that cationic lipidic dendrons are able to disrupt anionic vesicles and their ability to do this increases as the number of surface amino groups increases. Although cationic, these dendrons do not show preference for anionic liposomes and exhibit hydrophobic interactions with all liposomes but may affect anionic liposomes over a period of time. The membrane disruption model suggests that dendrons may be useful as fusion catalysts. As well as their possibilities to act as drug delivery vectors, in their own right, they may also be used to improve vesicle-mediated delivery.

The commercial availability of PAMAM has led to the increased use of dendrimers as cell transfection agents, which is a complicated, multi-step process. It is believed that transfection is mediated by endocytosis, and there is evidence that release from the endosome is the step that determines transfection efficiency (Rolland, 1998). The results of these studies show that dendrons can disrupt bilayer membranes and suggests that they may have the ability to permeate from endosomes as they have shown that they can enter through anionic membranes over a period of time. Dendrons have been reported with enhanced transfection activities. This is an observation attributed to their more flexible structures (Tang *et al.*, 1996).

The speculative membrane disruption model does not provide definitive answers but is does form a simple physical picture that suggests how cationic dendrons may behave in different carrier-mediated applications.

CHAPTER FOUR

THE INTERACTION OF CATIONIC DENDRONS WITH ALBUMIN AND THEIR DIFFUSION THROUGH CELLULOSE MEMBRANES

4.1 INTRODUCTION

4.1.1 Membrane permeability and diffusion

In the late 1800's, Overton discovered that substances that dissolve in lipids pass more easily into the cell than those that dissolve in water. This was some of the first evidence that cells were surrounded by a lipid membrane. The phospholipid membrane of cells can greatly modify the permeation of molecules into a cell. The membrane acts as a barrier to passive diffusion of water-soluble molecules. However, substances that dissolve in lipids pass more easily into the cell. The correlation between permeability and solubility in lipids is appropriately named Overton's Rule (Al-Awqati, 1999). Overton concluded that solubility in the boundary of the cell is selective and that permeability is enhanced by the lipophilicity of the molecule. Overton also suggested cholesterol based or lipidic oil based material was incorporated into the cell boundary (Al-Awqati, 1999). On the basis of this theory and further research, it was hypothesised that cell membranes are porous constructs of lipid domains. The porous channels allow the transport of hydrophilic molecules and the lipidic regions aid transport of hydrophobic molecules (Singer and Nicolson, 1972). Different membrane transport processes include facilitated diffusion, active transport, filtration and endocytosis but in this chapter, focus will be placed on passive diffusion.

Passive diffusion is the most significant transport mechanism for the majority of drugs, with the physicochemical properties of both the drug and the permeation barriers (membranes) being the major rate determinants for transport (Higuchi *et al.*, 1981). For the membrane its lipophilic character and the presence of water pores (Higuchi *et al.*, 1981), the membrane surface area available for absorption (Levine, 1970) and the presence of stagnant diffusion layers (Hayton, 1980) are all considered to be important factors influencing membrane transport. The characteristics of a molecule influencing transport rates and permeability are size, lipophilicity, hydrogen bonding capability and extent of ionisation. Various mathematical models have been developed to describe the relation between drug structure and membrane permeation. Compounds are able to move based on their thermal energy in the direction of a concentration gradient (passive diffusion). For charged molecules the electrochemical potential difference across a biological membrane may be an additional driving force for passive diffusion (Camenisch *et al.*, 1996). Cations migrate to the negatively charged membrane side (basolateral) and anions to the positively charged membrane side (apical).

4.1.2 Passive diffusion in solution

Passive diffusion of substances through liquids, solids and membranes is a process of considerable importance in the pharmaceutical sciences (Flynn and Yalkowsky, 1972). The rate of diffusion of a solute is expressed by Fick's first law:

$$\frac{dm}{dt} = -DA\frac{dC}{dx} \qquad (1)$$

where dm is the amount of solute (mg) diffusing in the time dt (sec) across an area A (cm^2) under the influence of a concentration gradient dC/dx (mg mol^{-1} cm^{-1}). D is

known as the diffusion coefficient (cm^2 sec^{-1}). It is not strictly constant but varies with concentration at constant temperature. The negative sign in Eq. (1) is necessary because diffusion occurs in the opposite direction to that of increasing concentration (Fig. 4.1). The diffusion coefficient (cm^2/s) of spherical particles that are of colloidal dimensions is given by Eq. (2), the Stokes-Einstein equation.

$$D = \frac{RT}{6\pi\eta r N_A} \qquad (2a)$$

where r is the radius of the spherical particle (cm), η is the viscosity of the liquid medium (g/cm.s), R is the gas constant, T is the thermodynamic temperature (K) and N_A is Avogadro's constant. Eq. (2a) can also be represented as:

$$D = \frac{kT}{6\pi\eta r} \qquad (2b)$$

where k is the Boltzmann constant.

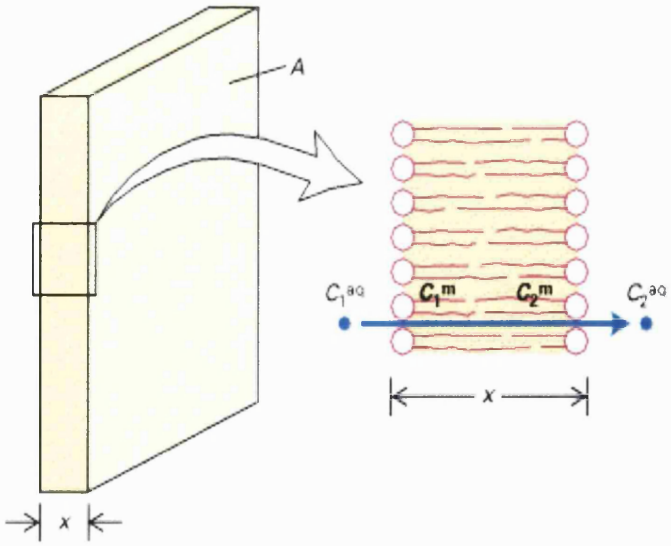

Fig. 4.1. *A membrane model showing how Fick's law can be applied. The blue arrow represents the direction of movement of the diffusant through a cross-sectional area A.* $(C_1^{aq}-C_2^{aq})/x$ *is the concentration gradient where* x *is the membrane thickness.*

It is important to note that Fick's first law refers to the rate of diffusion in the steady state of flow. When studying a change in concentration of diffusant with a non-steady state of flow, Fick's second law is applied to the system. The second law is represented by an equation that emphasises the change in concentration with time at a definite location, rather than the mass diffusing across a unit area of barrier in unit time. Following derivation (Martin, 1993), the equation for Fick's second law is represented as:

$$\frac{dC}{dt} = D \frac{d^2C}{dx^2} \qquad (3)$$

This is a one-dimensional representation of Fick's second law and only represents diffusion in the x direction. In a diffusion system consisting of donor and receptor compartments, maintaining a low concentration of diffusant in the receptor compartment is referred to as "sink conditions" (Martin, 1993). Sink conditions can be maintained by regularly replacing the liquid in the receptor compartment and represent a description of steady state, in terms of the second law. The concentration will not be maintained at an exact constant value, but will vary slightly with time. This can be referred to as a quasi-stationary state which can be assumed to be under steady state conditions (Martin, 1993).

Hydrodynamics predict the existence of a stagnant liquid layer near a surface (Camenisch *et al.*, 1996). With regard to this assumption and membranes, such stagnant aqueous boundary layers are often referred to as the unstirred layers. In model studies, stirring is used achieve homogenous bulk liquids. For passive diffusion, these aqueous layers are assumed to form significant permeation barriers.

Stirring of the bulk liquid leads to disruption of the aqueous layer and has a favourable effect on permeability. "*In vivo* the thickness of the stagnant aqueous diffusion layers is influenced by mechanical mixing due to agitated flow of the intestinal fluid or blood flow. Therefore, it is sometimes believed that *in vivo*, the stagnant aqueous diffusion layers are nearly non-existent and have no effect on drug absorption" (Camenisch *et al.*, 1996).

4.1.3 Cellulose membranes

Cellulose and its derivatives provide a very important class of basic materials for membranes, mainly due to the fact that cellulose is a very hydrophilic polymer but is not water soluble, which is related to its crystallinity and the intermolecular hydrogen bonding between its hydroxyl groups (Sakai, 1994). Cellophane and other types of regenerated cellulose are mainly used as materials for dialysis membranes, since they allow the diffusion of ions and low molecular weight solutes but they do not permit the diffusion of proteins or macromolecules of high molecular weight (Sakai, 1994), while cellulose acetate and nitrate are used for microfiltration/ultrafiltration processes and cellulose triacetate is used in reverse osmosis membranes for desalting applications. However, due to medical applications of dialysis membranes (haemodialysis), they represent one of the major membranes marketed worldwide.

The diffusion of dendritic structures through membranes does not seem to have been investigated. During this study the diffusion of lipidic cationic dendrons was studied using regenerated cellulose membranes. Kreuter and co-workers studied the membrane transport of liposomes (Kreuter *et al.*, 1981) and nanoparticles (Kreuter *et al.*, 1983) containing steroidal drugs. It was also found that captopril was delivered more efficiently by nanoparticles compared to a solution, across a number of

different membranes (Müller and Kreuter, 1999). Loftsson *et al.* (2002) studied drug permeability through semi-permeable cellophane membranes using cyclodextrins.

4.1.4 Interaction of molecules with albumin

Albumin is the most abundant protein in mammalian systems, and plays an important role in the transport and deposition of a variety of endogenous and exogenous substances in blood (Kragh-Hansen, 1981). Albumin is a relatively large multi-domain protein (Fig. 4.2) and its ability to fluctuate between isomeric forms in aqueous solution could assist in adapting the albumin molecule to bind ligands with a diverse nature with high affinity.

Apart from size, the body distribution of colloidal drug carrier systems is influenced by surface characteristics. They represent the major determinant for protein adsorption in biological fluids and may modify particle interaction with specific plasma membrane receptors, thus leading to elimination of the particles from the systemic circulation. The mechanism of protein adsorption on particle surfaces in conjunction with the recognition of such coated particles by monocytes and macrophages is the opsonisation process. Opsonisation seems to be influenced by the surface curvature of the carrier system, smaller carriers leading to a reduced adsorption of proteins and opsonins and in turn to a reduced uptake of such systems by phagocytic cells (Harashima *et al.*, 1994).

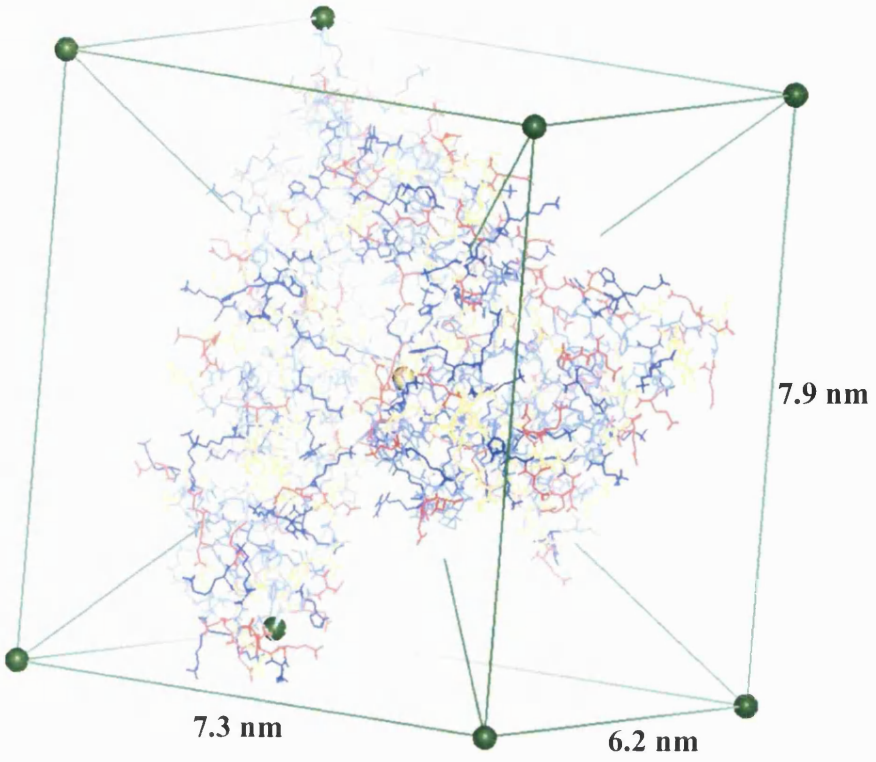

Fig. 4.2. *A molecular model of serum albumin showing the minimum dimensions required if placed in a box. The molecule is colour coded by polarity where; yellow = neutral; red = negative acid; and blue = positive base.*

Little information is known about biological properties of dendrimers. More information is required about how dendrimers influence cells and biomolecules which is crucial for further investigations of therapeutic applications of dendrimers. In this study, the interaction between lipidic cationic dendrons and bovine serum albumin (BSA) was studied using a dynamic dialysis process. The interaction between PAMAM dendrimers and BSA has been studied using fluorescence techniques (Klajnert and Bryszewska, 2002). Chiba *et al.* (2003) studied the interactions between sugar-coated dendrimers and BSA using interfacial tensiometer, surface tensiometer, fluorescence and circular dichroism (CD) spectroscopies.

Here we investigate the diffusion and permeability of cationic lipidic dendrons across cellulose membranes. The interaction of these molecules with bovine serum albumin is also studied using dynamic dialysis.

4.2 MATERIALS AND METHODS

4.2.1 Synthesis of the cationic dendrons

The amphipathic dendrons having three lipidic 14-carbon chains coupled to dendritic lysine head groups with 8, 16 or 32 free terminal amino groups were synthesised by solid phase peptide synthesis. They were the same series of dendrons studied in Chapter 3 (1a-c) and can be seen in Fig. 3.3. This series of dendrons were radiolabelled with tritium and were water-soluble. The synthetic methods are described in detail in Chapter 2. The following studies were carried out for all three of the radiolabelled series and the molecular weights of the dendrons ranged from 1588 for 8 amino groups to 4660 for 32 amino groups.

4.2.2 Dynamic dialysis

Dynamic dialysis was used to study the diffusion of the dendrons and their interaction with BSA. Dynamic dialysis is a simple method for studying the protein binding of small molecules (Meyer and Guttman, 1968), which is based on the determination of the rate of dialysis of small molecules from a protein-containing compartment. The time course of disappearance of small molecule from a protein compartment is followed for extended periods of time. This kinetic approach is more rapid than other methods such as equilibrium dialysis and ultrafiltration.

4.2.3 Diffusion studies

Two types of regenerated cellulose membranes were used during the study and both were obtained from Spectra/Por, Spectrum Labs. Inc. (USA). Unlike native cellulose which is highly crystalline and rigid, regenerated cellulose is largely amorphous and highly swollen by water. The first type of dialysis membrane used was Spectra/Por 2 and the second was Spectra/Por 7. The physical properties of the two membranes are

stated in Table 4.1. Spectra/Por 2 membranes contained traces of sulfides and heavy metals and needed to be prepared before use. The preparation required Spectrum Sulfide Removal solution and Spectrum Heavy Metals Cleaning solution which were obtained from Spectrum Labs. Inc. (USA). The sulfide removal kit contained two separate wash solutions and the cleaning process was completed in 10 min. The Heavy Metals Cleaning solution was a chelating rinse which stripped the heavy metals from the membrane. The Spectra/Por 7 membrane had been pre-treated chemically to minimize the content of heavy metals and sulfide contaminants. Preparation required soaking of the membrane in a large volume of deionised water for 30 min to remove the sodium azide preservative.

Table 4.1. *The physical properties of Spectra/Por 2 and 7 dialysis membranes used for the studies, where MWCO = molecular weight cut off.*

Dialysis Membrane	**MWCO**	**Flat Width (mm)**	**Diameter (mm)**	**Volume/Length (ml/cm)**
Spectra/Por 2	12,000	25	16	2
Spectra/Por 7	25,000	24	15	1.8

To study diffusion of the dendrons, aliquots (100 μg/5 ml) of dendron solutions were placed in 7 cm length dialysis membranes which were sealed at both ends using magnetic weighted closures to form a bag (donor). The membranes were dialysed against 500 ml (receptor) of phosphate buffer solution (PBS, pH 7.4, ICN Biomedicals Inc., USA), at 25°C for up to 24 h with constant stirring using a magnetic stirrer. Sink conditions were maintained during the experiments by replacing the liquid in the receptor compartment at sampling intervals. The amounts of dendrons interacting with the membranes and diffusing through the membranes were quantified by scintillation counting (Beckman LS6500 scintillation counter,

Beckman Instruments, USA). Samples to quantify diffusion were taken and measured at 4 hr intervals and the accumulative amounts of dendrons diffusing, were also calculated. During the initial experimental set up, samples to quantify diffusion were taken at 10 min intervals to determine if there was a delay in diffusion from the donor compartment to the receptor compartment, but this was not the case. Adsorption to the cellulose membranes was quantified at the end of each 24 h experiment and was calculated as a percentage of the initial amounts of dendrons added. Diffusion studies were also repeated in the presence of NaCl at different molar concentrations to determine the effect of salts. The NaCl concentration in the dialysis bag was kept constant (0.01 M) and that of the external solution was increased from 0.2 M to 0.8 M.

4.2.4 Dendron-albumin interaction studies

The experimental set-up for these studies was similar to that for the diffusion studies (4.2.3) but the 5 ml aliquots placed in the dialysis membranes were various molar mixtures of BSA and dendrons. The molar ratios of dendrons to albumin studied were; 0.5:1, 1:1, 2:1, 3:1 and 4:1. BSA was 99% fraction V, molar mass about 66 kDa and obtained from Sigma Chemical Co., UK. The amounts of dendrons diffusing through the membrane in the presence of BSA were quantified and compared to control studies where BSA was absent. All solutions were buffered (PBS, pH 7.4) and 0.8 M NaCl was added, with constant stirring throughout.

4.2.5 Apparent diffusion coefficient (*D*)

The apparent diffusion coefficient of the dendrons was calculated using Stokes-Einstein equation (see Eq. 2b);

$$D = \frac{kT}{6\pi\eta r} \qquad (2b)$$

where; k is the Boltzmann constant (1.38066 x 10^{-16} g.cm^2/s^2); T is the temperature at 298 K; η is the viscosity (0.01 g/cm.s) and π is taken as 3.14. The value for r (radii of the dendrons) was taken as the apparent hydrodynamic diameters which were calculated using molecular simulation software (Quanta 96 and CHARMm). The radii of the dendrons with 8, 16 and 32 amino groups were 1.05, 1.20 and 1.40 x 10^{-7} cm, respectively (see Table 3.1).

4.2.6 Apparent membrane partition coefficient (*K*)

Diffusion in the system studied obeyed Fick's second law. If sink conditions are maintained in the receptor compartment, the apparent membrane partition coefficient can be calculated using Eq.4 (Martin, 1996).

$$\frac{dm}{dt} = \frac{DAKC_d}{x} \qquad (4)$$

Where dm/dt is the amount of material diffusion through in unit time, t; D is the apparent diffusion coefficient; A is the cross-sectional area, which was kept constant at 11.96 cm^2 and; K is the apparent membrane partition coefficient; C_d is the concentration in the donor compartment (g/cm^3); and x is the average thickness of the membrane which was measured using microscopy, to be approximately 4 x 10^{-3} cm (40 μm).

4.2.7 Apparent membrane permeability coefficient (*P*)

The apparent membrane permeability coefficient, also called the 'apparent permeability', has units of linear velocity (cm/s) and can be calculated using Eq. 5 which includes parameters from Eq. 4.

$$P = \frac{DK}{x} \qquad (5)$$

4.2.8 Octanol-water partition coefficient (P_{ow})

Aqueous solutions were made up of the three radiolabelled dendrons. For each dendron, 0.20 μmol of dendron was solubilised in 400 μl double deionised water. Each solution was mixed with 400 μl 1-octanol (Sigma Chemical Co., UK) and was left to shake for 24 h at 25°C. The mixtures were then allowed to stand for 2 h and the two phases were separated from the layers. The scintillation counts were measured for the separate phases and the amounts of dendrons were quantified. The Log P_{ow} values were calculated using Eq. 6.

$$P_{ow} = \frac{O_c}{W_c} \qquad (6)$$

where O_c is the concentration of dendrons in the octanol phase and W_c is the concentration of dendrons in the water phase.

4.2.9 Thermodynamics of diffusion

Permeation of gases, liquids and solutes through membranes requires an energy of activation for the small molecules to move through the matrix of the barrier material (Martin, 1993). This fact is expressed in the Arrhenius equation (Eq. 7 and 8).

$$P = P_0 e^{-Ep/RT} \qquad (7)$$

$$\ln P = \ln P_0 - Ep/RT \qquad (8)$$

in which P is the membrane permeability, P_0 is a factor independent of temperature and proportional to the number of molecules entering the membrane and to the probability that these molecules have sufficient energy to engage in the diffusion

process. *Ep* is the energy of activation for permeation in J/mol, and *T* is the absolute temperature (°K) and *R* is the molar gas constant (8.314 J/K/mol).

Diffusion studies of the dendrons were carried out at 15°C (288°K), 25°C (298°K) and 37°C (310°K) for 10 h and the permeabilities of the dendrons were calculated at the different temperatures. An Arrhenius-like plot (ln *P* vs 1/*T*) produced a straight line with a gradient equal to the energy of activation for permeation (*Ep*). This energy was calculated for all three dendrons.

4.2.9 Molecular modelling and analysis

Molecular modelling and analysis of the dendrons and BSA was performed using a combination of Quanta 96 (version 96.0516) and CHARMm (version 23.2). Molecular graphics of BSA were obtained using the software program 'Spock' which was developed in 1998 by Jon A. Christopher at Texas A+M University.

4.3 RESULTS AND DISCUSSION

Note: In the respective figures, the distribution of data values is represented by showing a single data point, representing the **mean** *value of the data, and the error bars represent the overall* **distribution** *of the data.*

4.3.1 Diffusion studies

Fig. 4.3 represents the accumulative results after 24 h dialysis using a membrane with a 12 kDa MWCO (Spectra/Por 2). The percentage of dendrons diffusing, as expected, decreased with an increase in molecular size and number of amino groups. Adsorption complicates interpretation, as approximately 50% of each dendron adsorbs to the cellulose membrane. Fig. 4.4 represents the corresponding accumulative release data for the three dendrons from the dialysis tubing in the absence of albumin and NaCl. Sink conditions were maintained during the experiments. As can be seen from the diffusion profiles in Fig. 4.4, there is no delay or lag-time for diffusion in the system used. This can be explained by the fact that when cellulose membranes are in contact with water, they swell to form a porous network of fluid-filled channels, unlike non-porous solid membranes. Similar observations have been made by other researchers using porous cellulose and artificial membranes (Nolan *et al.*, 2003, Salamat-Miller *et al.*, 2002, Corrigan *et al.*, 1980, Hammouda *et al.*, 1993, Liu, H. *et al.*, 2000). The diffusion profiles in Fig. 4.4 (also see Appendix 7) were used to calculate the dm/dt values required for determination of K values using Eq. (4). The diffusion profiles for all three molecules show an initial burst and then represent more linear release profiles from 4-24 h (see Appendix 7 for a linear plot). This can be explained by the fact that, as the dendrons diffuse, they adsorb to the membrane and within the pores resulting in a hindered diffusion process. The use of a membrane that had a 25 kDa MWCO (Spectra/Por 7) and was free from impurities did not significantly alter these results. The high

cationic charge of the dendrons accompanied by the complex cellulose membrane structure and thickness (40 μm) hinders movement through the dialysis membrane (see Fig. 4.5a and b) but adsorption plays a significant retarding effect.

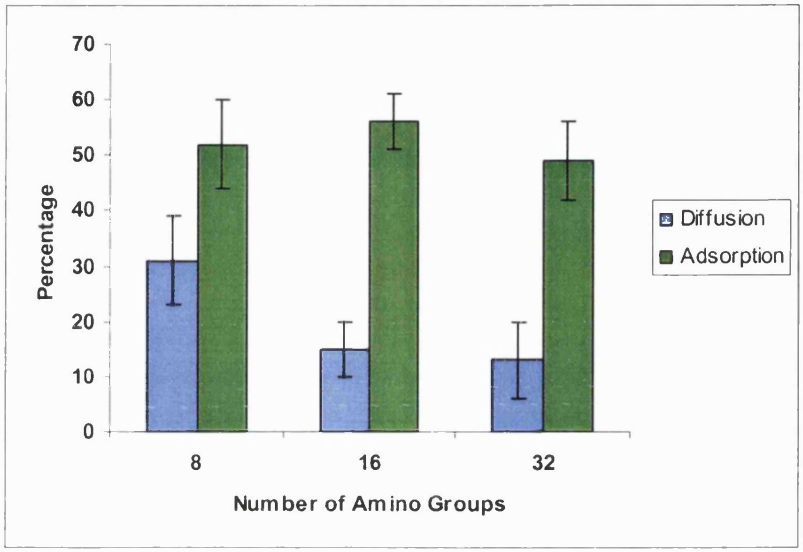

Fig. 4.3. *Results representing the accumulative percentage diffusion of the dendrons through the dialysis membrane in the absence of albumin & NaCl and the percentage adsorption of the dendrons to the membrane after 24 hours at 25°C.*

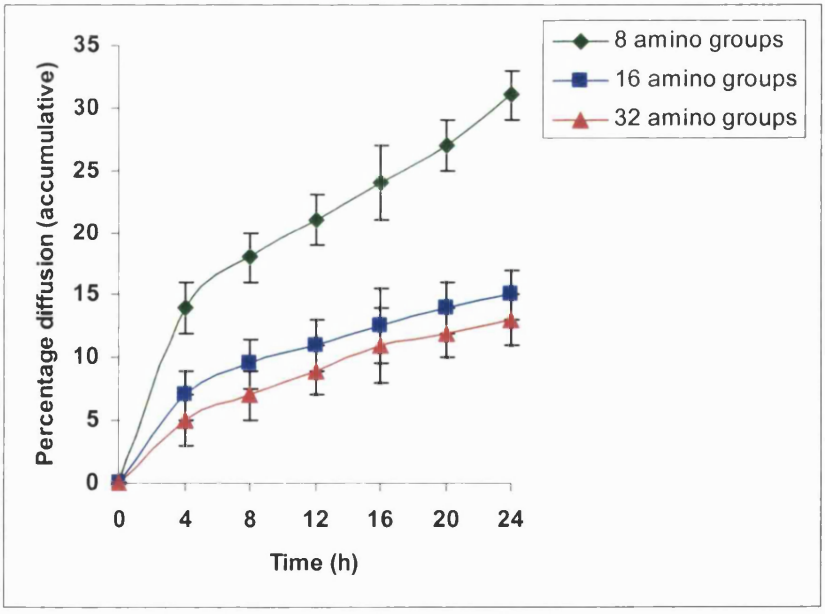

Fig. 4.4. *The percentage diffusion profiles of the three dendrons, in the absence of albumin & NaCl, over 24 h at 25°C.*

Adsorption of the dendrons to the cellulose membrane was reversible and was quantified following thorough washing of the membranes after completion of the experiments. Although the lipidic nature of the dendrons contributes to their adsorption effects, another factor is their cationic surface. In the case of regenerated cellulose membranes, some of the $-CH_2OH$ groups are oxidised to –COOH in air (Canas *et al.*, 2002). This gives a weak anionic charge to these membranes which can reduce the passage of cationic molecules such as dendrons and aid their adsorption.

Fig. 4.5a

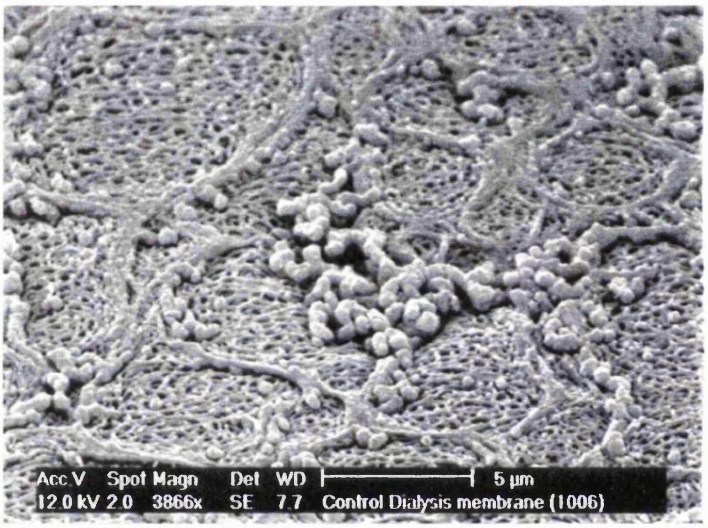

Fig. 4.5b

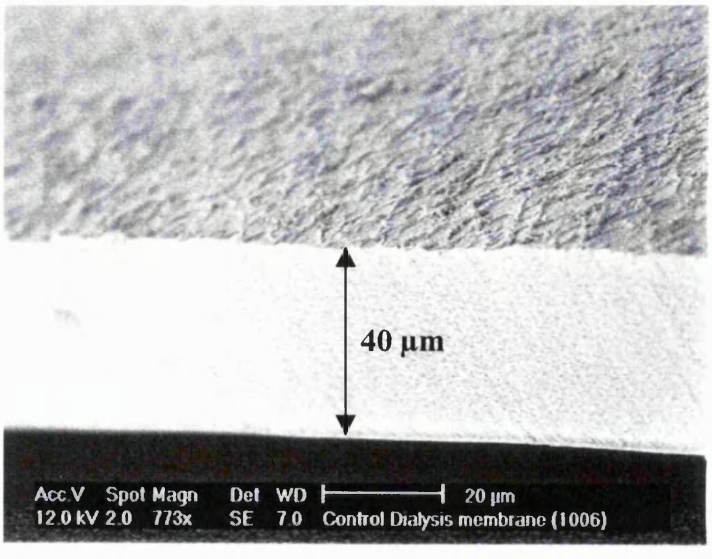

Fig.4.5. *Shows scanning electron micrographs of the cellulose membrane (Spectra/Por 2), representing* ***a)*** *the complex fibrous structure and pores, and* ***b)*** *the membrane cross-section showing the thickness (see Appendix 5).*

Predicting hindered diffusion of colloids has relevance to both theoretical and practical aspects of related membrane filtration processes such as ultrafiltration and microfiltration. The usual approach in hydrodynamic models has been to represent the porous medium of membranes as straight cylindrical pores founded in track-etched membranes. Since many real membrane systems closely resemble arrays of fibres with fluid-filled interstices, one would prefer a more realistic geometric model of the fibrous microstructure. Further, it is obvious that there is a great need for a better understanding of the effects of colloidal interactions on the partition and diffusion of colloids in membrane pores (Pujar and Zydney, 1994).

The influence of salt in the aqueous media was also studied. As seen in Figs. 4.6 and 4.7, increasing NaCl concentrations decreased dendron adsorption to the membrane and improved transport across the membrane. 0.8 M NaCl eliminated adsorption for all three dendrons. After 24 h in the presence of 0.8 M NaCl at 25°C, there was a 33% increase in the amount of 8 amino group dendron, diffusing through the membrane. With 16 and 32 amino group dendrons, the amounts diffusing were doubled.

Canas *et al.* (2002) studied the electrochemical and electrokinetic parameters for cellulose membranes in contact with NaCl and $NaNO_3$ solutions. The electric potential difference at both sides of a membrane when it is separating two solutions of the same electrolyte but different concentrations is called the "membrane potential". Canas *et al.* (2002) determined that when the salt concentration is equal on both sides of the membrane, the membrane potential is approximately zero. If the internal salt concentration is kept constant, an increase in the salt concentration of the external solution produces a negative membrane potential value. The cellulose

membrane behaves as a weak cation exchanger and this agrees with results reported in the literature for different cellulose membranes (Kimura *et al.*, 1984).

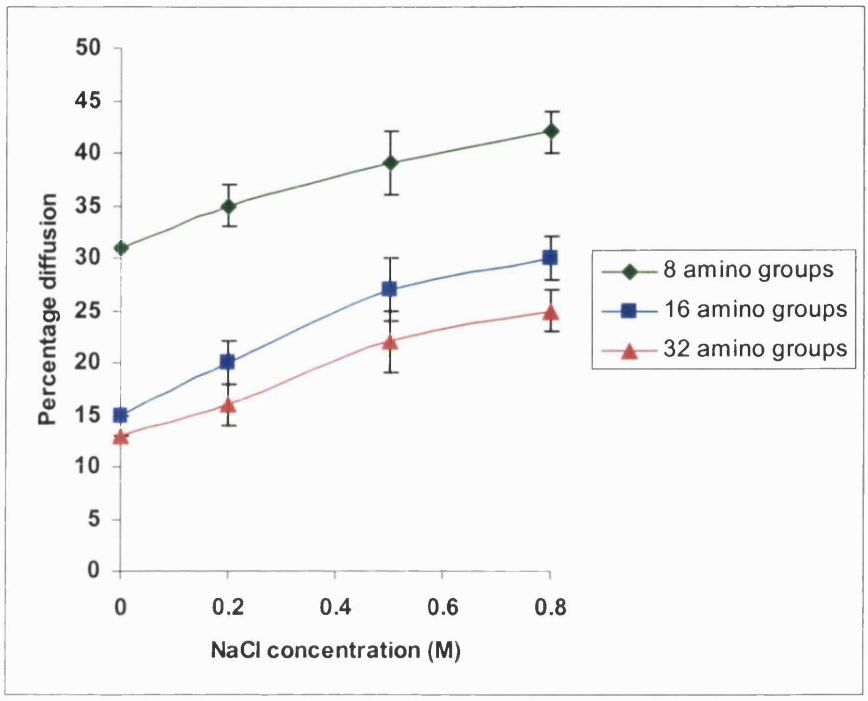

Fig. 4.6. *Showing an increase in percentage diffusion through the membrane over 24 h at 25°C, of the dendrons as NaCl concentration is increased.*

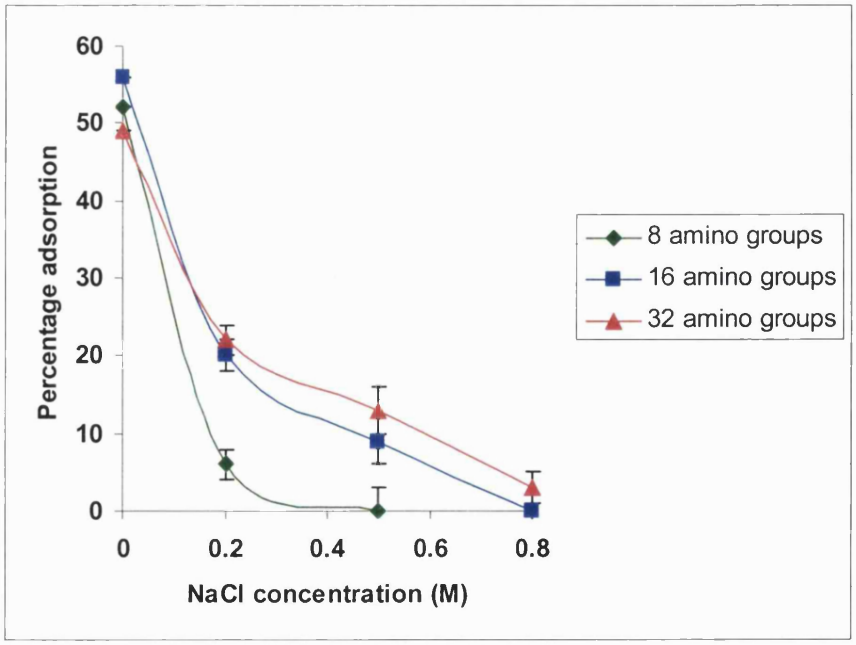

Fig. 4.7. *Showing a decrease in percentage adsorption to the membrane after 24 h at 25°C, of the dendrons as NaCl concentration is increased.*

During these studies, when a buffer was not used, the solution inside the dialysis bag became acidic with time and this was due to some of the $-CH_2OH$ groups being oxidised to –COOH in air. Canas *et al.* (2002) determined that the cation exchange properties of the membrane were more relevant when the membrane was in contact with NaCl solutions than when in contact with $NaNO_3$. A higher permeability was obtained with NaCl solutions than with $NaNO_3$. The use of a pH buffer, in this system, was important. Low pHs which can be attributed to the effects of the cellulose membranes, can lead to ionisation of amino groups present in the dendron structure, which in turn can hinder diffusion of the dendrons.

4.3.2 Apparent membrane diffusion and permeability coefficients

On the basis of Fick's second law, in a system maintaining sink conditions, apparent membrane permeability P and membrane diffusion coefficient D were calculated for each dendron. Fig. 4.8 shows the P and D values for the three dendrons. For the dendrons studied, the diffusion coefficient and permeability decrease with the increasing size and number of amino groups. The apparent diffusion coefficient decreases linearly with size, whereas the apparent permeability decreases in an exponential manner with size.

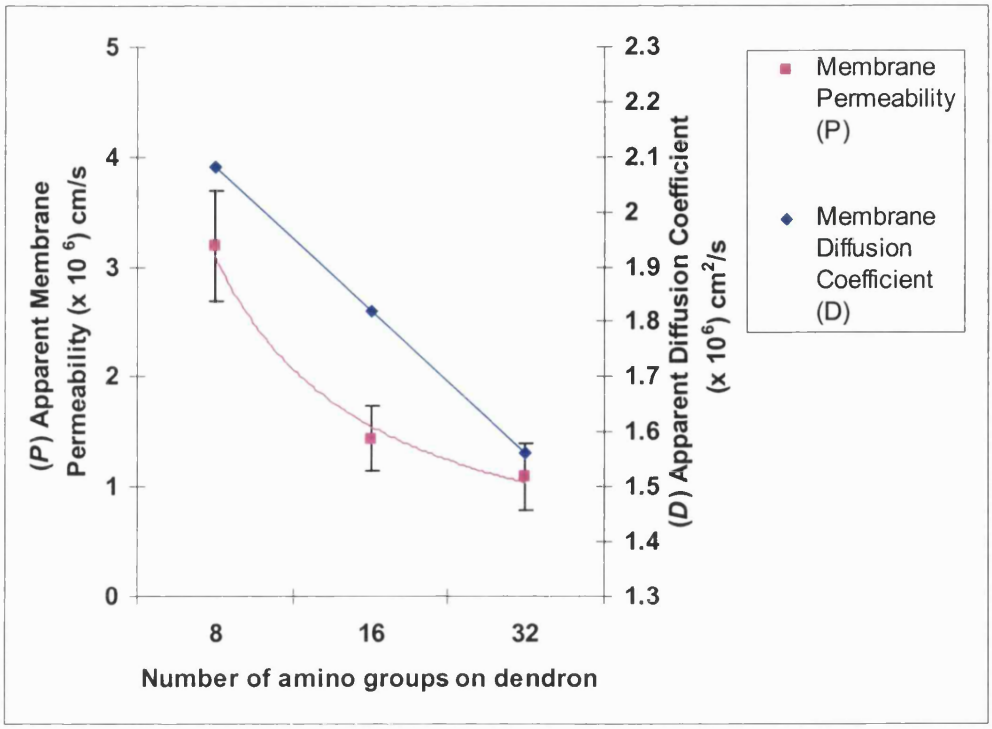

Fig. 4.8. *Membrane permeability and diffusion coefficients for the three dendrons which were calculated at 25°C.*

This can be attributed to the cationic lipidic nature of the dendrons combined with the complex structure of the cellulose membrane. We attempted to use the Perrin or shape factor (F) to better understand the results of our diffusion experiments. The Perrin factor is defined as the ratio of the apparent frictional coefficient for an ellipsoid to that of a sphere having an identical volume and hence, a minimum frictional coefficient (f_0 or f_{min}), and can be informative as an estimate for the deviation from a spherical shape (Tanford, 1961). The ratio is calculated as follows, $F = f_{exp}/f_0$ where, $f_{exp} = 6\pi\eta R_H$ and $f_0 = 6\pi\eta R_S$ in which R_S, as defined for a sphere, is equal to $(3mw.\ \acute{\upsilon}/4\pi N)^{1/3}$ and R_H is the measured hydrodynamic radius. In the expressions above, η is the viscosity, $\acute{\upsilon}$ is the partial specific volume, and N is Avogadro's number. The partial specific volume, $\acute{\upsilon}$, of a molecule is a measure of the change in volume (in ml) of the solution per gram of the molecule in that solution. $\acute{\upsilon}$

= V/mw, where V is the molar volume of the molecule. Table 4.2 shows values for R_H and V for the three dendrons determined using molecular analysis software.

Table 4.2. *Showing the molecular weights, hydrodynamic radii and molar volumes of the three dendrons studied.*

Number of Amino Groups	Molecular Weight	Hydrodynamic Radius (R_H) (nm)	Molar Volume (V) (cm^3)
8	1588	1.05	845
16	2612	1.20	1495
32	4660	1.40	2582

Calculated F values for the dendrons with 8, 16 and 32 amino groups were 1.52, 1.48, and 1.43 respectively and are represented in Fig. 4.10. A value of F in the range of 1.25–1.40 represents a protein or polypeptide which has minimal deviation from a globular (spherical) shape. However, molecules with F values which deviate substantially from unity are suggestive of a non-spherical or ellipsoid shape (Salamat-Miller, 2002). The calculated value of F for the 8 amino dendron, 1.52, is suggestive of a moderately elongated shape. In contrast, an F value of 1.43 for the 32 amino dendron is suggestive of a more globular molecule.

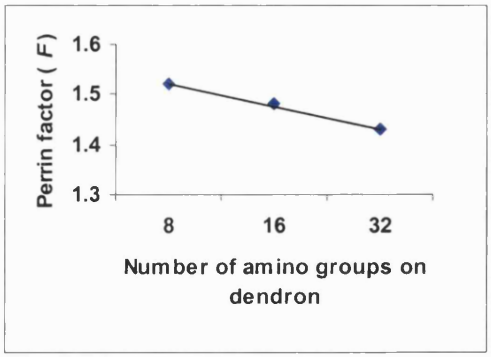

Fig. 4.9. *A graph showing how the Perrin or shape factor decreases with the number of amino groups which suggests the formation of a more globular molecule as size increases.*

As Fig. 4.9 shows, an increase in the number of terminal amino groups leads to the formation of a more globular dendron. In theory the globular (spherical) shape of the 32 amino dendron would have the smallest translational friction in the solution and, therefore, result in a faster rate of diffusion in the liquid-filled channels of the porous membrane. This, however, is not the case and as the lipidic factor is equal for all three dendrons, the increasing cationic charge may be hindering the diffusion of the dendrons. Another factor to consider is the formation of large dendron aggregates in aqueous media, due to their amphiphilic nature.

4.3.3 Membrane and octanol/water partition coefficients

The apparent membrane partition coefficient (K), defined as $C_{membrane}/C_{water}$, is an indication of the affinity which the dendrons have for the cellulose membrane. Fig. 4.10 shows the K values for the 8, 16 and 32 amino group dendrons. The smallest dendron has a K value of 6.13×10^{-3} - approximately twice that of dendrons with 16 (3.16×10^{-3}) or 32 (2.80×10^{-3}) amino groups suggesting a greater affinity towards the cellulose membrane. The K values show that as the number of terminal amino groups of the dendrons increase, the molecule becomes more hydrophilic. This is in agreement with the log P_{ow} values which were calculated from measured octanol/water partition coefficients. The average log P_{ow} values were –0.423, –0.569 and –0.618, respectively for 8, 16 and 32 amino dendrons. Fig 4.11 shows a linear correlation between K and log P_{ow} values.

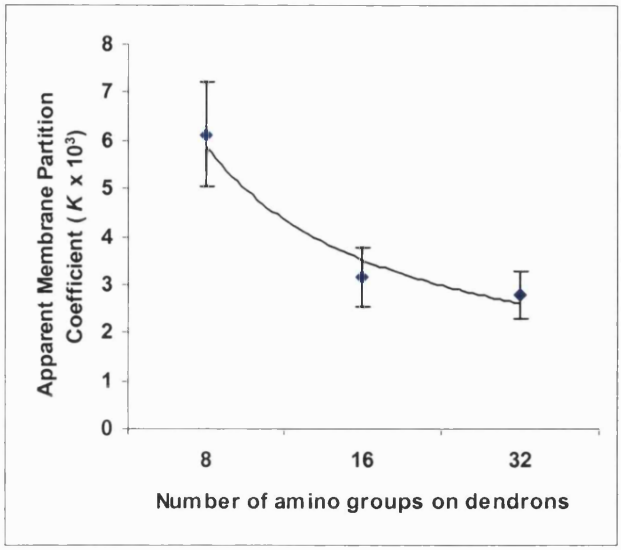

Fig. 4.10. *A graph showing the apparent membrane partition coefficient (K) values for the three dendrons at 25°C.*

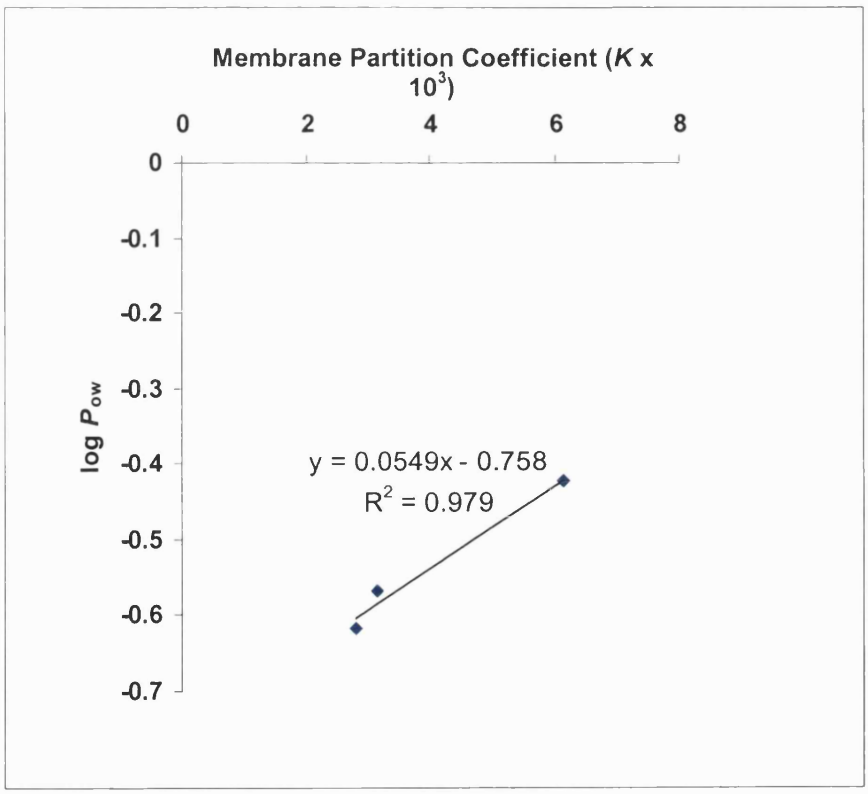

Fig. 4.11. *A graph showing a linear correlation between membrane partition coefficient (K) and log P_{ow} values.*

4.3.4 Thermodynamics of diffusion

Using Eq. 8 ($\ln P = \ln P_0 - Ep/RT$), an Arrhenius-like plot was constructed (Fig. 4.12) to calculate the energy of activation for permeation (Ep) for each of the dendrons. The straight line of the plot is represented by; $y = c + mx$, where $y = \ln P$, $c = \ln P_0$, $m = -Ep/R$ and $x = 1/T$.

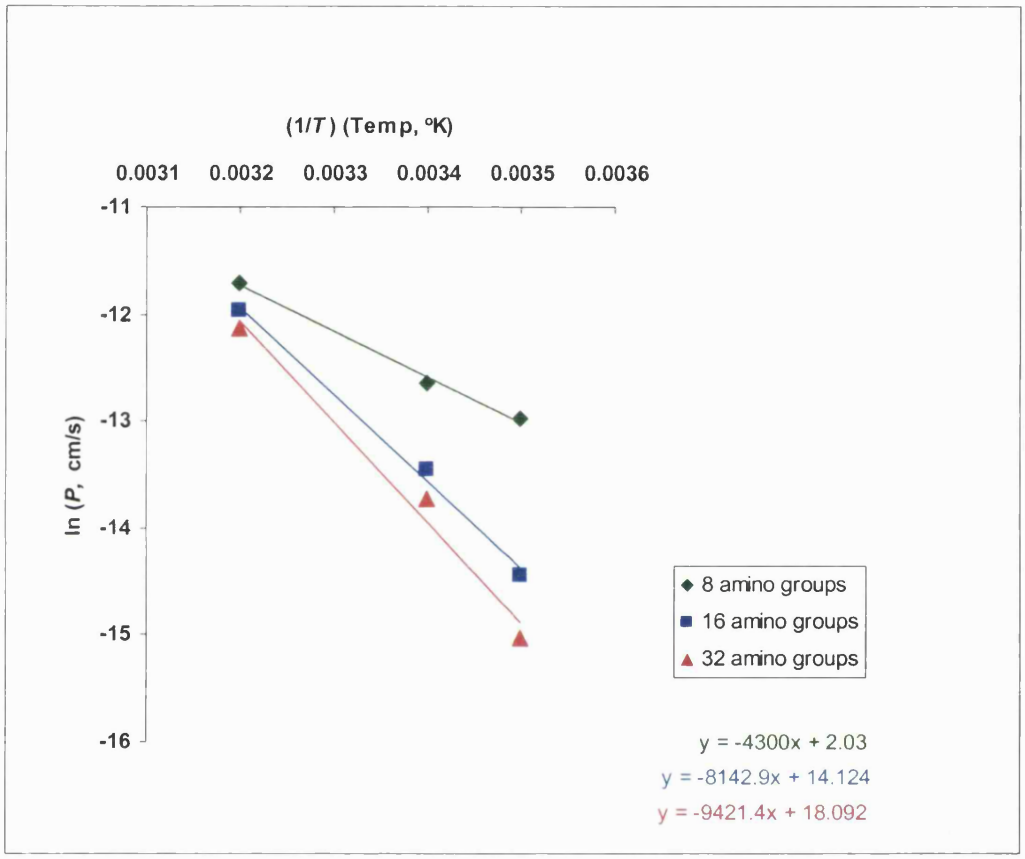

Fig. 4.12. *An Arrhenius-like plot (ln permeability versus reciprocal absolute temperature) for the diffusion of the three dendrons, where the slopes of the lines are equal to the energy of activation for permeation.*

From Fig. 4.12, the respective activation energies for dendrons with 8, 16 and 32 amino groups were 517, 979 and 1133 kJ/mol. This shows that the smallest dendron, which is more lipophilic, requires a much lower activation energy to engage in the diffusion process, in comparison to the larger and more hydrophillic dendrons. Blank *et al.* (1967) showed that the apparent activation energies for permeation through

human skin by lower alcohols (ethanol to pentanol) and higher or less polar alcohols (hexanol to octanol) were 69 kJ/mol and 42 kJ/mol, respectively. The larger less polar alcohols penetrate the skin more rapidly and the smaller polar compounds have higher activation energies.

4.3.6 Dendron-albumin interaction studies

As can be seen in Fig. 4.13, the dendrons are relatively large in comparison to conventional drugs that bind to albumin.

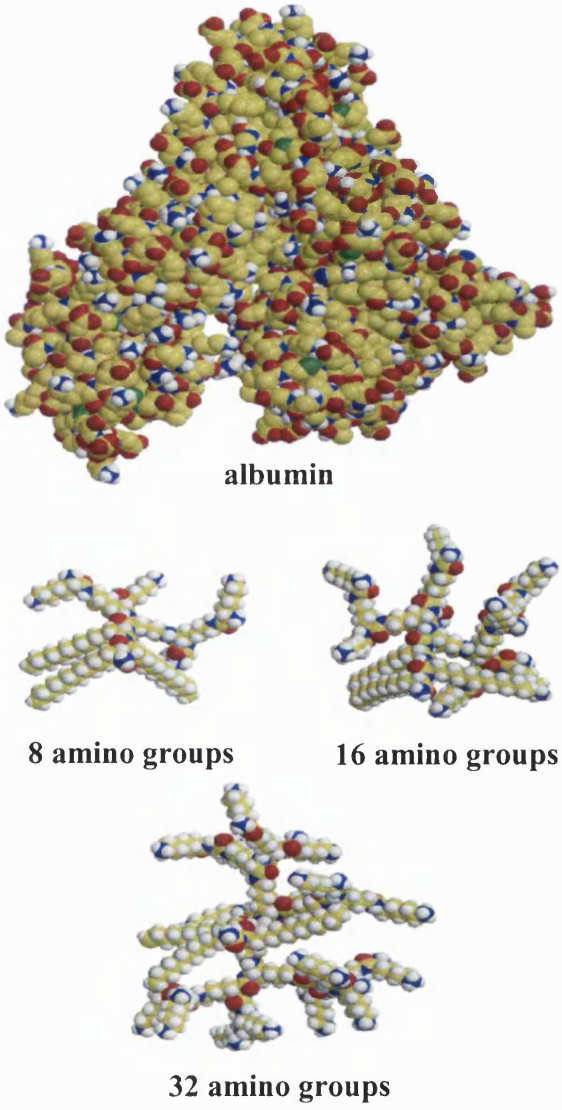

Fig. 4.13. *Scale molecular models of albumin in comparison with 8, 16 and 32 amino group dendrons.*

Initial studies were carried out with the smallest dendron. The amounts of dendron was kept constant (100 μg) and were placed in 5 ml aliquots in dialysis tubing with various concentrations of BSA, which were 1, 3, 5 and 10 % w/v. The mixtures were diffused for 24 h at 25°C and a control experiment absent of BSA was performed. 0.8 M NaCl was added to the systems to minimise adsorption to the cellulose membranes. Fig. 4.14 shows the diffusion profiles for the dendron with 8 amino groups. There is a significant difference in the profiles of the control experiment and the albumin- containing experiments.

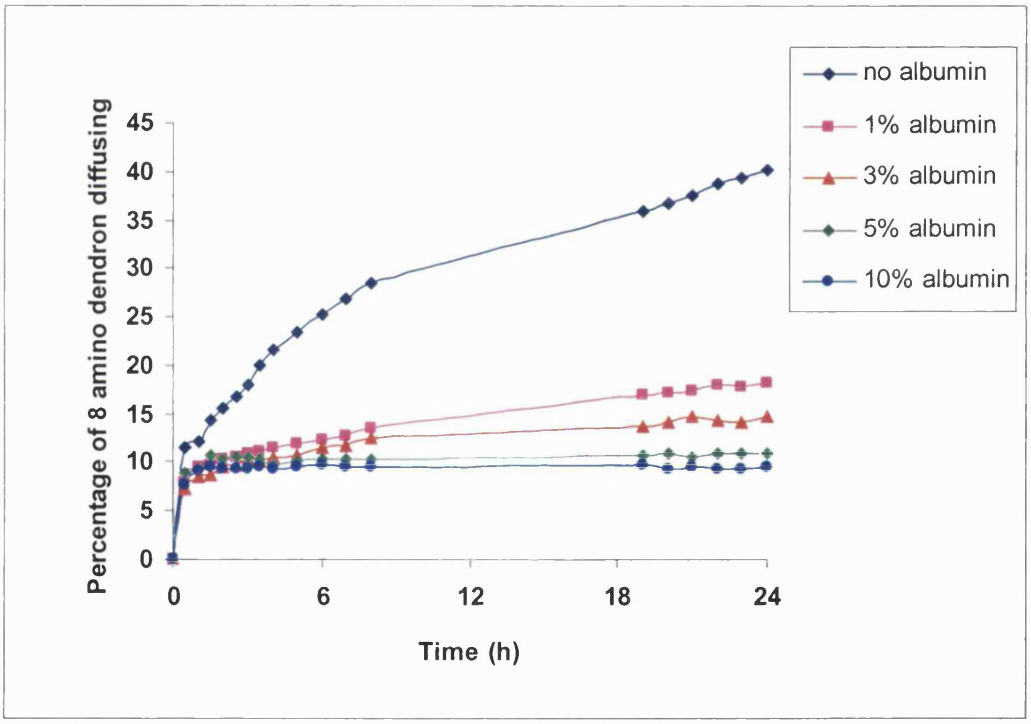

Fig. 4.14. *The diffusion profiles of dendrons with 8 amino groups and how various concentrations of albumin (BSA) affects the average percentage of dendrons diffusing over 24 h at 25°C.*

The presence of 1% w/v of albumin reduced the percentage of diffusion of dendrons by more than 50%. As the albumin concentrations increased, the effects were not as significant but did result in a reduction of the percentage of diffusion from the dialysis bag with increasing albumin concentrations. Albumin is the most abundant

protein in plasma with a typical concentration of 5% w/v and contributes 80% to colloid osmotic blood pressure (Carter and Ho, 1994). The results showed that the smallest dendron interacted with albumin but the mechanism of interaction was not clear. Before commencing further studies, more information about albumin was obtained using software and molecular modelling analysis templates from CHARMm. BSA consists of 578 amino acids and has a net formal charge of –15; this information is detailed in Table 4.3.

Table 4.3. *The composition of amino acids in bovine serum albumin showing the number of each amino acid and their contribution to the formal charge.*

Amino acid	Number of amino acid	Formal charge contribution
Ala	61	
Arg	24	+24
Asn	17	
Asp	35	–35
Cys	35	
Glu	62	–62
Gln	20	
Gly	11	
His	15	(uncharged)
Ile	8	
Leu	59	
Lys	58	+58
Met	6	
Phe	31	
Pro	24	
Ser	24	
Thr	28	
Trp	1	
Tyr	18	
Val	41	

All of the amino acids are in a single polypeptide chain and the molecule is built from three structurally homologous domains (I, II and III). Each domain is the product of two sub-domains (IA, IB, etc.) (Peters, 1996).

Considering regions of high anionic charge on the albumin surface, electrostatic interactions were expected. To understand the distribution of the charge on the surface of the albumin molecule, plots of electrostatic potential on the molecular surface were constructed. Fig. 4.15 shows six different views of an albumin molecule where blue represents a positive potential and red represents a negative potential. As the respective colours become darker, the corresponding charge increases in potential.

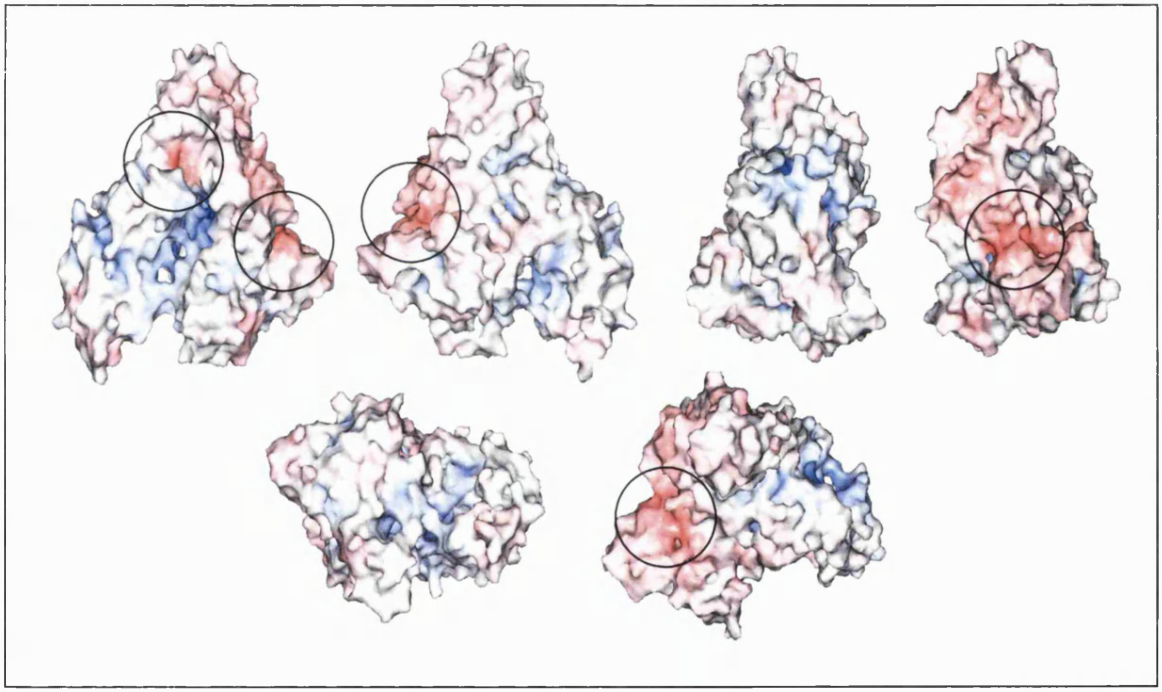

Fig. 4.15. *Six different views of the albumin molecule showing the electrostatic potential on the molecular surface where blue denotes a cationic charge and red denotes an anionic charge.*

In Fig. 4.15, the deeper red regions of the albumin molecule which are circled indicate an electrostatic potential in the region of –25 to –35 mV. The paler pink regions indicate an electrostatic potential in the region of –5 to –20 mV, depending on the intensity of the red colour. This shows that the albumin molecule has regions of anionic charge on the surface which can potentially interact with the cationic

dendrons. Due to the comparable dimensions of dendron and BSA molecules, it was not expected that the dendrons could penetrate into the protein matrix. To further understand the interactions between cationic dendrons and albumin, at a molecular level, different molar ratios were mixed and analysed.

The results, represented in Fig. 4.16, show that none of the dendrons interact with albumin in a stoichiometric manner but there is a degree of interaction. Approximately two dendrons with 8 amino groups interacted with three albumin molecules. Dendrons with 16 and 32 amino groups interacted with approximately four and five albumin molecules, respectively.

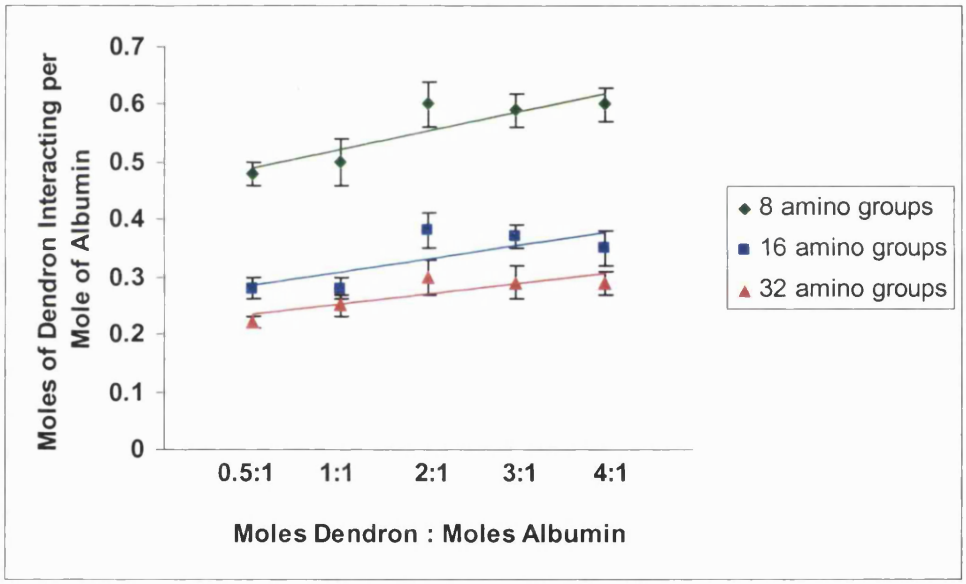

Fig. 4.16. *Moles of dendrons interacting per mole of albumin at various molar ratios after 24 h at 25°C.*

The results show that cationic dendrons interact with albumin and the dendrons bridge the albumin molecules. As the size of the dendron increases, so does the number of terminal amino groups resulting in a greater bridging capacity. The mechanism by which the bridging occurs is likely to be electrostatic. Klagnert *et al.* (2003) studied the interactions between PAMAM dendrimers and BSA. They used dendrimers of generation 3.5 (COOH terminal groups) and two of generation 4 (NH_2

and OH terminal groups). Using spectral assays they found that the biggest changes in the spectral shape and its position were observed for PAMAM dendrimers of generation 4 with amino group terminals. No effect was found for hydroxy-terminated dendrimers. The group also observed that BSA fluorescence was strongly quenched by amino-terminated dendrimers but was poorly quenched by dendrimers with COOH and OH terminal groups. To determine whether the cationic amino terminals were involved in the interaction with BSA, further studies were conducted with the smallest dendron. The 8 terminal amino groups were acetylated ($-COCH_3$) to neutralise the cationic charge (molecule 1d) and mixed with albumin under the same conditions as previously. Fig. 4.17 shows the diffusion profiles for dendrons with 8 amino groups, which are amino-terminated and acetate-terminated, in the presence of albumin.

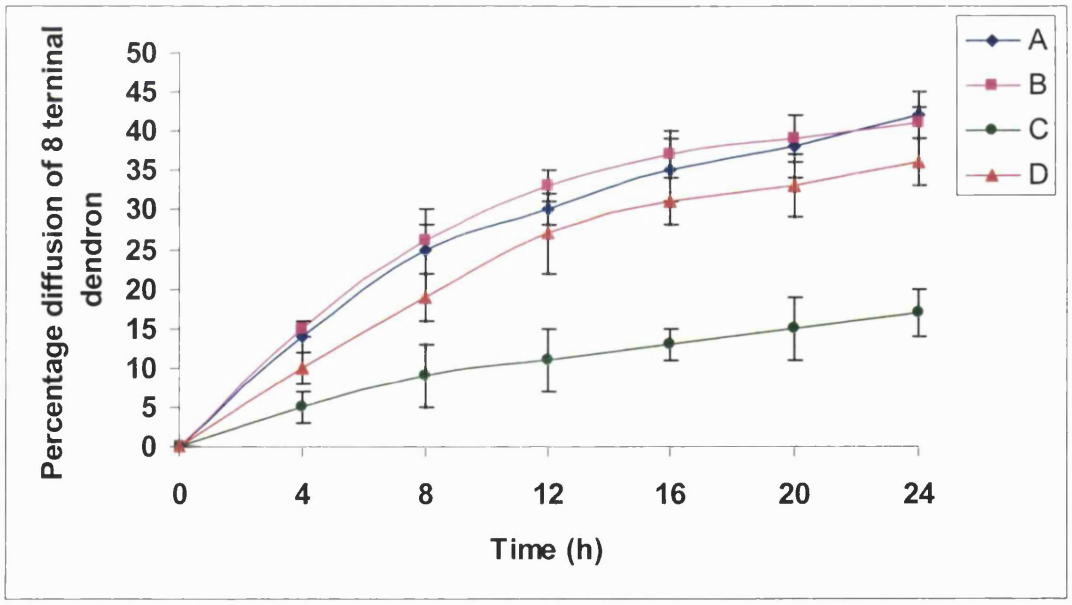

Fig. 4.17. *The percentage diffusion profiles of dendrons with 8 terminal groups and the effects of different terminal groups on their interaction with BSA at 25°C over 24 h. Profile A= amino-terminated dendrons without BSA; Profile B= acetate-terminated dendrons without BSA; Profile C= amino-terminated dendrons with BSA (1:2); Profile D= acetate-terminated dendrons with BSA (1:2).*

Amino and acetate-terminated dendrons showed almost identical diffusion profiles in the absence of albumin and approximately 40% of each dendron diffused over a 24 h period. When albumin was added, there was a significant difference between the diffusion profiles of both dendrons. The acetate-terminated dendron exhibited 36% diffusion over 24 h and was slightly lower, but similar to when the albumin was absent. However, only 17% of the amino-terminated dendron diffused over 24 h when albumin was present. This also suggests that the cationic terminal groups interact with albumin whereas the neutral acetate groups do not seem to have a significant interaction with albumin. This study also showed, when albumin was absent, that the diffusion of charged dendrons and neutral dendrons did not differ in the system used. This indicates that the interactions between dendrons and BSA are probably of electrostatic nature. That is why they are the weakest for neutral acetate-terminated dendrons. At pH 7.4 (the pH of blood), BSA has the negative net charge (–15); therefore, amino-terminated cationic dendrons have the biggest impact on the protein. However, serum albumin molecules are not uniformly charged within the structure and in physiological pH, domain I (–11) and domain II (–7) are negatively ionised (Carter and Ho, 1994), giving the place for possible contact between the BSA surface and the cationic amino-terminated dendrons.

4.4 CONCLUSION

These studies show that NaCl improved the transport of cationic lipidic dendrons through cellulose membranes. High molar concentrations of NaCl (0.8 M) were shown to eliminate dendron adsorption to the cellulose membranes. The mechanisms by which this occurred are unclear and whether NaCl affects the dendrons, membrane or both needs to be determined. The apparent values for membrane permeability P, membrane diffusion coefficient D and the membrane partition coefficient K values were calculated for each dendron. P and D values were highest for the 8 amino group dendron. The membrane partition coefficient K was greatest for the 8 amino group dendron. This was also the case with octanol/water partition coefficient studies. Calculations based on experimental values and molecular modelling analysis showed that the shapes of the dendrons become more quasi-spherical with each generation of growth.

The stoichiometry of dendron: albumin interactions was found to be 1:1.5, 1:4 and 1:5 for the dendrons with 8, 16 and 32 amino groups, respectively. Although the mode of this interaction is still unclear, molecular modelling studies of the dendrons and albumin reveal the possibility of electrostatic interactions. This possibility was strengthened by the fact that the diffusion of acetate-terminated dendrons (neutral) was not reduced by albumin, unlike the diffusion of amino-terminated (cationic) molecules.

CHAPTER FIVE

THE SYNTHESIS AND PROPERTIES OF A NOVEL DIDENDRON

The design of a stable didendron can lead to the production of a molecule which possesses unique characteristics. The supramolecular architectures arising from such polymers have the potential to produce interesting properties and the scope for synthesising functional tri- and quadratic dendritic structures. A major potential of such structures will be the ability to incorporate different peripheral functionalities on each segment of a multi-dendron molecule. In the case of didendrons, their dumbbell-like shape can allow for the "bar" to be modified and possess unique properties in its own right. In this chapter, the viscosities of these didendrons will be studied, together with a general discussion regarding viscosity of dendrimers.

5.1 INTRODUCTION

5.1.1 Multi-functionalised dendrimers

Block copolymers composed of poly(ethylene glycol) (PEG) have been utilised in various drug delivery systems because of their high solubility in water, non-immunogenicity and improved biocompatibility (Gref *et al.*, 1994). Choi *et al.*, (1999) reported the concept of a copolymer which takes advantage of the above mentioned copolymers and dendrimers. Their aim was to conjugate linear PEG with a dense globular poly(L-lysine) dendrimer to produce a block copolymer using liquid phase peptide synthesis (Fig. 5.1). They showed that this linear polymer/dendrimer block copolymer assembled spontaneously with plasmid DNA, forming a water-

soluble complex which increased the stability of the complexed DNA. Choi and co-workers then expanded on this idea and developed a barbell-like triblock copolymer, poly(L-lysine) dendrimer- *block* -poly(ethylene glycol)- *block* -poly(L-lysine) dendrimer (PLLD-PEG-PLLD) (Fig 5.2). These triblock copolymers also spontaneously formed a complex with DNA (Choi *et al.*, 2000) and did not show cytotoxicity towards cells as did the linear copolymers such as PLL.

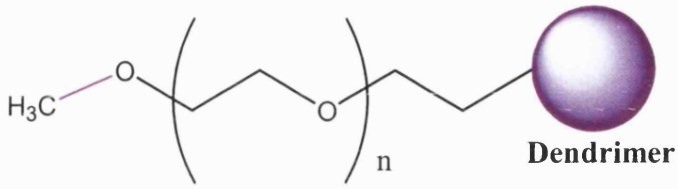

Fig. 5.1. *A structural representation of a linear poly(ethylene glycol)-block-poly(L-lysine) dendrimer.*

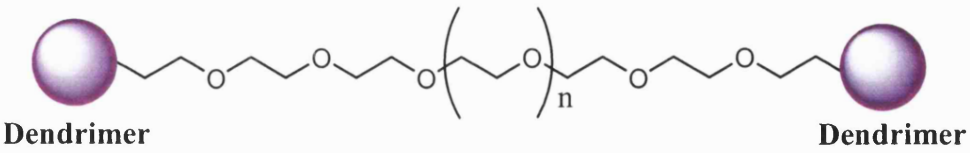

Fig. 5.2. *A structural representation of a barbell-like triblock copolymer, poly(L-lysine) dendrimer- block -poly(ethylene glycol)- block -poly(L-lysine) dendrimer (PLLD-PEG-PLLD).*

As discussed previously, the location of the functional group or attachment can change the properties of a dendritic molecule. Apart from the site of functionality, the number of different functional groups within the dendrimer also influences its properties. Two functions being present in one molecule is very important for certain applications and, e.g. for the examination of such compounds which try to mimic

biological systems (Sadamoto *et al.*, 1996). The bifunctionalisation of dendrimers has already been realised in different combinations. Wang *et al.* (1996) joined aniline or phenyl derivatives on the periphery of a dendrimer with an anthracene moiety as the core unit and obtained electroluminescent diodes this way. The alternative dendrimer, in which one function is situated in the core and the other one in the branching units, has been prepared, e.g. by Balzani *et al.* (1998). It consists of an osmium complex in the centre and several ruthenium complexes in the branches, leading to a "light-harvesting effect".

Wooley *et al.* (1993) succeeded in a combination of unlike functions on the periphery of a dendrimer by coupling two differently functionalized dendrons. Thus, the linkage of a polynitrile-determined dendron and a benzylic ether dendron leads to dendrimers with an enhanced macromolecular dipole moment, whereas the analogous coupling of lipophilic benzyl ether dendrons and hydrophilic carboxylate-functionalized dendrons leads to globular amphiphilic dendrimers (Hawker *et al.*, 1993). The latter are able to stabilize emulsions of water in dichloromethane over a long period of time. Ganesh *et al.* (2002) described the synthesis of benzyl ether dendrimers that are bifunctionalised at their peripheries using phenolic functionalities. They determined that for this synthesis to be facile, it was necessary to have one of the two phenolic groups in dihydroxybenzyl alcohol more reactive than the other.

The field of trifunctionalised dendrimers has been explored by Salamończyk *et al.* (2002). Using a developed method for the synthesis of phosphorus-based dendrimers involving chemistry of trivalent phosphorus derivatives, they reported a highly efficient synthesis of new heteroorganic dendrimers having different chalcogen

atoms bound to a branching phosphorus at different 'layers' of a dendrimer. In this chapter, two different synthetic strategies to produce didendrons will be discussed.

5.1.2 Viscosity of dendrimers

Fréchet (1994) made a macroscopic analogous comparison of dendrimers and linear polymers, stating they are like "green peas" and "cooked spaghetti", respectively. This analogy was in reference to the monodisperse, globular nature of dendrimers compared with the entangled linear polymers. In general terms the intrinsic viscosity [η] of linear polymers can be described by the Mark-Houwink-Sakurada equation;

$$[\eta] = K M^{a}$$

Where M is the molecular weight of the polymer and K and a are constants for the given polymer. According to this equation, intrinsic viscosity is directly proportional to the molecular weight. Dendrimers only obey this relation until a certain threshold is reached (Fréchet, 1994). This can be explained by the fact that dendrimers undergo a transition from a linear to a more globular shape with increasing molecular weight and generations of growth.

Interdendrimer interactions and the intrinsic viscosity of dendrimers have been studied by experimental (Uppuluri *et al.*, 1998, Prosa *et al.*, 1997, Jockusch *et al.*, 2001, Mourey *et al.*, 1992, Fréchet *et al.*, 1994) and theorectical (Mansfield, 2000, Pavlov *et al.*, 2002) means.

In general, the literature cited above, discusses the concept of dendrimers molecules having small intrinsic viscosities with the values highly dependent on the molecular weight (Pavlov *et al.*, 2002). Prosa *et al.* (1997) used small-angle x-ray scattering to characterise the single-particle scattering produced by dendrimers and hyperbranched polymers in dilute methanol solutions. They found that PAMAM dendrimers, G7 to G10, produced scatter patterns indicative of monodisperse, spherical particles with uniform internal segment densities. The hyperbranched polymers produced scatter patterns suggesting more irregular internal segment densities. Uppuluri and co-workers (1998) demonstrated that PAMAM dendrimers exhibited Newtonian flow behaviour, with constant viscosities, in ethylenediamine (EDA). This behaviour was consistent across a range of shear rates and shear stresses and there was no indication of interdendrimer entanglement of molecules. This study showed that an increase in dendrimer generation, resulted in an increase in the viscosity of the EDA solution.

5.2 MATERIALS AND METHODS

5.2.1 Didendron synthesis on solid support

METHOD C

This synthetic method required the design of a core which could be attached to a solid support and allow two-way growth of a dendritic structure. Thus cleavage of the resin would yield a crude didendron molecule.

5.2.1.1 Core design (Part I)

The first step was to prepare Boc-protected 2,3 diaminoproprionic acid (DAPA). DAPA (0.5 g, 3.56 mmol) was suspended in a 2:3 mixture of *tert*-butyl alcohol/water (15 ml) and 8 M aqueous NaOH was added drop-wise to adjust the pH=13. Di-*tert*-butyl dicarbonate (2.33 g, 10.68 mmol) in *tert*-butyl alcohol (5 ml) was added at room temperature. The pH value was adjusted to 11-12 and the reaction mixture was stirred overnight. Next the reaction mixture was diluted with water (6.25 ml) and solid citric acid was added to adjust the pH=3. The oil was then extracted with ethyl acetate (3 x 20 ml). After drying (anhydrous $MgSO_4$), the organic layer was evaporated. The residue was triturated with cold acetonitrile and the product was filtered and dried to yield 0.958 g di-(Boc)-2,3 diaminoproprionic acid (M_r = 303.57).

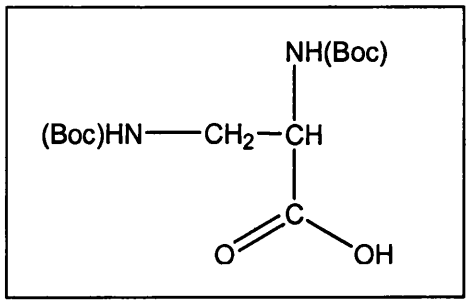

5.2.1.2 Core design (Part II)

The second step was to prepare Boc-6-aminocaproic acid. 6-aminocaproic acid (8 g, 61.7 mmol) was suspended in a 2:3 mixture of *tert*-butyl alcohol/water (240 ml) and

8 M aqueous NaOH was added drop-wise to adjust the pH=13. Di-*tert*-butyl dicarbonate (20 g, 91.6 mmol) in *tert*-butyl alcohol (40 ml) was added at room temperature. The pH value was adjusted to 11-12 and the reaction mixture was stirred overnight. Next the reaction mixture was diluted with water (50 ml) and solid citric acid was added to adjust the pH=3. The oil was then extracted with ethyl acetate (3 x 150 ml). After drying (anhydrous $MgSO_4$), the organic layer was evaporated. The residue was triturated with cold acetonitrile and the product was filtered and dried to yield 12.716 g Boc-6-aminocaproic acid (M_r = 230.5).

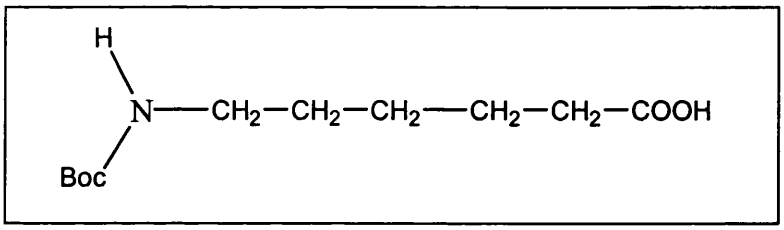

5.2.1.3 Core design (Part III)

The final step was to combine the Boc-protected DAPA and the Boc-protected aminocaproic acid to a solid support (*p*MBHA resin, capacity = 0.67 mmol/g). The following procedure used 3 times excess reagent for each step to ensure completion of each reaction (0.67 x 3 ≈2 mmol). The HBTU solution used contained 19.5 g HBTU in 100 ml DMF and the ninhydrin test was used to monitor each coupling and deprotection step.

1 g *p*MBHA resin was coupled to di-(Boc)-2,3 DAPA (606 mg, 2 mmol) using HBTU solution (4 ml) and DIEA (0.48 ml) to produce ***compound 1*** (Fig. 5.3). This was followed by deprotection of *compound 1* with TFA.

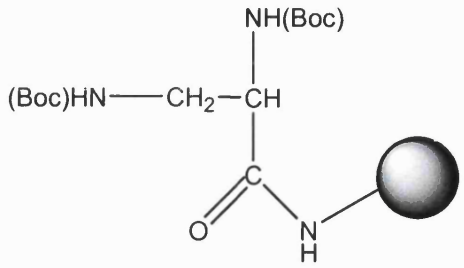

Fig. 5.3. *Compound 1 representing di-(Boc)-2,3 diaminoproprionic acid attached to pMBHA resin.*

Following deprotection, Boc-6-aminocaproic acid (924 mg, 2 x 2 mmol as diamine substitution) was added together with HBTU solution (8 ml) and DIEA (0.96 ml) and the reaction mixture was shaken to completion to produce ***compound 2*** (Fig. 5.4). This was the completed core structure to allow two-way dendritic growth to synthesise didendrons.

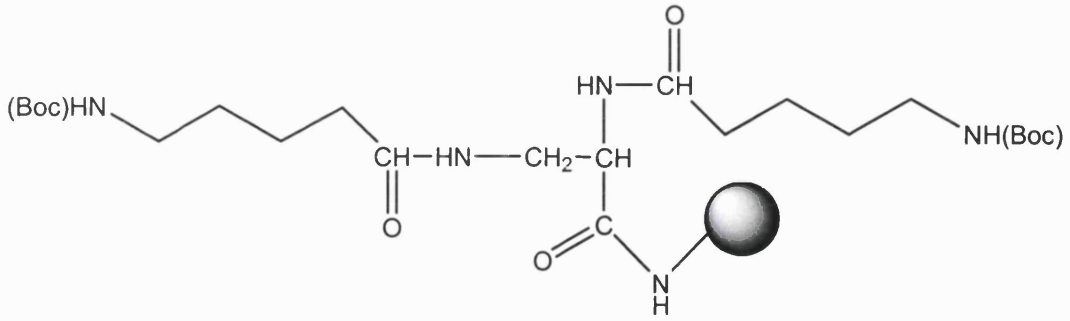

Fig. 5.4. *Compound 2 representing the final structure of the core.*

The dendritic two-way branching of these molecules was produced using the synthetic method previously described in section 2.10.1 (Method A) but the amounts of reagents used were doubled for each coupling/generation growth step. Cleavage and post-cleavage procedures were as described in Method A (Chapter 2).

5.2.2 Didendron synthesis by coupling single dendrons in liquid phase

METHOD D

This method was studied using glycine-tailed dendrons 2b, 2d, 2h, 2j, 2l and 2n (section 2.10.2). All of these dendrons were constructed on a PAM resin, leaving a free COOH at the end of the tail. Also each of these dendrons had their terminal groups acetylated to render the periphery inactive.

Excess of a particular dendron (3 molar quantities) was reacted with 1,12-diaminododecane (1 molar quantity) in DMF in the presence of HBTU and DIEA to couple two dendron molecules to each molecule of 1,12-diaminododecane. This reaction mixture was stirred overnight at room temperature and this procedure was carried out for each of the dendrons mentioned above.

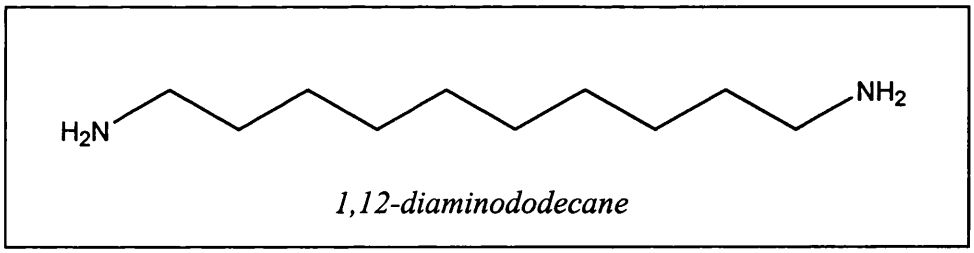

1,12-diaminododecane

The DMF was evaporated, followed by the addition of water. Chloroform was added to solubilise any unreacted 1,12-diaminododecane. All other components of the reaction were water soluble and had to be separated using HPLC.

5.2.3 Dynamic viscosity measurements

Dynamic viscosity of dendritic molecules was measured using an Anton Paar AMVn automated microviscometer (Ref. 1). This equipment is based on the "rolling ball" principle. The sample to be measured is introduced into a glass capillary in which a

steel ball rolls. The viscous properties of the test fluid can be determined by measuring the rolling time of the steel ball. The measuring system used was 'manually-filled' and this consisted of 1.5 mm diameter balls and two capillaries with diameters of 1.6 mm (capillary 1-400 µl volume) and 1.8 mm (capillary 2-510 µl volume). Capillary 1 was used to measure viscosities ranging from 0.3-10 mPa.s and capillary 2 could measure viscosities ranging from 2.5-70 mPa.s. All experiments were performed using different dendron concentrations (2.5-10 mg/ml) at various temperatures (25-55°C). All molecules were solubilised in double deionised water.

The exact determination of the viscosity required the measuring system and the AMVn to be calibrated, to determine the calibration constant, $K_1(\alpha)$ and the instrument constant, K_2 (Ref. 1).

5.2.3.1 Determining the viscosity

The rolling time "t_0" of a ball over a defined measuring distance in the capillary was measured for each sample. The dynamic viscosity of the sample is calculated from the calibration constant of the measuring system, the rolling time and the difference of density between the ball and sample, using the following formula (Ref. 1);

$$\eta = K_1(\alpha).t_0.(\rho_K - \rho_S)$$

where η is the dynamic viscosity of the sample (mPa.s); $K(\alpha)$ is the calibration constant of the measuring system (mPa.cm^3/g); t_0 is the rolling time for 100mm (s); ρ_K is ball density (7.85 g/cm^3); and ρ_S is the density of the sample (g/cm^3).

5.2.4 Molecular modelling and analysis

Molecular modelling and analysis of the dendrons and didendrons was performed using a combination of Quanta 96 (version 96.0516) and CHARMm (version 23.2). ChemOffice software from CambridgeSoft was also used to prepare diagrammatic and three-dimensional structures.

5.2.5 Self-assembling dendritic aggregates

A series of terminal-acetylated dendrons (2d, 2f, 2h and 2j) were solubilised in water in concentrations of 1 mg/ml and 5 mg/ml. They were studied for their self-assembling properties and analysed with a Mastersizer X, for size measurements, and a Zetasizer 3000, for zeta potential measurements. Both instruments were manufactured by Malvern Instruments, Malvern, UK (section 3.2.4).

5.2.6 Micrograph images

Light micrographs were taken using the Nikon Microphot-FXA light microscope which was attached to a Sony UP-860CE video graphic printer. Paint Shop Pro 5 (Jasc Software) was used to capture images directly from the microscope (see Appendix 5).

5.3 RESULTS AND DISCUSSION

Note: In the respective figures, the distribution of data values is represented by showing a single data point, representing the **mean** *value of the data, and the error bars represent the overall* **distribution** *of the data.*

5.3.1 Didendron synthesis

Method C successfully produced three didendron molecules (**3a-c**) which are summarised in Table 5.1 (see Appendix 4 for characterisation data). All three molecules were water-soluble (see Appendix 6) and the apparent hydrodynamic diameters were calculated using molecular analysis software. The didendron with 2 x 16 terminal lysine (2 x 32 amino groups) is diagramatically represented in Fig 5.5.

Table 5.1. *Summary of the three didendron molecules synthesised using Method C.*

Molecule	Terminal Lys	Terminal NH_2	M_r	Hydrodynamic Diameter (nm)
3a	2 x 8	2 x 16	4130	4.7
3b	2 x 16	2 x 32	8226	5.4
3c	2 x 32	2 x 64	16418	6.3

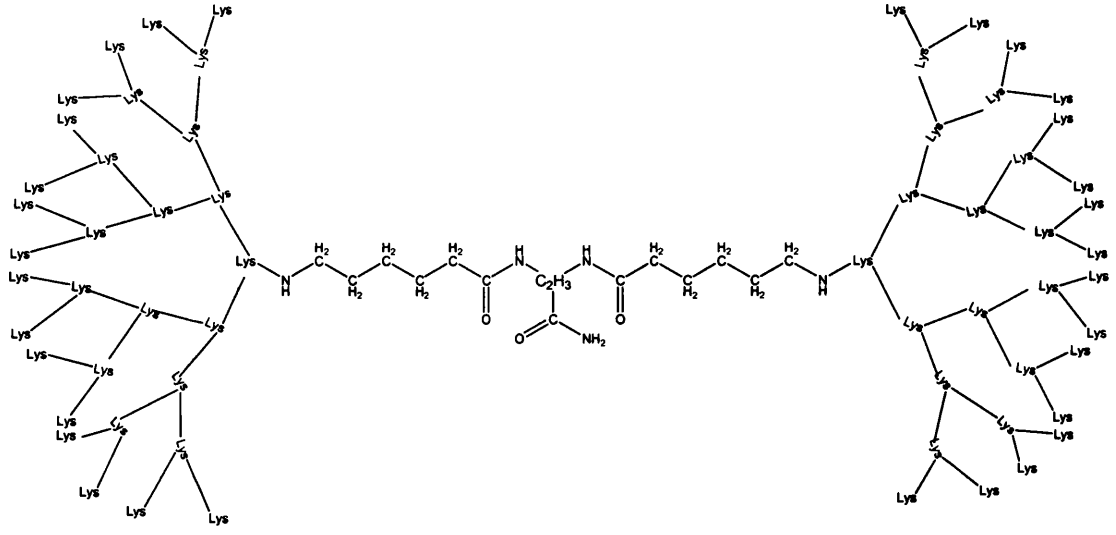

Fig.5.5. *A diagrammatic representation of the structure of a didendron molecule, with 2 x 16 terminal lysine (3b), synthesised using Method C.*

The yields of molecules 3a, 3b and 3c were 82%, 71% and 59% respectively. The reduction in yield, with growth of the molecules, is likely to be caused by steric hindrance. Thus preventing complete coupling to the reactive terminal lysines resulting in incomplete molecules. Although the yields were adequate, further addition of excess reagents and lengthening of coupling reaction times, did not produce any significant improvements in the yields. Method C did however prove highly successful when compared to Method D. Method C provided the crude molecule following cleavage of the solid support but Method D proved to be very difficult and not economical.

With Method D, the only way to isolate the required compound was using HPLC, which was a very tedious and unsuccessful method. As the synthetic approach required the use of excess dendrons, this resulted in dendrons which were not coupled to the diaminododecane, as well as sub-compounds. In most instances, the required molecules were not found. Evidence of didendron formation was only found when the reaction involved molecules 2b and 2l. Both of these molecules had only 16 terminal groups, presenting with the least steric hindrance to the reaction and this was the critical factor when compared to the length of the glycine tail. On this evidence, the lack of dendritic branching was the rate determining step.

Fig. 5.6 shows to scale, the wire molecular models of molecules 3a-c. An increase in steric hindrance of the terminal groups, as the didendrons grew, is evident from these models. Fig. 5.7 represents solid 'solvent accessible surface' models of the didendrons 3a-c. Each model is represented along its longest possible *x-axis* distance against its longest possible *y-axis* distance. The position of the *x-axis* is based on the position of the lipidic didendron core.

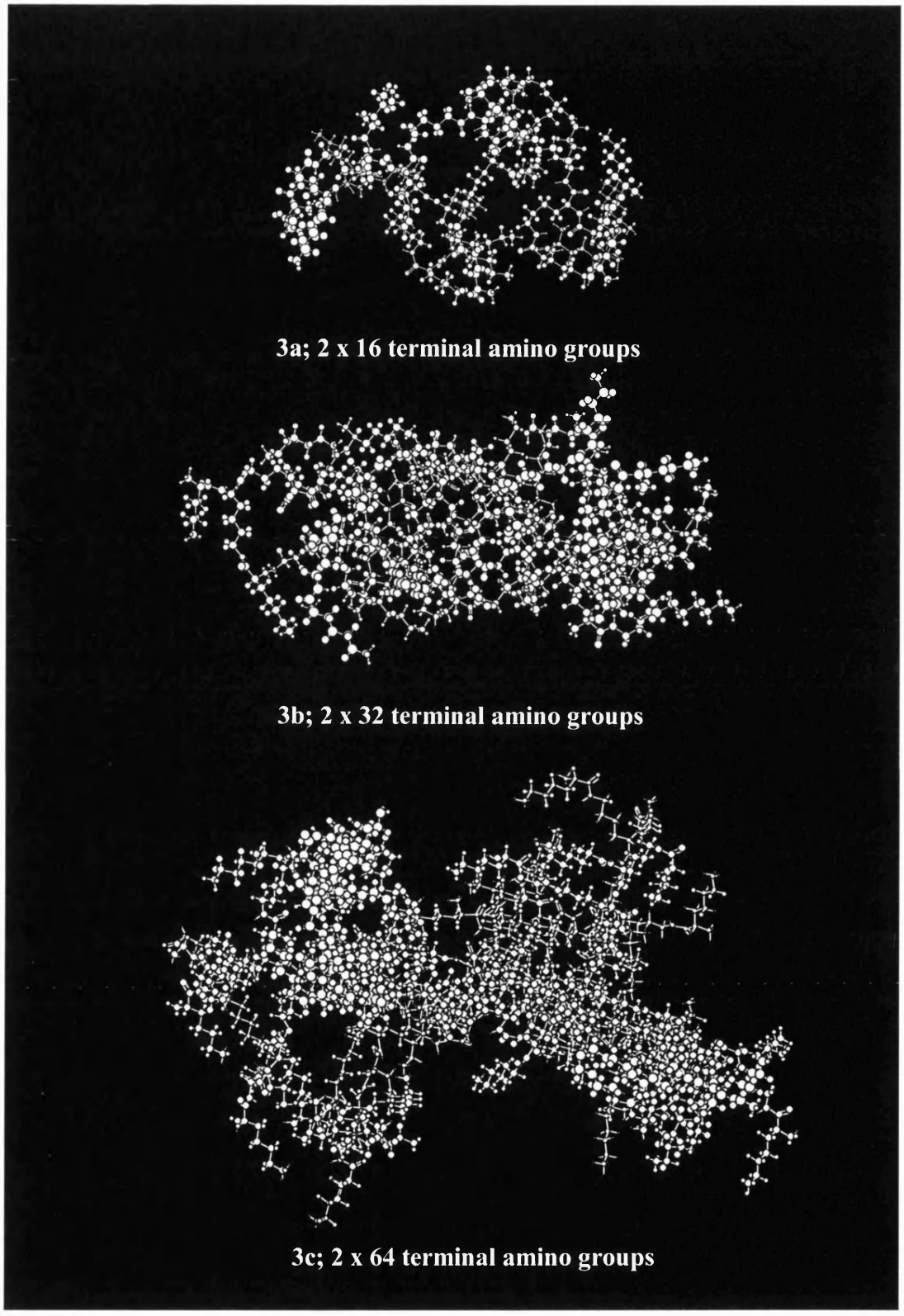

Fig. 5.6. *Scale molecular wire models of the didendrons 3a-c which were synthesised using Method C.*

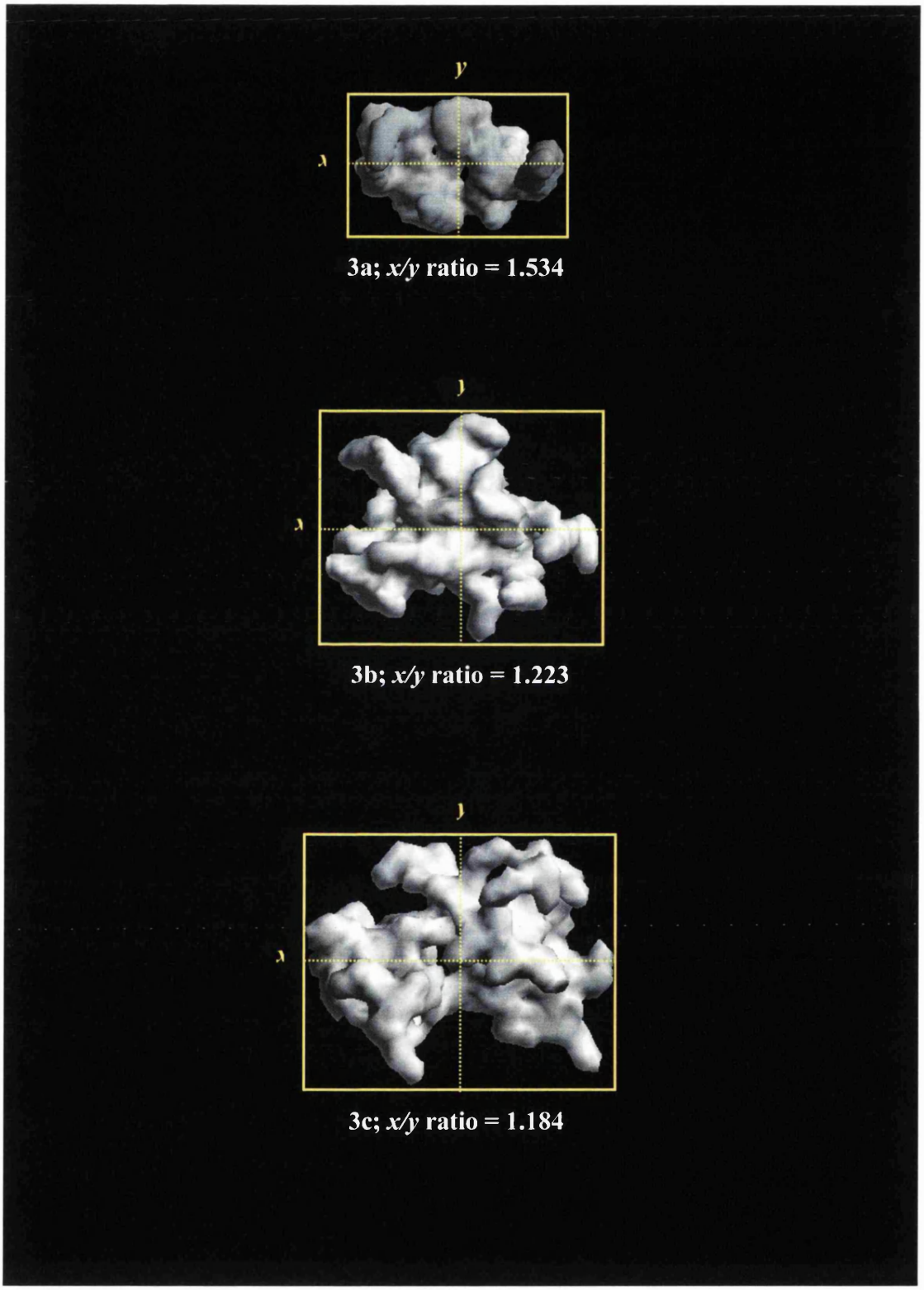

Fig. 5.7. *'Solvent accessible surface' models of didendrons 3a-c showing the x/y axis ratios for the three molecules.*

As shown in Fig. 5.7, the *x/y axis* ratios for didendrons 3a, 3b and 3c were 1.534, 1.223 and 1.184. This shows that the didendrons with the lowest numbers of terminal amino groups had more elongated shapes. Further molecular modelling and simulation studies showed that, with increasing generation growth, the didendrons became denser and spherical in shape as branching became more condensed. It is important to note that the structural confirmations of these molecules will vary in different systems. The confirmations shown here are representative of the didendrons being in an aqueous environment at pH 7.4.

5.3.2 Viscosity studies

5.3.2.1 Dynamic viscosity (η)

Fig. 5.8 shows how the dynamic viscosities, for the didendrons 3a-c, vary with didendron concentration at 25°C.

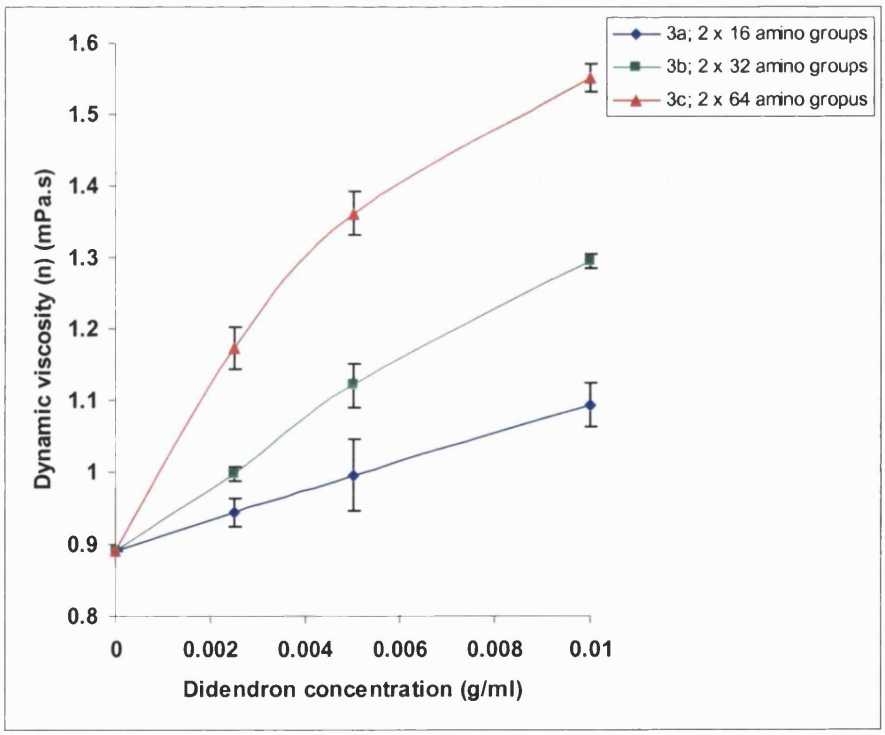

Fig. 5.8. *The dynamic viscosities (η) of didendrons 3a-c versus increasing didendron concentration (g/ml) at 25°C.*

As can be seen in Fig. 5.8, all three molecules show an increase in dynamic viscosity with increasing didendron concentration. The intercept on the *y-axis* corresponds to the viscosity of the water at 25°C (0.8904 mPa.s). At the maximum concentration of 10mg/ml, the dynamic viscosities for molecules 3a, 3b and 3c are 1.0935, 1.2943 and 1.5512 mPa.s, respectively. Compared to molecules 3a and 3b, 3c appears to deviate more from a linear relationship and this was also evident with repeat experiments.

The viscosities of the three didendrons were also shown to change linearly with increases in temperature (Fig. 5.9). The concentration of each didendron was 10mg/ml and the viscosity of water at the various temperatures was also determined as a control measure.

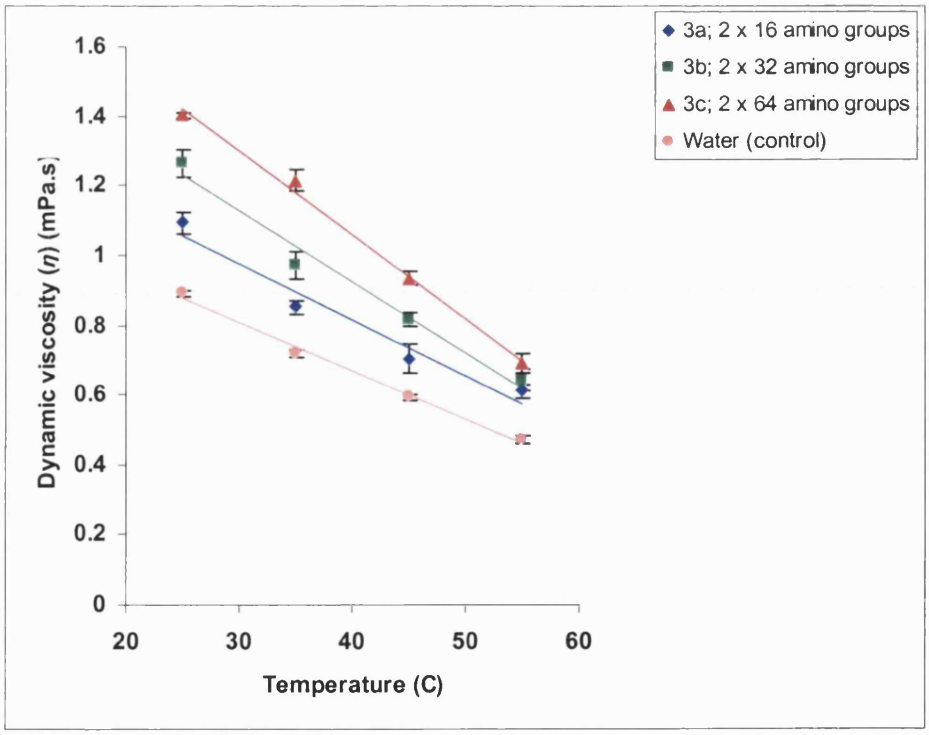

Fig. 5.9. *The dynamic viscosities (η) of didendrons 3a-c versus increasing temperature(°C), with didendron concentrations of 10 mg/ml.*

Fig. 5.9 shows that all three didendrons exhibit a linear decrease in dynamic viscosity as temperature increases. When increasing the temperature from 25°C to 55°C, molecule 3a shows a decrease in dynamic viscosity by 44%; molecule 3b shows a decrease by 49%; 3c shows a decrease by 51%; and water shows a decrease by 47%. The graph also shows, that at 55°C, the dynamic viscosities of all three didendrons become similar and fall in the range of 0.61 (for 3a) to 0.69 (for 3c) mPa.s. At 55°C, the dynamic viscosity of water was 0.47 mPa.s.

Further viscosity studies were performed using single dendrons in comparison with the didendron 3c (2 x 64 amino groups, M_r = 16441). The two dendron molecules were 2e (64 amino groups, M_r = 10884) and 2m (128 amino groups, M_r = 16559). The studies were performed at 25°C and the results are displayed in Fig. 5.10.

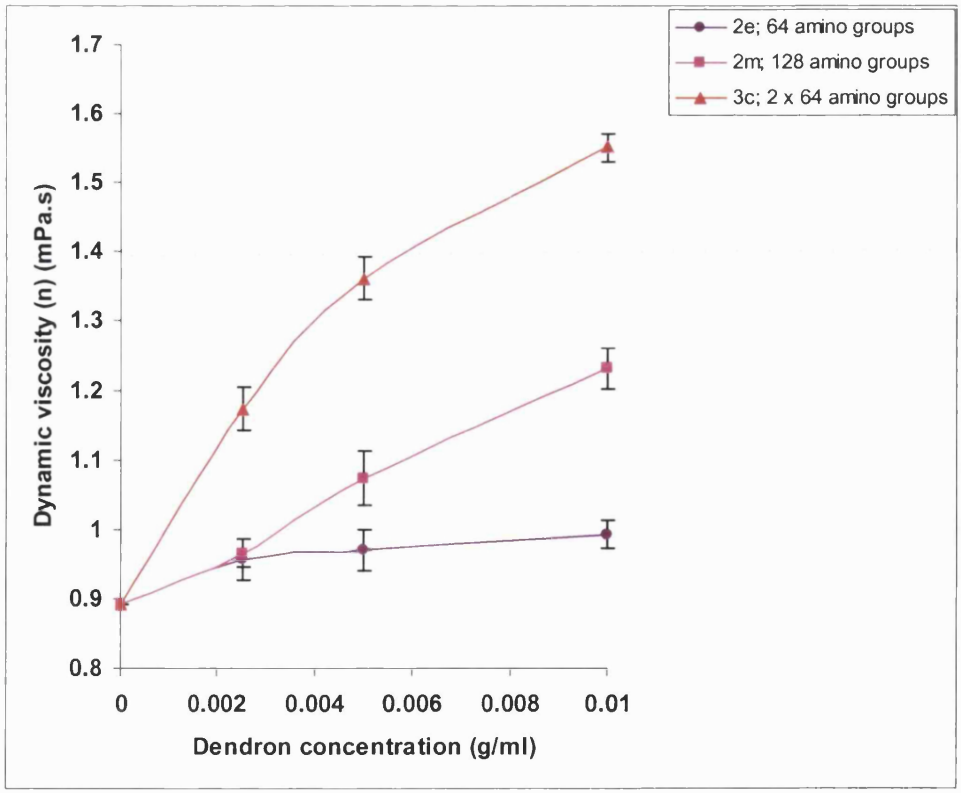

Fig. 5.10. *A comparison of dynamic viscosities (η) of molecules 2e, 2m and 3c of different concentrations (g/ml) at 25°C.*

As expected, molecule 2e had the lowest dynamic viscosities at all concentrations (0.9921 mPa.s at 10 mg/ml). However, there was a large difference between the results for molecules 2m and 3a, despite both molecules having the same number of terminal amino groups and similar molecular weights. At a maximum concentration of 10 mg/ml, molecule 3c had a dynamic viscosity of 1.5512 mPa.s. At the same concentration, molecule 2m had a dynamic viscosity of 1.2314 mPa.s. Thus molecule 3c has a dynamic viscosity 25% greater than 2m. An explanation regarding the lower dynamic viscosity of 2m can be based on its shape and confirmation. Molecular simulations showed that dendrons 2m, with 128 terminal amino groups, had a denser and more spherical confirmation in water (hydrodynamic diameter = 5.2 nm). Didendrons 3c (hydrodynamic diameter = 6.3 nm), had more elongated shapes and had more potential for didendron 'tangling' because of their dumbbell-like structure.

5.3.2.2 Intrinsic viscosity ([η])

To determine the intrinsic viscosities of the didendrons, further calculations and formulae had to be applied.

Dynamic viscosity, $\eta = \dfrac{\textbf{shear stress}}{\textbf{shear rate}}$ **(Pa.s)**

Using the dynamic viscosity, the relative viscosity (η_{rel}) can be calculated with the equation;

Relative viscosity, $\eta_{rel} = \dfrac{\eta}{\eta^0}$

; where η^0 is the dynamic viscosity of the pure solvent (e.g. water) at a given temperature. As it is a ratio, relative viscosity has no units and can be used to calculate the specific viscosity (η_{sp}).

Specific viscosity, $\eta_{sp} = \eta_{rel} - 1$ and as with the relative viscosity, it has no units. The specific viscosity is required to calculate the reduced viscosity (η_{red}).

Reduced viscosity, $\eta_{red} = \eta_{sp}/c$ where c is the concentration (g/l). It has units of reciprocal concentration (l/g) and is related to the **intrinsic viscosity** $[\eta]$ by the Huggins-Kramer equation:

$\eta_{red} = [\eta] + k^1 [\eta]^2 c$; where c is the concentration. Fig.5.11 shows a plot of reduced viscosity versus concentration. The *y*-intercept is the intrinsic viscosity $[\eta]$ and the slope is equal to $k^1 [\eta]^2$.

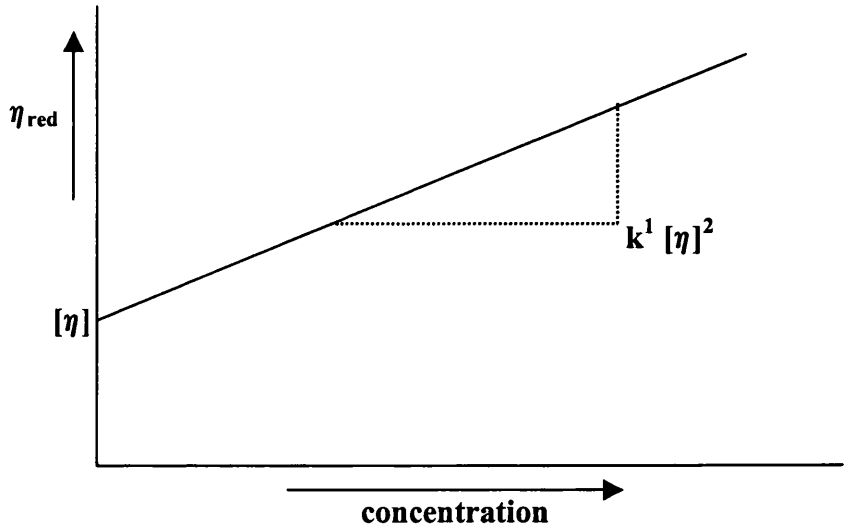

Fig. 5.11. A linear plot representing the Huggins-Kramer equation, $\eta_{red} = [\eta] + k^1 [\eta]^2 c$, *to determine the intrinsic viscosity.*

The reduced viscosity, η_{red}, is a measure of the specific capacity of the polymer to increase the relative viscosity.

Based on the above formulae, Table 5.2 contains the required data, to produce a Huggins-Kramer plot (Fig. 5.12) for the didendrons (3a-c) to determine their intrinsic viscosities at 25°C, where η^0 = 0.8904 mPa.s and concentration is expressed as g/l.

Table 5.2. *Values for dynamic, relative, specific and reduced viscosities for didendrons 3a-c, at different concentrations in water at 25°C.*

Molecule	Concentration (g/l)	η (mPa.s)	η_{rel}	η_{sp}	η_{red} (l/g)
3a	2.5	0.9435	1.060	0.060	0.0240
	5	0.9954	1.118	0.118	0.0236
	10	1.0935	1.228	0.228	0.0228
3b	2.5	0.9979	1.121	0.121	0.0484
	5	1.1214	1.259	0.259	0.0518
	10	1.2943	1.454	0.454	0.0454
3c	2.5	1.1731	1.317	0.317	0.1268
	5	1.3617	1.529	0.529	0.1058
	10	1.5512	1.742	0.742	0.0742

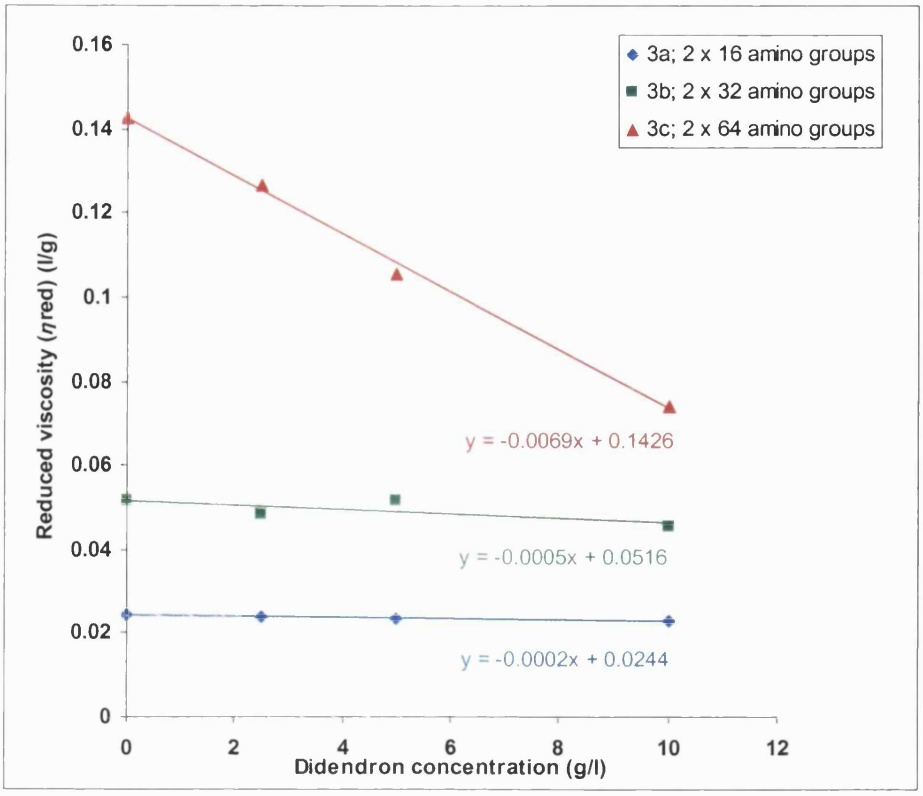

Fig 5.12. *A Huggins-Kramer plot for didendrons 3a-c for viscosity measurements at 25°C.*

Using a Huggins-Kramer plot in Fig. 5.12, the intrinsic viscosities [η] for didendrons 3a, 3b and 3c are 0.0244, 0.0516 and 0.1426 l/g, respectively. The [η] value for 3b is approximately twice that of 3a, but the [η] value for 3c is approximately thrice that of 3b. The shapes and directions of the plots for all molecules were not as expected, when compared to Fig 5.11. All three didendrons had decreasing reduced viscosities (η_{red}), with increasing concentration, resulting in negative values for the slopes, although this was clearly evident with 3c. This shows that with increasing concentration, 3c has a lower capacity to affect the relative viscosity of the system.

It is important to note that the intrinsic viscosity of a polymer is the limiting value of the reduced viscosity, at infinite dilution of the polymer. The use of equations such

as Huggins-Kramer have been used successfully to determine properties of linear polymers but whether they can be applied to branched and dendritic polymers requires further investigation. The dendrons and didendrons, when in aqueous solution, exhibited Newtonian flow behaviour. This is consistent with findings by Uppuluri *et al.* (1997) who studied flow properties of PAMAM dendrimers in EDA. Rietveld and Bedeaux (2001) studied the viscosity of poly(propylene imine) dendrimer solutions in methanol. They also concluded that the dendrimers do not interpenetrate and demonstrate Newtonian flow behaviour at every concentration (volume fractions ranged from 1 to 100%).

Mourey *et al.* (1992) discovered that one of the unique properties that poly(benzyl ether) dendrimers show, is that the intrinsic viscosity goes through a maximum at the fourth generation of growth. Tande *et al.* (2001) have attempted to rationalise this behaviour using dendrimer functionality (f), dendrimer generation (g) and Einstein's relation for suspension viscosity. Einstein showed the intrinsic viscosity $[\eta]$ for hard spheres is given by;

$$[\eta] = 2.5\,\Phi/c \qquad (\text{where } c \rightarrow 0)$$

where Φ is the volume fraction of polymer in a solvent (ratio of polymer volume to total volume) and c the polymer concentration (ratio of polymer mass to total volume). Thus, $[\eta]$ is merely the ratio of polymer volume (V) to polymer mass (M).

The dendrimer volume was taken to a first approximation as;

$$V \sim g^3$$

or the linear dimension grows steadily with generation number thereby making the volume increase accordingly. Using the above molecular mass scaling, Tande and co-workers found;

$$[\eta] \sim V/M \sim g^3/[f\text{-}1]^g$$

This equation has a maximum at G4 which is where Mourey *et al.* (1992) found their maximum for poly(benzyl ether) dendrimers. In general, the intrinsic viscosity maximum (g_{max}) is given by;

$g_{max} = 3/ln(f\text{-}1)$ for any functionality.

According to Tande *et al.* (2001) "This is a crude calculation, yet, does serve to show the reason why the peculiar intrinsic viscosity maximum is seen. The molecular volume can at most scale with g^3 while the mass is set by the functionality and scales with a power law in generation number. Eventually the power law becomes the dominant factor and the intrinsic viscosity decreases, in other words, the volume does not suddenly collapse, rather the mass increases faster than the volume". The authors have stated that, although the above application gives us some insight into the viscosimetric behaviour of dendritic structures, further research is required.

Fréchet *et al.* (1994) researched the intrinsic viscosities of dendrimers and found that, when the generation increases beyond a certain point, the intrinsic viscosity begins to decline, contrary to the behaviour of linear polymers (Fig. 5.13). They conducted the experiment using polyether dendrimers and polystyrene. This effect is believed to be

a consequence of the globular shapes of high generation dendrimers leaving them unable to 'tangle' with one another as linear polymers do.

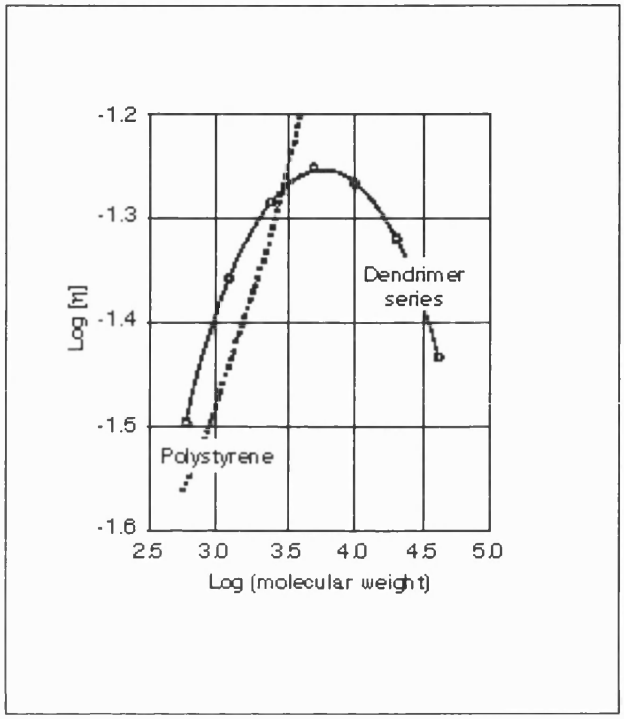

***Fig. 5.13**. Intrinsic viscosity behaviour of polyether dendrimers and of polystyrene (from Fréchet et al. (1994) J. Macromol. Sci., Pure Appl. Chem., **A31**, 1627-1645).*

Although most dendrimers have been found to predominantly exhibit Newtonian flow behaviour, some studies have shown PAMAM dendrimers to have non-Newtonian behaviour at higher shear rates (Uppuluri *et al.*, 2000).

5.3.3 Self-assembling dendritic aggregates

Dendrons 2d, 2f, 2h and 2j were solubilised in water in concentrations of 1mg/ml and 5 mg/ml. All four molecules had the terminal groups acetylated, with 2d and 2f having two glycine molecules in their tail; whilst 2h and 2f had three glycine

molecules in their tail. Molecules 2d and 2h had 32 terminal groups (colourless clear solutions), whereas 2f and 2j had 64 terminal groups (pale yellow clear solutions).

The dendrons with 64 terminal groups did not form structures at either concentration. However, the dendrons with 32 terminal groups formed some interesting aggregates when placed on a glass microscope slide. The formation of these structures was consistent at concentrations of 1 mg/ml and 5 mg/ml. Fig. 5.14 shows some examples of these structures which were formed with dendron 2d.

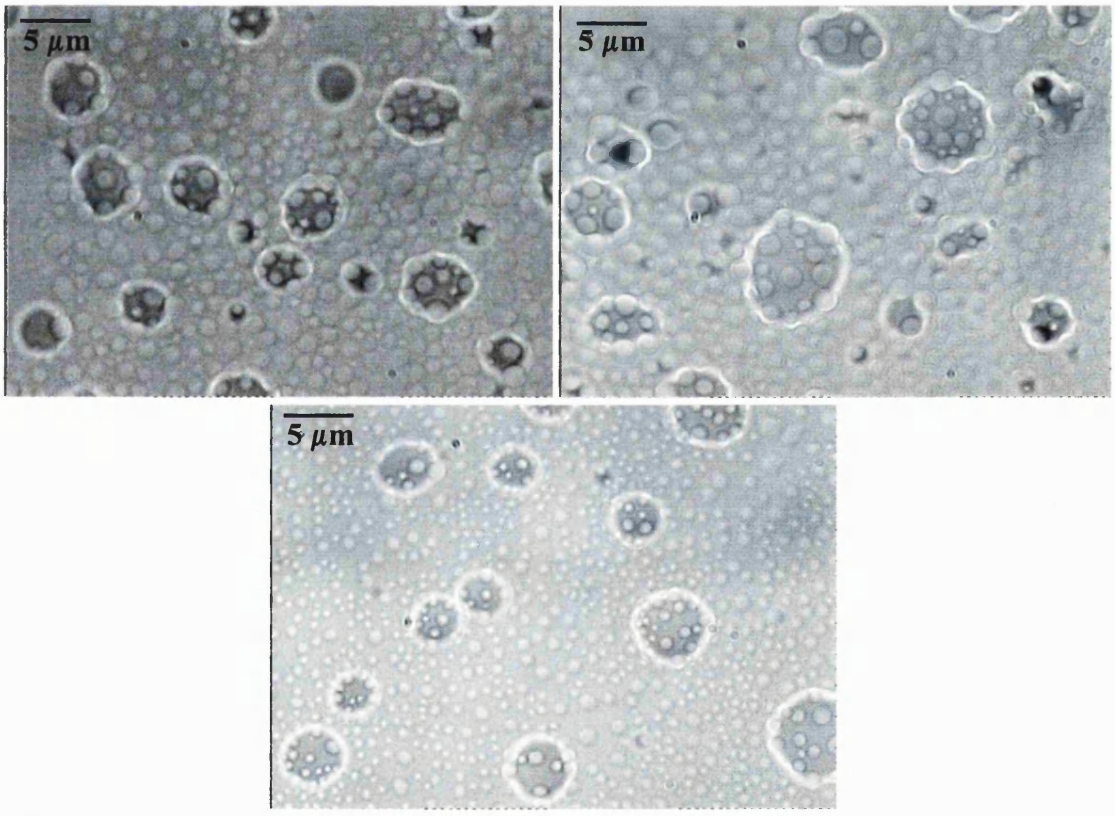

Fig. 5.14. *Examples of molecular aggregates formed on a glass slide by a solution of dendrons 2d (1mg/ml, 32 terminal groups).*

Fig. 5.15 shows some examples of these structures which were formed with dendron 2h.

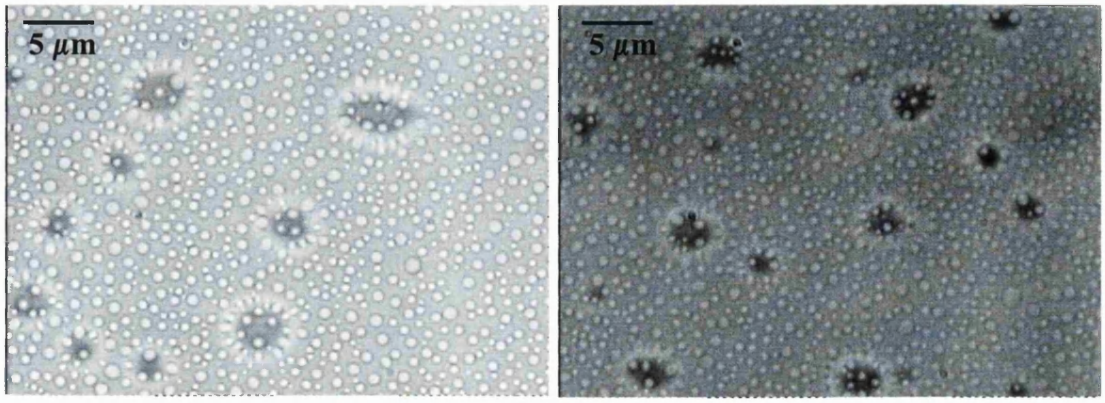

Fig. 5.15. *Examples of molecular aggregates formed on a glass slide by a solution of dendrons 2h (1mg/ml, 32 terminal groups).*

As can be seen from Figs. 5.14 and 5.15, dendrons 2d and 2h form very similar looking aggregates. The larger structures, which seem to attract the smaller structures onto their surfaces, vary in size from 1-10 μm. The smaller structures appear to be of a more uniform size, ranging from 0.5-1 μm. Despite their definite formation, these structures could not be analytically detected in solution, which was colourless and clear. Their formation was only evident when the solutions were placed on glass slides with cover-slips on top. The formation of these aggregates was not instantaneous and took approximately 5 min and only formed when an air bubble was present under the cover-slip. The structures were only visible where pockets of air were present and when exposed to the lamp of the microscope. To exclude the interference of contaminants, slides and cover-slips were washed with chromic acid, but formation of the structures was still evident.

The dynamic viscosities for dendrons 2d (M_r = 5444) and 2h (M_r = 5501) were determined for various concentrations at 25°C and are shown in Fig. 5.16. The two dendrons of similar molecular weights, had almost identical dynamic viscosities and increases in concentrations only produced very small increases in dynamic viscosity.

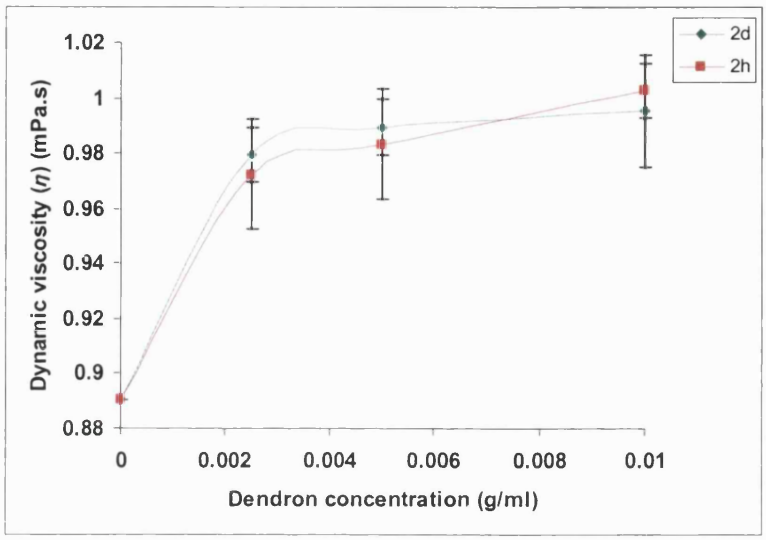

Fig. 5.16. *A comparison of dynamic viscosities (η) of molecules 2d and 2h of different concentrations (mg/ml) at 25°C.*

Although the mechanism by which these structures form is still unclear, it provides an interesting platform for further research and investigation into the self-assembling properties of dendritic structures. A possible explanation could be based on recent observations made by Sommer and co-workers (2004). They were studying the evaporation of liquid drops containing 60nm nanospheres and the resulting deposition patterns which were formed. They used mirror-polished clean surfaces and found that slow evaporation, with a uniform surface tension, resulted in a well-ordered distribution of self-assembled particles forming circular deposition patterns.

As with the aggregates formed by the dendrons, the presence of air was important for the self-assembly of the nanospheres (Sommer *et al.*, 2004). The nanospheres began deposition at the air/liquid/solid-contact line. Although, the dendron solution was not evaporated intentionally, slow evaporation of the water on the slide due to the light of the microscope was an important factor for the formation of these aggregates. This explains why formation of the aggregates was only evident after exposure to the light of the microscope, for approximately 5 min. To understand this pattern of formation further, investigations into the effects of surface tension, gravity and temperature would need to be studied in such systems.

5.4 CONCLUSION

Method C was a successful synthetic approach to produce a didendron structure on a solid support. Three novel polylysine didendrons (3a-c), which were water soluble, were synthesised and their viscosities were studied. With all three molecules, dynamic viscosity increased as didendron concentration increased. This appeared to be a linear relationship for molecule 3a but as didendron generation increased (3b and 3c), there was evidence of a non-linear relationship. All three molecules showed a linear decrease in dynamic viscosity with increasing temperature.

Comparative viscosity studies with single dendrons, showed that a didendron with 128 peripheral amines (2 x 64) had a dynamic viscosity 25% greater than that of a single dendron with 128 peripheral amines.

Using a Huggins-Kramer plot, the intrinsic viscosities for the didendrons were determined. The intermediate didendron (2 x 32 amino groups-3b) had an intrinsic viscosity twice that of the smallest didendron (2 x 16 amino groups-3a). The intrinsic viscosity of the largest didendron (2 x 64 amino groups-3c) was approximately three times that of the intermediate molecule and six times that of the smallest molecule. The reason for this large increase in intrinsic viscosity is unclear. The reduced viscosities of 3a and 3b remained approximately constant with increasing didendron concentration. The reduced viscosity of 3c decreased as its concentration increased. The didendrons and dendrons studied, exhibited Newtonian flow behaviour.

Two polylysine acetate-terminated dendrons (32 peripheral groups) were shown to produce unusual aggregates on glass microscope slides, the mechanism by which they form is still unclear. The aggregates only form in the presence of air pockets

under the cover-slip and their formation is influenced by heat from the light of the microscope.

CHAPTER SIX

CONCLUSIONS AND FUTURE PERSPECTIVES

We have developed dendritic molecules with varying structural properties using different synthetic approaches. Studying these molecules, with regard to their physicochemical behaviour, has helped us to gain further insight into their properties such as shape, diffusion, permeability, adsorption, viscosity and structural confirmation. *In vitro* studies of the interaction of dendrons with lipidic membranes and albumin have produced data which can help us understand some biological properties which dendritic molecules may possess.

The interaction of cationic lipidic dendrons with charged and neutral liposomes showed that the initial interactions between the dendrons and liposome membranes were hydrophobic. This was the case, regardless of the membrane charge and preference was not shown towards anionic liposomes. However, with time, the cationic dendrons caused disruption of the anionic membranes but did not affect the cationic and neutral membranes, suggesting a delayed influence of electrostatic forces. Significant effects of the dendrons on anionic liposomal membranes were also evident during dendron-entrapping studies. Following centrifugation, to remove non-entrapped dendrimer, the liposomes were resuspended to form abnormal large vesicular structures with myelin-like figures. This suggested that a combination of mechanical force, electrostatic attraction and the amphiphilic nature of the dendrons produced a surfactant-like solubilisation effect. Further investigation into the

interaction of cationic dendritic molecules with anionic membranes may enlighten us with information about how such molecules may behave at a cellular level. This in turn can provide us with knowledge which can be used to synthesise a dendritic molecule with optimal properties with regard to cellular entry and minimal toxicity.

Diffusion of cationic lipidic dendrons through cellulose membranes produced results as expected, the smallest dendrons having the higher rates of diffusion. However, adsorption of the dendrons to the cellulose membranes was the cause of much hindrance to the diffusion process. Sodium chloride proved to be a solution of this hindrance. At higher molar concentrations, sodium chloride eliminated adsorption of the dendrons to the membranes and improved the transport of dendrons across the membranes. The mechanism by which this occurred is still unclear but points us in a direction which requires further investigation. The three dendrons used had the same number of lipidic chains but different numbers of peripheral amines. Membrane and octanol-water coefficient calculations showed that the dendrons become more hydrophilic with increasing numbers of peripheral amines. Perrin factor calculations suggested that the dendrons become more quasi-spherical with each generation of growth.

Dendron-albumin interaction studies showed that cationic lipidic dendrons do interact with bovine serum albumin but the method is still unclear. Dynamic dialysis studies showed that the stoichiometry of dendron: albumin interactions was found to be 1:1.5, 1:4 and 1:5 for the dendrons with 8, 16 and 32 amino groups, respectively. Molecular modelling and analysis of the dendrons and albumin suggested the possibility of electrostatic interaction as the dendrons are too large to be involved in ligand-receptor interactions. This theory was further enhanced by experimenting with

acetate-terminated dendrons for which the cationic charges were neutralised. In the presence of albumin, the diffusion of amino-terminated dendrons was decreased whereas the diffusion of acetate-terminated dendrons was not affected. To gain a better understanding of processes such as membrane diffusion and serum protein interactions, the dendrons should be exposed to biological systems. Even *in vitro* experiments using biological membranes and whole blood may provide some valuable answers.

As well as synthesising other dendrons, didendrons having a dumbbell-like shape were also synthesised. Following the successful synthesis of a series of novel didendron molecules (polylysine) with free peripheral amines, the viscosities of these molecules (in water) were studied in comparison with single dendrons. As well as increasing with the size of the molecules, the dynamic viscosities of the dendrons and didendrons increased with concentration and decreased with temperature. In comparison with single dendrons, having the same number of peripheral amines (128), the didendron showed a 25% increase in dynamic viscosity. Another interesting observation seen with dendrons and smaller didendrons (32 and 64 peripheral amines) was that the reduced viscosities were approximately constant as concentrations of the molecules increased. However, with the larger didendrons (128 peripheral amines), the reduced viscosity decreased with an increase in concentration. The reduced viscosity is a measure of the specific capacity of the polymer to increase the relative viscosity (the relative viscosity being the ratio of the dynamic viscosity of a specified solution of the polymer to the dynamic viscosity of the pure solvent). Understanding the rheological properties of dendritic structures is crucial for gaining insight into their interactions and shapes at a molecular level. This information would be crucial to successful pharmaceutical applications of dendritic

structures. Whether dendrimers obey the viscosity laws of linear polymers is still debatable and is an area which requires much thought and investigation. Didendron chemistry is currently undergoing further investigation in our laboratories, with regard to bifunctionalisation and dual radiolabelling. Each dendritic section of the didendron can be synthesised using different radiolabels and also possess different surface functionalities using a combination of Boc and Fmoc chemistry.

Two acetate-terminated dendrons (32 peripheral groups), constructed of polylysine with a glycine tail, were shown to produce unusual aggregates. The formation of these structures was evident only on glass slides after a period of approximately five minutes. The cause of this phenomenon is still unknown and these self-assembling properties need to be studied further.

The potential for dendritic structures to be successful vehicles for drug and gene delivery is evident. At this stage it is pivotal to focus on the fundamental aspects of dendritic structure and molecular confirmation. This will enable us to design and synthesise dendritic molecules with particular functions and properties in mind. To fully understand these functions and properties, emphasis has to be put on physicochemical aspects such as viscosity, diffusion, affects of pH and temperature, molecular interactions and how different solvent systems may change the dendritic confirmation. This will provide us with the pharmaceutical knowledge to commercially produce an efficient and stable molecule, with chemists and material scientists playing an important role. Only when this is achieved, will there be light at the end of the tunnel, regarding biocompatibility and biodistribution.

APPENDIX I

Sources of chemicals and reagents used for dendron synthesis

Chemical/Reagent	Source
1,12-diaminododecane	Aldrich Chemical Co., Dorset, UK
2-(1H-Benzotriazole-1-yl-1,1,3,3-tetramethyluronium hexaflurophosphate (HBTU)	Severn Biotech Ltd, Worcester, UK
2,3-diaminopropionic acid	Aldrich Chemical Co., Dorset, UK
2-methyl-2-propanol	Aldrich Chemical Co., Dorset, UK
6-aminocaproic acid	Aldrich Chemical Co., Dorset, UK
Boc-Gly-OH	Calbiochem-Novabiochem AG, Laufelfingen, Switzerland
Boc-Gly-PAM resin	Calbiochem-Novabiochem AG, Laufelfingen, Switzerland
Boc-Lys(Boc)-OH	Calbiochem-Novabiochem AG, Laufelfingen, Switzerland
Chloroform	BDH Laboratories, Poole, UK
Citric acid	Lancaster, Morecambe, UK
Dichloromethane (DCM)	BDH Laboratories, Poole, UK
Ethanol	BDH Laboratories, Poole, UK
Ethyl acetate	BDH Laboratories, Poole, UK
Glacial acetic acid	BDH Laboratories, Poole, UK
HCl	BDH Laboratories, Poole, UK
Hydrogen fluoride (HF)	Air Products Plc, Cheshire, UK
L-lysine	Calbiochem-Novabiochem AG, Laufelfingen, Switzerland
Magnesium sulphate dried	BDH Laboratories, Poole, UK
Methanol	BDH Laboratories, Poole, UK
N,N-diisopropylethylamine (DIEA)	Avocado Research Chem. Ltd, Lancashire, UK
N,N-dimethylformamide (DMF)	Rathburn Chemicals Ltd, Walkerburn, UK

NaOH	BDH Laboratories, Poole, UK
Ninhydrin	Avocado Research Chem. Ltd, Lancashire, UK
p-cresol	Avocado Research Chem. Ltd, Lancashire, UK
Phenol	Avocado Research Chem. Ltd, Lancashire, UK
*p*MBHA resin	Calbiochem-Novabiochem AG, Laufelfingen, Switzerland
Potassium cyanide	Aldrich Chemical Co., Dorset, UK
Pyridine	BDH Laboratories, Poole, UK
Radiolabelled L-lysine, (4,5 - ^{3}H)	Moravek Biochemicals, California, USA
Trifluoroacetic acid (TFA)	KMZ Chemicals, Surrey, UK
Trimethylsilyl trifluoromethanesulfonate (TMSOTf)	Aldrich Chemical Co., Dorset, UK
A-aminotetradecanoic acid	Aldrich Chemical Co., Dorset, UK

APPENDIX II

Mass spectra data for dendrons

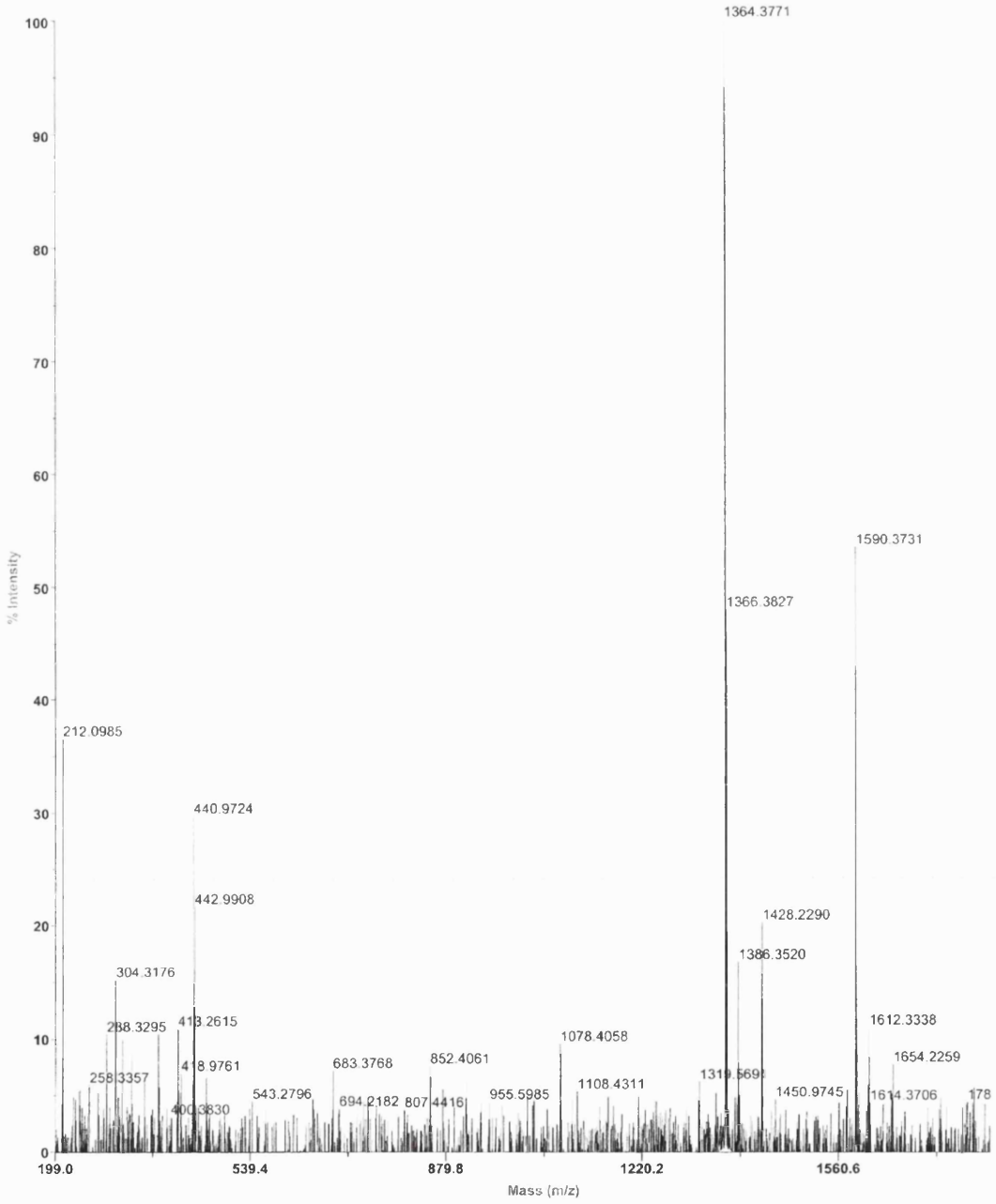

Molecule 1a **($C_{84}H_{168}N_{18}O_{10}$ [1588])**

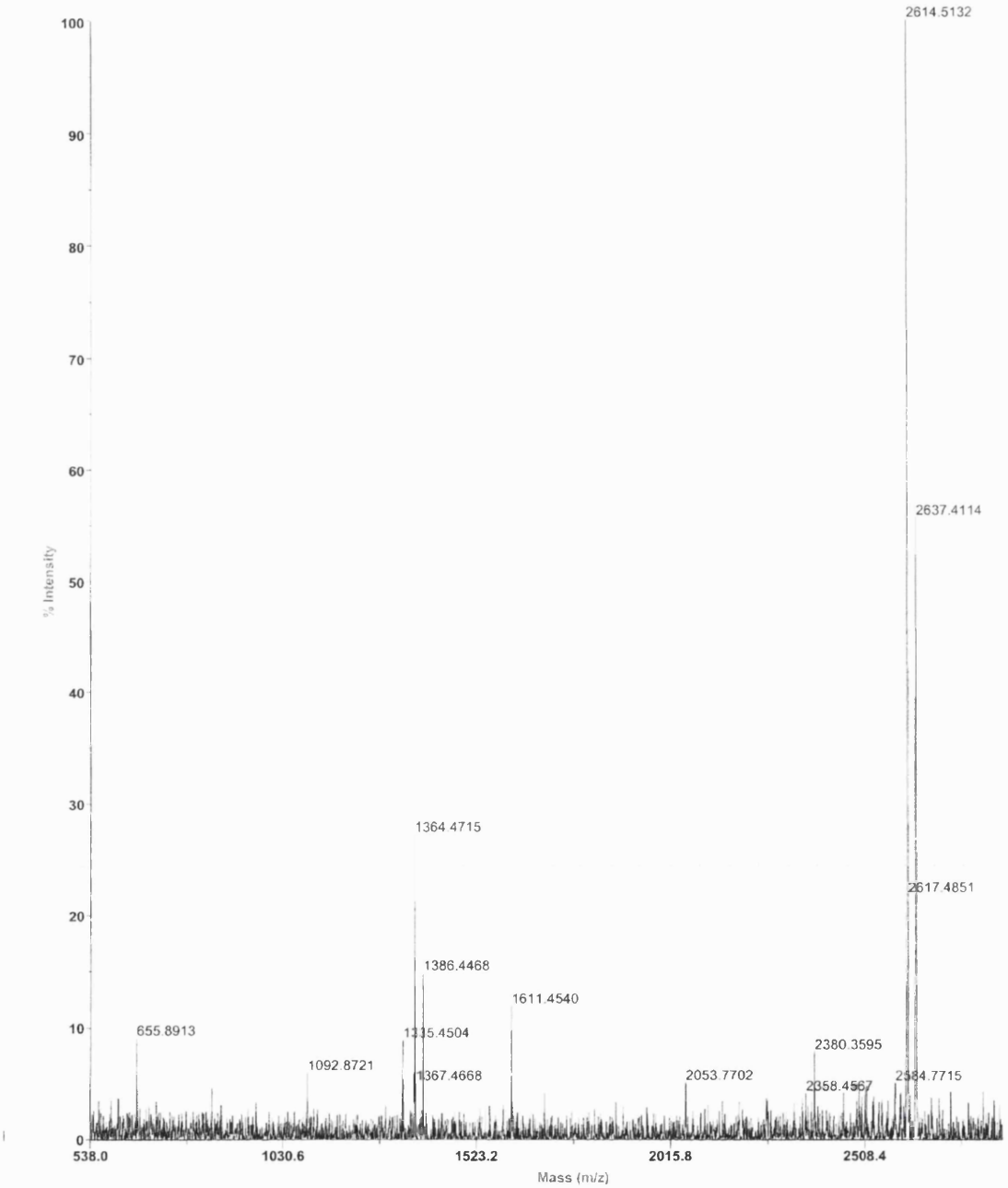

Molecule 1b **($C_{132}H_{264}N_{34}O_{18}$ [2612])**

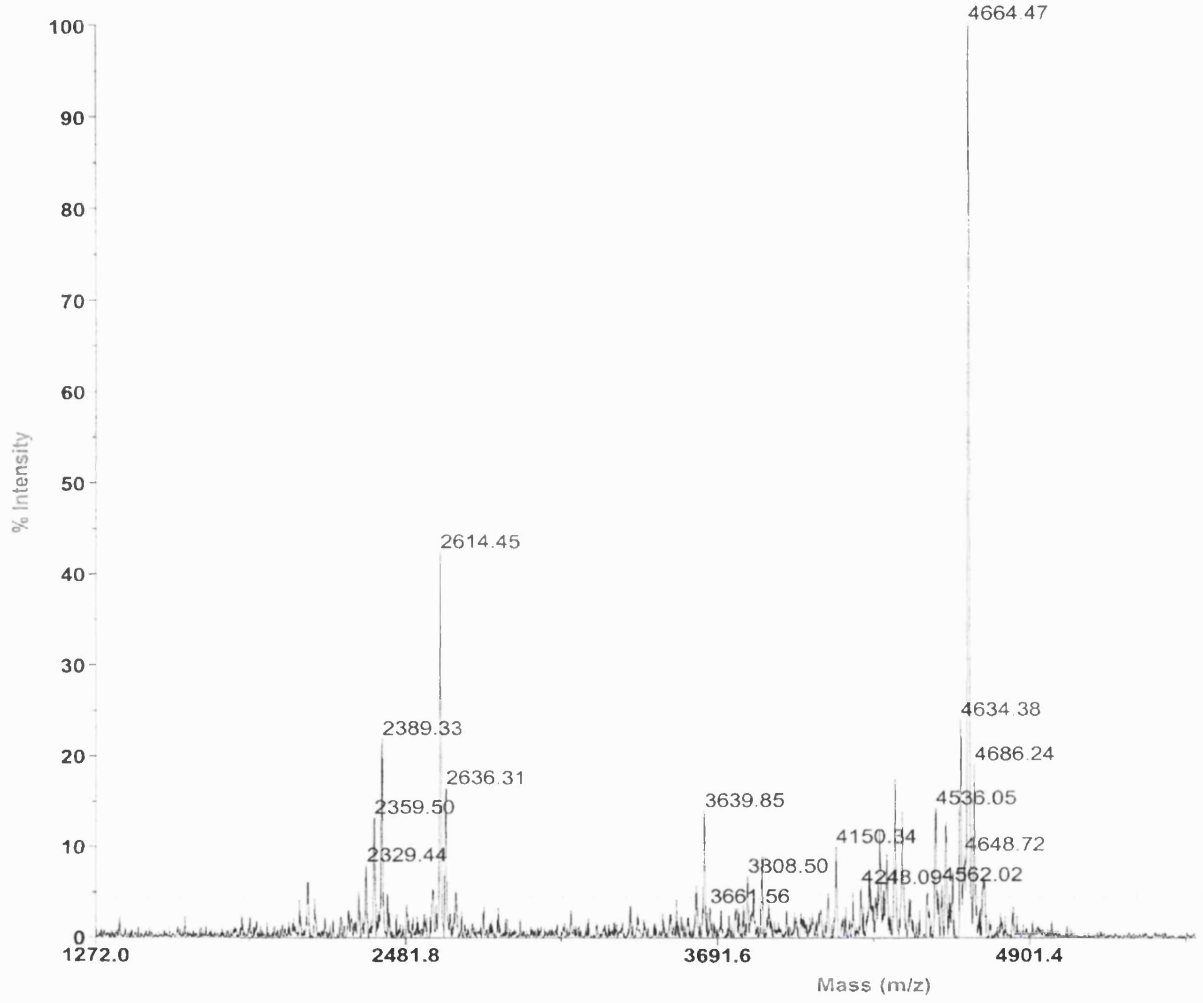

Molecule 1c **($C_{228}H_{456}N_{66}O_{34}$ [4660])**

Molecule 1d
MS m/z (%) $C_{100}H_{184}N_{18}O_{18}$ [1924] : 1926 (47) [M + 2H], 1785 (45), 1231 (79), 817 (15), 345 (47)

Molecule 1e
MS m/z (%) $C_{164}H_{296}N_{34}O_{34}$ [3284] : 3307 (67) [M + Na], 3102 (23), 2915 (45), 1678 (24), 1008 (45), 925 (79), 613 (56)

Molecule 1f
MS m/z (%) $C_{292}H_{520}N_{66}O_{66}$ [6004] : 6027 (13) [M + Na], 6008 (56) [M + 4H], 5024 (34), 4556 (11), 4112 (13), 2678 (28)

Molecule 2a
MS m/z (%) $C_{94}H_{188}N_{32}O_{18}$ [2052] : 2052 (87) [M], 1890 (23), 942 (81), 729 (12), 328 (64)

Molecule 2b
MS m/z (%) $C_{126}H_{220}N_{32}O_{34}$ [2724] : 2748 (54) [M + H + Na], 2098 (56), 1093 (26), 890 (19), 856 (72), 457 (39)

Molecule 2c
MS m/z (%) $C_{190}H_{380}N_{64}O_{34}$ [4100] : 4102 (79) [M + 2H], 4017 (34), 3024 (39), 2780 (90), 2558 (35), 1037 (42)

Molecule 2d
MS m/z (%) $C_{254}H_{444}N_{64}O_{66}$ [5444] : 5446 (32) [M + 2H], 5201 (49), 4920 (13), 3670 (21), 1140 (56), 1112 (13), 746 (35)

Molecule 2e
MS m/z (%) $C_{382}H_{764}N_{128}O_{66}$ [8196] : 8219 (24) [M + Na], 8134 (56), 7924 (22), 6903 (87), 4102 (13), 3245 (89)

Molecule 2f
MS m/z (%) $C_{510}H_{892}N_{128}O_{130}$ [10884] : 10888 (12) [M + 4H], 8898 (79), 6894 (51), 4352 (36), 2045 (42), 678 (93)

Molecule 2g
MS m/z (%) $C_{192}H_{383}N_{65}O_{35}$ [4157] : 4160 (67) [M + 3H], 4024 (45), 2789 (71), 2567 (50), 1789 (27)

Molecule 2h
MS m/z (%) $C_{256}H_{447}N_{65}O_{67}$ [5501] : 5524 (13) [M + Na], 5501 (58) [M], 4990 (91), 2093 (49), 1748 (17), 734 (65)

Molecule 2i
MS m/z (%) $C_{384}H_{767}N_{129}O_{67}$ [8253] : 8255 (41) [M + 2H], 8202 (67), 7654 (88), 6904 (83), 5674 (34), 2088 (91)

Molecule 2j
MS m/z (%) $C_{512}H_{895}N_{129}O_{131}$ [10941] : 10965 (39) [M + H + Na], 10888 (67), 9890 (83), 7460 (91), 5894 (71), 2007 (12), 1348 (76), 955 (82), 867 (48)

Molecule 2k
MS m/z (%) $C_{100}H_{197}N_{35}O_{21}$ [2223] : 2223 (74) [M], 1998 (64), 1887 (18), 1670 (89), 563 (83)

Molecule 2l
MS m/z (%) $C_{132}H_{229}N_{35}O_{37}$ [2895] : 2897 (49) [M + 2H], 2895 (36) [M], 2802 (86), 2330 (67), 1010 (41)

Molecule 2m
MS m/z (%) $C_{772}H_{1541}N_{259}O_{133}$ [16559] : 16564 (22) [M + 5H], 16560 (12) [M + H], 14674 (94), 12786 (56), 8902 (88), 5788 (82), 5678 (42), 4055 (83)

Molecule 2n
MS m/z (%) $C_{1028}H_{1797}N_{259}O_{261}$ [21935] : 21981 (26) [M + 2Na], 21902 (19), 18334 (92), 16866 (31) 12225 (69), 8676 (89), 6044 (29)

APPENDIX III

HPLC data for dendrons

Project Name:	dendrimer		
Sample Name:	S-71		
Vial:	43	Sample Type:	Standard
Injection:	1	Volume:	100.00
Channel:	486	Run Time:	25.0 min
Date Acquired:	07/26/91 05:04:17 PM	Date Processed:	07/26/91 05:29:36 PM
SampleWeight:	1.00000	Dilution:	1.00000
Acq Meth Set:	amphipep2		
Processing Method:	amphipep2		

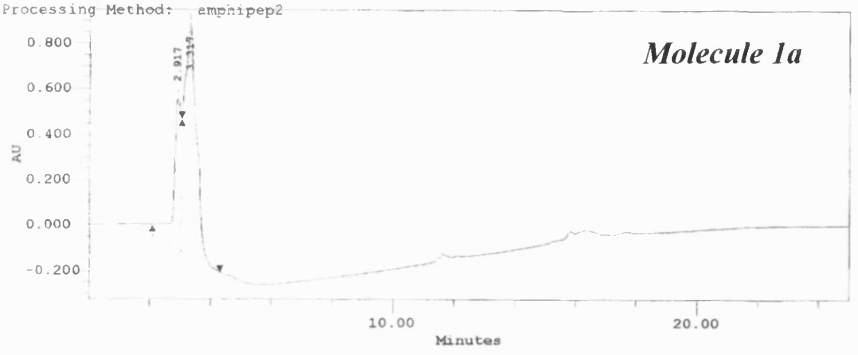

Project Name:	dendrimer		
Sample Name:	S-72		
Vial:	44	Sample Type:	Standard
Injection:	1	Volume:	100.00
Channel:	486	Run Time:	25.0 min
Date Acquired:	07/26/91 05:31:06 PM	Date Processed:	07/26/91 05:56:27 PM
SampleWeight:	1.00000	Dilution:	1.00000
Acq Meth Set:	amphipep2		
Processing Method:	amphipep2		

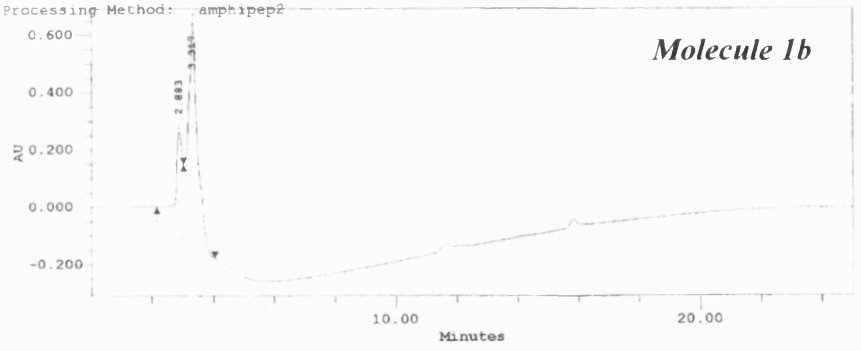

Project Name:	dendrimer		
Sample Name:	S-74		
Vial:	45	Sample Type:	Standard
Injection:	1	Volume:	100.00
Channel:	486	Run Time:	25.0 min
Date Acquired:	07/26/91 05:57:52 PM	Date Processed:	07/26/91 06:23:10 PM
SampleWeight:	1.00000	Dilution:	1.00000
Acq Meth Set:	amphipep2		
Processing Method:	amphipep2		

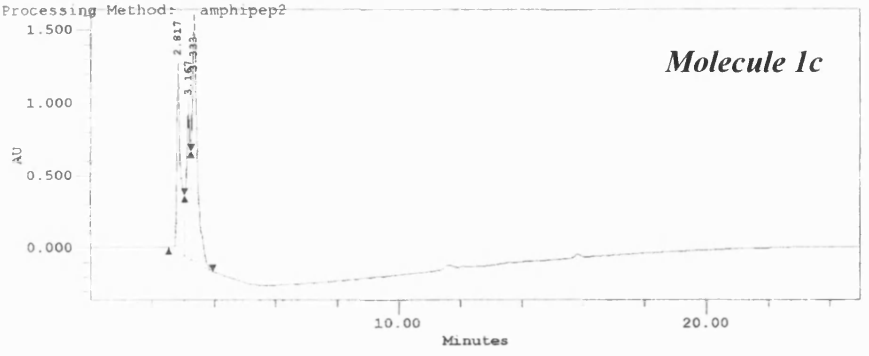

Peak data:

Molecule	Retention Time (min)	Area (uV.sec)	Height (uV)
1a	2.917	11668550	660008
1b	2.883	7248071	363704
1c	2.817	11929354	1242522
1d	3.431	9345632	456738
1e	3.217	6026478	657783
1f	3.099	5678482	878436
2a	2.233	12375899	1125778
2b	2.491	12664795	364767
2c	2.355	7253355	600285
2d	2.517	11354647	658821
2e	2.350	10567838	377688
2f	3.125	8566356	1255789
2g	2.890	7887463	1167585
2h	3.614	7355657	385987
2i	2.855	8784662	875632
2j	3.913	5758748	576883
2k	2.191	12664768	1367483
2l	2.361	11357688	1147590
2m	4.121	6758732	365782
2n	5.343	5668784	267789

With some of the molecules (1a-f), a peak was observed at the retention time of 3.317. This indicated that acetic acid was present, following the initial lyophilisation. Further lyophilisation using excess water aided the removal of the acetic acid.

APPENDIX IV

Didendron characterisation data

Mass Spectra Data for Didendron Synthesis

Core Design – Part I; di-(Boc)-2,3 diaminoproprionic acid

MS m/z (%) $C_{13}H_{24}N_2O_6$ [304] : 328 (100) [M + H + Na], 304 (62), 216 (22), 102 (7)

Core Design – Part II; (Boc)-6-aminocaproic acid

MS m/z (%) $C_{11}H_{21}NO_4$ [231] : 255 (100) [M + H + Na], 231 (37), 131 (9)

Molecule 3a

MS m/z (%) $C_{194}H_{392}N_{63}O_{33}$ [4130] : 4153 (15) [M + Na], 4130 (67), 3996 (91), 3512 (45), 2166 (51), 1188 (42)

Molecule 3b

MS m/z (%) $C_{386}H_{776}N_{127}O_{65}$ [8226] : 8249 (77) [M + Na], 8229 (15) [M + 3H], 7362 (67), 5433 (50), 4613 (45), 2984 (85), 2026 (39)

Molecule 3c

MS m/z (%) $C_{770}H_{1544}N_{255}O_{129}$ [16418] : 16441 (39) [M + Na], 16362 (79), 16124 (88), 15348 (45), 9431 (46), 8127 (83), 6142 (91) 4726 (32)

HPLC Data for Didendron Synthesis

Molecule	Retention Time (min)	Area (uV.sec)	Height (uV)
3a	4.520	5263855	350998
3b	4.466	7248071	393704
3c	4.221	4929354	242522

APPENDIX V

Sample preparation for microscopy

All samples for microscopy were provided in an aqueous medium. Dendrimers were in solution and liposomes were in suspension.

Light Microscopy

An aqueous drop of the sample was placed on a clean glass slide and covered with a cover slip and examined using a Nikon Microphot-FXA Light Microscope. No further treatment of the sample was performed. Images were captured either digitally as "tif" files or prints were taken using a video graphic printer.

(see Figures 3.7a-d; Figure 5.14; Figure 5.15)

Transmission Electron Microscopy

An aqueous drop of the sample was placed onto a carbon coated copper grid (400 mesh), excess removed with filter paper, and a drop of negative stain added for contrast (1% Phosotungstic acid). The prepared sample was viewed and photographed under a FEI/Philips CM 120 Transmission Electron Microscope, using Kodak So163 Film and printed on Ilford multi-grade paper.

(see Figure 3.2)

Scanning Electron Microscopy

An aqueous sample was adhered onto an SEM stub using carbon discs, then gold coated in an Emitech K550 Sputter Coater for 2 minutes at 30 mA. The coated sample was viewed under a FEI/Philips XL 20 Scanning Electron Microscope. Images were captured either digitally as "tif" files or prints were taken using a video graphic printer.

(see Figures 4.5a-b)

APPENDIX VI

Solubility data of the molecules synthesised

Molecule	Aqueous Solubility (mg/ml)
1a	3.8
1b	4.1
1c	4.5
1d	1.8
1e	2.1
1f	2.2
2a	-
2b	-
2c	-
2d	2.4
2e	4.6
2f	1.3
2g	-
2h	2.4
2i	-
2j	1.4
2k	-
2l	-
2m	5.1
2n	-
3a	2.1
3b	1.9
3c	2.3

The exact solubilities of molecules 2a, 2b, 2c, 2g, 2i, 2k, 2l, and 2n were not determined. All of these molecules exhibited aqueous solubility during lyophilisation when excess solvent was used.

APPENDIX VII

Linear representation of diffusion profiles (4-24 h) seen in Fig. 4.4.

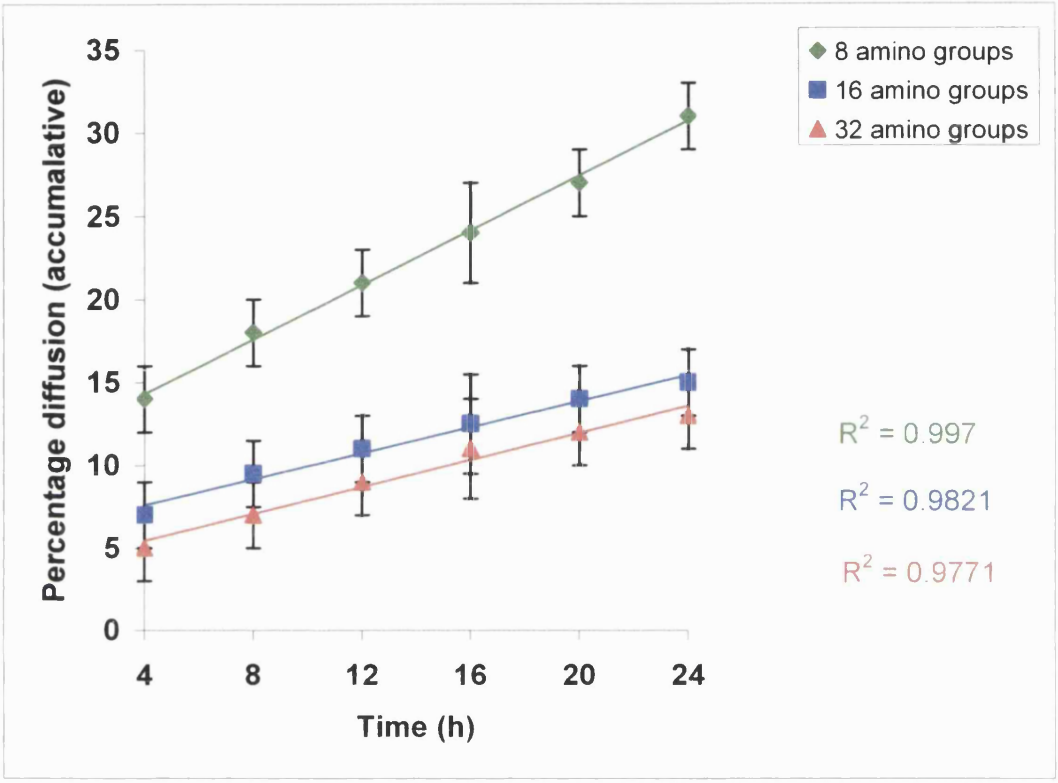

The accumulative percentage diffusion profiles of molecules 1a-c, in the absence of albumin and NaCl, from 4 h to 24 h at 25 ℃.

PUBLICATIONS

Purohit, G., Sakthivel, T., Florence, A.T. (2001) Interaction of cationic partial dendrimers with charged and neutral liposomes. *Int. J. Pharm.*, **214**, 71-76.

Purohit, G., Sakthivel, T., Florence, A.T. (2003) The interaction of cationic dendrons with albumin and their diffusion through cellulose membranes. *Int. J. Pharm.*, **254**, 37-41.

REFERENCES

Reference 1: AMVn Automated Microviscometer Instruction Handbook (2001). Published by Anton Paar GmbH, Graz, Austria.

Al-Awqati, Q. (1999) One hundred years of membrane permeability: Does Overton still rule? *Nat. Cell Biol.*, **1**, 201-202.

Al-Jamal, K.T., Sakthivel, T., Florence, A.T. (2003) Dendrisomes: cationic lipidic dendron vesicular assemblies. *Int. J. Pharm.*, **254**, 33-36.

Alonso, B., Moran, M., Casado, C.M., Lobete, F., Losada, J., Cuadrado, I. (1995) Electrodes modified with electroactive films of organometallic dendrimers *Chem. Mater.*, **7**, 1440-1442.

Arima, H., Kihara, F., Hirayama, F., Uekama, K. (2001) Enhancement of gene expression by polyamidoamine dendrimer conjugates with α-, β-, and γ-cyclodextrins. *Bioconjugate Chem.*, **12**, 476-484.

Balzani, V., Capagna, S., Denti, G., Juris, A., Serroni, S., Venturi, M. (1998) Designing dendrimers based on transition-metal complexes. Light-harvesting properties and predetermined redox patterns. *Acc. Chem. Res.*, **31**, 26–34.

Bangham, A.D., Standish, M.M., Watkins, J.C. (1965) Diffusion of univalent ions across the lamellae of swollen phospholipids. *J. Mol. Biol.*, **13**, 238-253.

Banno, Y., Ohki, K., Morita, T., Yoshioka, S., Nozawa, Y. (1986) Involvement of the membrane fluidity of lactosylceramide-targeted liposomes in their intrahepatic uptake. *Biochem. Int.*, **12**, 865–871.

Bar-Haim, A., Klafter, J. (1998) Geometric versus energetic competition in light harvesting by dendrimers. *J. Phys. Chem. B*, **102**, 1662 – 1664.

Baru, M.B., Mustaeva, L.G., Gorbunova, E.Y., Vagenina, I.V., Kitaeva, M.A., Cherskii, V.V. (1999) Spectrophotometric monitoring in continuous-flow Boc-based solid-phase peptide synthesis. *J. Peptide Res.*, **54**, 263-269.

Bezouška, K. (2002) Design, functional evaluation and biomedical applications of carbohydrate dendrimers (glycodendrimers). *Rev. Mol. Biotechnology*, **90**, 269-290.

Blank, I.H., Scheuplein, R.J., MacFarlane, D.J. (1967) Mechanism of percutaneous absorption. 3. The effect of temperature on the transport of non-electrolytes across the skin. *J. Invest. Dermatol.*, **49**, 582-589.

Bodanszky, M. (1984) Reversible blocking of amino and carboxyl groups. In: *Principles of Peptide Synthesis.* Bodanszky, M., ed. Berlin, Springer-Verlag, 59-118.

Camenisch, G., Folkers, G., Waterbeemd, H.V.D. (1996) Review of theoretical passive drug absorption models: Historical background, recent developments and limitations. *Pharma. Acta Helv.*, **71**, 309-327.

Campagna, S., Denti, G., Serroni, S., Juris, A., Venturi, M., Ricevuto, V., Balzani, V. (1995) Dendrimers of nanometer size based on metal complexes: Luminescent and redox-active polynuclear metal complexes containing up to twenty-two metal centres. *Chem. Eur. J.*, **1**, 211-221.

Canas, A., Ariza, M.J., Benavente, J. (2002) A comparison of electrochemical and electrokinetic parameters determined for cellophane membranes in contact with NaCl and $NaNO_3$ solutions. *J. Colloid Interface Sci.*, **246**, 150-156.

Carter, D. C., Ho, J. X. (1994) Structure of serum albumin. *Adv. Protein Chem.*, **45**, 153-203.

Chen, C.Z., van Dyk, T., Dhurjati, P., LaRossa, R., Cooper, S.L. (2000) Quaternary ammonium functionalized dendrimers as effective antimicrobials: structure-activity studies. *Biomacromolecules*, **1**, 473–480.

Cherestes, A., Engel, R. (1994) Dendrimeric ion exchange materials. *Polymer. Commun.*, **35**, 3343-3344.

Chiba, T., Yoshimura, T., Esumi, K. (2003) Physicochemical properties of aqueous mixed solutions of sugar-persubstituted poly(amidoamine)dendrimers and bovine serum albumin. *Colloids and Surfaces A: Physicochem. Eng. Aspects*, **214**, 157-165.

Choi, J.S., Joo, D.K., Park, J.S. (2000) Synthesis of a barbell-like triblock copolymer, poly(L-lysine) dendrimer- *block* -poly(ethylene glycol)- *block* -poly(L-lysine) dendrimer and its self-assembly with plasmid DNA. *Proc. Int. Symp. Control. Release Bioact. Mater.*, **27**, 618-619.

Choi, J.S., Lee, E.J., Choi, Y.H., Jeong, Y.J., Park, J.S. (1999) Poly(ethylene glycol)-block-poly(L-lysine) dendrimer: novel linear polymer/dendrimer block copolymer forming a spherical water-soluble polyionic complex with DNA. *Bioconjugate Chem.*, **10**, 62–65.

Cloninger, M.J. (2002) Biological applications of dendrimers. *Curr. Opinion Chem. Biol.*, **6**, 1-7.

Corrigan, O.I., Farvar, M.A., Higuchi, W.I. (1980) Drug membrane transport enhancement using high energy drug polyvinylpyrrolidone (PVP) co-precipitates. *Int. J. Pharm.*, **5**, 229-238.

de Gennes, P.G., Hervet, H. (1983) Statistics of "Starburst" polymers. *J. Phys. Lett.*, **44**, 351-360.

Dennig, J., Duncan, E. (2002) Gene transfer into eukaryotic cells using activated polyamidoamine dendrimers. *Rev. Mol. Biotechnology*, **90**, 339-347.

Donaruma, L.G., Vogl, O., Ottenbrite, R.M. (1980) In: *Anionic Polymeric Drugs*. New York, Wiley, 34-51.

Dubber, M., Lindhorst, T.K. (2001) Trehalose-based octopus glycosides for the synthesis of carbohydrate-centred PAMAM dendrimers and thiourea-bridged glycoclusters. *Org. Lett.*, **3**, 4019-4022.

Duncan, R. (1997) Drug targeting: Where are we now and where are we going? *J. Drug Targ.*, **5**, 1-4.

Dvornic, P.R., Tomalia, D.A. (1996) Molecules that grow like trees. *Sci. Spectra.* **5**, 36-41.

El-Sayed, M., Ginski, M., Rhodes, C., Ghandehari, H. (2002) Transepithelial transport of poly(amidoamine) dendrimers across Caco-2 cell monolayers. *J. Control. Rel.*, **81**, 355–365.

El-Sayed, M., Kiani, M.F., Naimark, M.D., Hikal, A.H., Ghandehari, H. (2001) Extravasation of poly(amidoamine) (PAMAM) dendrimers across microvascular network endothelium. *Pharm. Res.*, **18**, 23-28.

Emanuel, N., Kedar, E., Bolotin, E.M., Smorodinsky, N.I., Barenholz, Y. (1996) Preparation and characterization of doxorubicin- loaded sterically stabilized immunoliposomes. *Pharm. Res.*, **13**, 352–359.

Erickson, B.W., Merrifield, R.B. (1976) In: *The Proteins Vol II.* Neurath, H., Hill, R.L., eds. New York, Academic Press, 255-262.

Esfand, R., Tomalia, D.A. (2001) Poly(amidoamine) (PAMAM) dendrimers: from biomimicry to drug delivery and biomedical applications. *Drug Discov. Today*, 6, 427-436.

Ferruti, P. (1986) Polymers as matrices for drug release. In: *Targeting of Drugs with Synthetic Systems.* Gregoriadis, G., Senior, J., Poste, G., eds. NATO ASI Series, Series A: Life Sciences, Vol **113**, New York: Plenum Press, 165-183.

Fischer, D., Li, Y., Ahlemeyer, B., Krieglstein, J., Kissel, T. (2003) In vitro cytotoxicity testing of polycations: influence of polymer structure on cell viability and hemolysis. *Biomaterials*, **24**, 1121–1131.

Florence, A.T., Hussain, N. (2001) Transcytosis of nanoparticle and dendrimer delivery systems: evolving vistas. *Adv. Drug Del. Rev.*, **50**, S69–S89.

Flynn, G.L., Yalkowsky, S.H. (1972) Correlation and prediction of mass transport across membranes I: Influence of alkyl chain length on flux-determining properties of barrier and diffusant. *J. Pharm. Sci.*, **6**, 838-852.

Fontenot, J.D., Ball, J.M., Miller, M.A., David, C.M., Montelaro, R.C. (1991) A survey of potential problems and quality control in peptide synthesis by the fluorenylmethoxycarbonyl procedure. *Pept. Res.*, **4**, 19-25.

Fréchet, J.M.J. (1994) Functional polymers and dendrimers: Reactivity, molecular architecture, and interfacial energy. *Science*, **263**, 1710-1715.

Fréchet, J.M.J., Hawker, C.J., Wooley, K.L. (1994) The convergent route to globular dendritic macromolecules: A versatile approach to precisely functionalized three dimensional polymers and novel block copolymers. *J. Macromol. Sci., Pure Appl. Chem.*, **A31**, 1627-1645.

Fukushima, D., Yokoyama, S., Kezdy, F.J., Kaiser, E.T. (1981) Binding of amphiphilic peptides to phospholipid/cholesterol unilamellar vesicles: A model for protein-cholesterol interaction. *Proc. Natl. Acad. Sci. USA*, **78**, 2372-2736.

Gabizon, A, Price, D.C., Huberty, J., Bresalier, R.S., Papahadjopoulos, D. (1990) Effect of liposome composition and other factors on the targeting of liposomes to experimental tumours: biodistribution and imaging studies. *Cancer Res.*, **50**, 6371–6378.

Ganesh, R.N., Shraberg, J., Sheridan, P.G., Thayumanavan, S. (2002) Synthesis of difunctionalized dendrimers: an approach to main-chain poly(dendrimers). *Tetrahedron Lett.*, **43**, 7217–7220.

Gausepohl, H., Pieles, U., Frank, R.W. (1992) In: *Peptides, Chemistry and Biology, Proceedings of the 12th American Peptide Symposium.* Smith, J.A., Rivier, J.E., eds. Leiden: ESCOM, 523.

Gebhart, C.L., Kabanov, A.V. (2001) Evaluation of polyplexes as gene transfer agents. *J. Control. Rel.*, **73**, 401-416.

Gensch, T., Tsuda, K., Doll, G.C., Latterini, L., Weener, J.W., Schenning, A.P.H.J., Hofkens, J., Meijer, E.W., De Schryver, F.C. (2001) Microscopy and optical manipulation of dendrimer-built vesicles. *Pure Appl. Chem.*, **73**, 435–441.

Gilat, S.L., Adronov, A., Fréchet, J.M.J. (1999) Modular approach to the accelerated convergent growth of laser dye-labelled poly(aryl ether) dendrimers using a novel hypermonomer. *J. Org. Chem.*, **64**, 7474–7484.

Gossl, I., Shu, L., Schluter, A.D., Rabe, J.P. (2002) Molecular structure of single DNA complexes with positively charged dendronized polymers. *J. Am. Chem. Soc.*, **124**, 6860-6865.

Gref, R., Minamitake, Y., Peracchia, M.T., Trubetskoy, V., Torchilin, V., Langer, R. (1994) Biodegradable long-circulating polymeric nanospheres. *Science*, **263**, 1600-1603.

Gregoriadis, G. (1998) Liposomes in drug targeting. In: *Cell Biology: A Laboratory Handbook*, 2nd ed. London, Academic Press, 131-136.

Gregoriadis, G., Davis, C. (1979) Stability of liposomes in vivo and in vitro is promoted by their cholesterol content and the presence of blood cells. *Biochem. Biophys. Res. Commun.*, **89**, 1287–1293.

Gregoriadis, G., Ryman, B.E. (1972) Fate of protein-containing liposomes injected into rats. An approach to the treatment of storage diseases. *Eur. J. Biochem.*, **24**, 485-491.

Haensler, J., Szoka, F.C. Jr (1993) Polyamidoamine cascade polymers mediate efficient transfection of cells in culture. *Bioconjugate Chem.*, **4**, 372–379.

Hammouda, Y.E., Kasim, N.A., Nada, A.H. (1993) Formulation and in vitro evaluation of verapamil HCl suppositories. *Int. J. Pharm.*, **89**, 111-118.

Harashima, H., Sakata, K., Funato, K., Kiwada, H. (1994) Enhanced hepatic uptake of liposomes through complement activation depending on the size of liposomes. *Pharm. Res.* **11**, 402–406.

Hawker, C. J., Fréchet, J. M. J. (1990) Preparation of polymers with controlled molecular architecture. A new convergent approach to dendritic macromolecules. *J. Am. Chem. Soc.*, **112**, 7638-7647.

Hawker, C.J., Wooley, K.L., Fréchet, J.M.J. (1993) Solvatochromism as a probe of the microenvironment in dendritic polyethers: transition from an extended to a globular structure. *J. Am. Chem. Soc.*, **115**, 4375–4376.

Hawker, C.J., Wooley, K.L., Fréchet, J.M.J. (1993a) Unimolecular micelles and globular amphiphiles: Dendritic macromolecules as novel recyclable solubilization agents. *J. Chem. Soc., Perkin Trans. 1*, 1287–1297.

Hayton, W.L. (1980) Rate-limiting barriers to intestinal drug absorption: A review. *J. Pharmacokin. Biopharm.*, **8**, 321-334.

Higuchi, W.I., Ho, N.F.H., Park, J.Y., Komiya, I. (1981) Rate limiting steps and factors in drug absorption. In: *Drug Absorption.* Nimmo, L.F., Prescott, W.S., eds. Lancaster, MTP Press, 35-60.

Inoue, K. (2000) Functional dendrimers, hyperbranched and star polymers. *Prog. Polym. Sci.*, **25**, 453-571.

Jansen, J.F.G.A., de Brabander-van den Berg, E.M.M., Meijer, E.W. (1994) Encapsulation of guest molecules into a dendritic box. *Science*, **266,** 1226-1229.

Jansen, J.F.G.A., Meijer, E.W., de Brabander-van den Berg, E.M.M. (1995) The dendritic box, shape-selective liberation of encapsulated guests. *J. Am. Chem. Soc.*, **117**, 4417–4418.

Jayaraman, G., Li, Y., Moore, J.A., Cramer, S.M. (1995) Ion-exchange displacement chromatography of proteins: dendritic polymers as novel displacers. *J. Chromatogr.*, **702**,143-155.

Jevprasesphant, R., Penny, J., Jalal, R., Attwood, D., McKeownb, N.B., D'Emanuele, A. (2003) The influence of surface modification on the cytotoxicity of PAMAM dendrimers. *Int. J. Pharm.*, **252**, 263–266.

Jevprasesphant, R., Penny, J., Attwood, D., McKeownb, N.B., D'Emanuele, A. (2003) Engineering of dendrimer surfaces to enhance transepithelial transport and reduce cytotoxicity. *Pharm. Res.*, **20**, 1543-1550.

Jockusch, S., Turro, N.J., Ottaviani, M.F., Tomalia, D.A. (2002) An EPR and fluorescence depolarization study of intermolecular interactions of dendrimers at medium and highly concentrated aqueous solutions. *J. Colloid Interface Sci.*, **256**, 223-227.

Junge, D.M., McGrath, D.V. (1997) Photoresponsive dendrimers. *Chem. Commun.*, 857–858.

Kaiser, E., Colescott, R.L., Bossinger, C.D., Cook, P.I. (1970) Color test for detection of free terminal amino groups in the solid-phase synthesis of peptides. *Anal. Biochem.*, **34**, 595– 598.

Kimura, Y., Lim, H.J., Iijima, T. (1984) Membrane potentials of charged cellulosic membranes. *J. Membr. Sci.*, **18**, 285-296.

Klajnert, B., Bryszewska, M. (2002) Fluorescence studies on PAMAM dendrimers interactions with bovine serum albumin. *Bioelectrochemistry*, **55**, 33-35.

Klajnert, B., Stanislawska, L., Bryszewska, M., Palecz, B. (2003) Interactions between PAMAM dendrimers and bovine serum albumin. *Biochim. Biophys. Acta*, **1648**, 115-126.

Knorr, R., Trzeciak, A., Bannwarth, W., Gillessen, D. (1989) New coupling reagents in peptide chemistry. *Tetrahedron Letters*, **30**, 1927-1930.

Kojima, C., Kono, K., Maruyama, K., Takagishi, T. (2000) Synthesis of polyamidoamine dendrimers having poly(ethylene glycol) grafts and their ability to encapsulate anticancer drugs. *Bioconjugate Chem.*, **11**, 910-917.

Kragh-Hansen, U. (1981) Molecular aspects of ligand binding to serum albumin. *Pharmacol. Rev.*, **33**, 17-53.

Kreuter, J., Higuchi, W.I., Ganesan, M.G. and Weiner, N.D. (1981) Delivery of liposome membrane-associated sterols through silastic membranes. *Biochim. Biophys. Acta*, **676**, 118–121.

Kreuter, J., Mills, S.N., Davis, S.S. and Wilson, C.G., (1983) Polybutylcyanoacrylate nanoparticles for the delivery of [^{75}Se]norcholestenol. *Int. J. Pharm.*, **16**, 105–113.

Kukowska-Latallo, J., Bielinska, A., Chen, C., Rymaszewski, M., Tomalia, D., Baker, J.R.J. (1998) Gene transfer using starburst dendrimers. In: *Self-assembling Complexes for Gene Delivery.* Kabanov, A.V., Felgner, P., Seymour, L. eds. Chichester, Wiley, 241-253.

Kukowska-Latallo, J.F., Bielinska, A.U., Johnson, J., Spindler, R., Tomalia, D.A., Baker Jr., J.R. (1996) Efficient transfer of genetic material into mammalian cells using starburst polyamidoamine dendrimers. *Proc. Natl. Acad. Sci. U.S.A.*, **93**, 4897–4902.

Kuzdzal, S.A., Monnig, C.A., Newkome, G.R., Moorefield, C.N. (1994) Dendrimer electrokinetic capillary chromatography: Unimolecular micellar behaviour of carboxylic acid terminated cascade macromolecules. *J. Chem. Soc., Chem. Commun.*, 2139-2140.

Lasic, D.D. and Papahadjopoulos, D. (1995) Liposomes revisited. *Science*, **267**, 1275–1276.

Lee, K.D., Hong, K., Papahadjopoulos, D. (1992) Recognition of liposomes by cells: in vitro binding and endocytosis mediated by specific lipid headgroups and surface charge density. *Biochim. Biophys. Acta.*, **1103**, 185–197.

Levine, R.R. (1970) Factors affecting gastrointestinal absorption of drugs. *Am. J. Diges. Dis.*, **15**, 171-188.

Liu, M., Fréchet, J.M.J. (1999) Designing dendrimers for drug delivery. *Pharm. Sci. Technol. Today*, **2,** 393-401.

Liu, M., Kono, K., Fréchet, J.M.J. (2000) Water-soluble dendritic unimolecular micelles: Their potential as drug delivery agents. *J. Control. Rel.*, **65**, 121-131.

Liu, H., Farrell, S., Uhrich, K. (2000) Drug release characteristics of unimolecular polymeric micelles. *J. Control. Rel.*, **68**, 167-174.

Loftsson, T., Másson, M., Sigurdsson, H.H. (2002) Cyclodextrins and drug permeability through semi-permeable cellophane membranes. *Int. J. Pharm.*, **232**, 35-43.

Loukas, Y.L., Jayasekera, P., Gregoriadis, G. (1995) Characterisation and photoprotection studies of a model γ-cyclodextrin-included photolabile drug entrapped in liposomes incorporating light absorbers. *J. Phys. Chem.*, **99**, 11035-11040.

Loukas, Y.L., Jayasekera, P., Gregoriadis, G. (1995a) Novel liposome-based multicomponent systems for the protection of photolabile agents. *Int. J. Pharm.*, **117**, 85-94.

Loup, C., Zanta, M., Caminade, A., Majoral, J., Meunier, B. (1999) Preparation of water-soluble cationic phosphorus-containing dendrimers as DNA transfecting agents. *Chem. Eur. J.*, **5**, 3644-3650.

Luo, D., Haverstick, K., Belcheva, N., Han, E., Saltzman, W.M. (2002) Poly(ethylene glycol)-conjugated PAMAM dendrimer for biocompatible high-efficiency DNA delivery. *Macromolecules*, **35**, 3456-3462.

Malik, N., Evagorou, E.G., Duncan, R. (1997) A PAMAM dendrimer-platinate. *Proc. Int. Symp. Control. Release Bioact. Mater.*, **24**, 107–108.

Malik, N., Wiwattanapatapee, R., Klopsch, R., Lorenz, K., Frey, H., Weener, J.W., Meijer, E.W., Paulus, W., Duncan, R. (2000) Dendrimers: relationship between structure and biocompatibility *in vitro* and preliminary studies on the biodistribution of ^{125}I-labelled polyamidoamine dendrimers *in vivo*. *J. Control. Rel.*, **65**, 133-148.

Mammen, M., Choi, S.K., Whitesides, G.M. (1998) Polyvalent interactions in biological systems: implications for design and use of multivalent ligands and inhibitors. *Angew. Chem. Int. Ed. Engl.*, **37**, 2754-2794.

Mansfield, M.L. (2000) Monte Carlo studies of dendrimers. Additional results for the diamond lattice model. *Macromolecules*, **33**, 8043-8049.

Martin, A.N. (1993) *Physical Pharmacy: Physical Chemical Principles in the Pharmaceutical Sciences*, 4th ed. Baltimore, Lippincott Williams and Wilkins, 324-329, 351-353, 400-402.

Martinez, J., Bali, J.P., Rodriquez, M., Castro, B., Laur, J., Lignon, M-F. (1985) Synthesis and biological activities of some pseudo peptide analogues of tetagastrin – The importance of the peptide backbone. *J. Med. Chem.*, **28**, 1874-1879.

Matsueda, G.R., Stewart, J.M. (1981) A p-Methylbenzhydrylamine resin for improved solid phase synthesis of peptide amides. *Peptides*, **2**, 45-50.

Matthews, O.A., Shipway, A.N., Stroddart, J.F. (1998) Dendrimers – Branching out from curiosities into new technologies. *Prog. Polym. Sci.*, **23**, 1-56.

Merrifield, R.B. (1963) Solid phase peptide synthesis I. The synthesis of a tetrapeptide. *J. Am. Chem. Soc.*, **85**, 2149-2153.

Meyer, M.C., Guttman, D.E. (1968) Novel method for studying protein binding. *J. Pharm. Sci.*, **57**, 1627-1629.

Milhem, O.M., Mobedi, H., Day, N., McKeown, N.B., Attwood, D., D'Emanuele, A. (2001) Development of dendrimer conjugates for drug delivery. *Polym. Mater. Sci. Eng.*, **84**, 721.

Miller, T.M., Neenan, T.X., Zayas, R., Blair, H.E. (1992) Synthesis and characterization of a series of monodisperse, 1, 3, 5, phenylene-based hydrocarbon dendrimers including $C_{276}H_{186}$ and their fluorinated analogues. *J. Am. Chem. Soc.*, **114**, 1018-1025.

Mitchell, A.R., Kent, S.B.H., Engelhard, M., Merrifield, R.B. (1978) A new synthetic route to tert. Butyloxycarbonylaminoacyl 4-(oxomethyl) pheneylacetamidomethyl resin – An improved support for solid phase peptide synthesis. *J. Org. Chem.*, **43**, 2845-2852.

Mizrahi, A., Ben-Ner, E., Katz, M.J., Kedem, K., Glusman, J.G., Libersat, F. (2000) Comparative analysis of dendritic architecture of identified neurons using the Hausdorff distance metric. *J. Comp. Neurol.* **422**, 415-428.

Mojsov, S., Mitchell, A.R., Merrifield, R.B. (1980) A quantitative evaluation of methods for coupling asparagine. *J. Org. Chem.*, **45**, 555-560.

Mori, A., Klibanov, A.L., Torchilin, V.P., Huang, L. (1991) Influence of the steric barrier activity of amphipathic poly-(ethyleneglycol) and ganglioside GM on the circulation time of liposomes and on the target binding of immuno-liposomes in vivo. *FEBS Lett.*, **284**, 263–266.

Mourey, T.H., Turner, S.R., Rubenstein, M., Fréchet, J.M.J., Hawker, C.J., Wooley, K.L. (1992) Unique behaviour of dendritic macromolecules: Intrinsic viscosity of polyether dendrimers. *Macromolecules*, **25**, 2401-2406.

Muijselaar, P.G.H.M., Claessens, H.A., Cramers, C.A., Jansen, J.F.G.A., Meijer, E.W., de Brabander-van den Berg, E.M.M., van der Wal, S. (1995) Dendrimers as pseudo-stationary phases in electrokinetic chromatography. *J. High. Resol. Chromatogr.*, **18**, 121-123.

Müller, B., Kreuter, J. (1999) Enhanced transport of nanoparticle associated drugs through natural and artificial membranes-a general phenomenon? *Int. J. Pharm.*, **178**, 23-32.

Naylor, A.M., Goddard, W.A., Kiefer, G.E., Tomalia, D.A. (1989) Starburst dendrimers 5. Molecular shape and control. *J. Am. Chem. Soc.*, **111**, 2339-2341.

Newkome, G.R. (1996) Heterocyclic loci within cascade dendritic macromolecules. *J. Heterocyclic Chem.*, **33**, 1445-1460.

Newkome, G.R., Moorefield, C.N., Baker, G.R., Saunders, M.J., Grossman, S.H. (1991) Unimolecular micelles. *Angew. Chem. Int. Ed. Engl.*, **30**, 1178-1180.

Newkome, G.R., Moorefield, C.N., Vogtle, F. (1996) Dendritic macromolecules: Concepts, syntheses, perspectives. Weinheim, VCH.

Newkome, G.R., Woosley, B.D., He, E., Moorefield, C.N., Güther, R., Baker, G.R., Escamilla, G.H., Merrill, J. (1996a) Supramolecular chemistry of flexible, dendritic based structures employing molecular recognition *J. Chem. Soc., Chem. Commun.*, 2737-2738.

Newkome, G.R., Yao, Z., Baker, G.R., Gupta, V.K. (1985) Cascade molecules: a new approach to micelles. A [27]-Arborol. *J. Org. Chem.*, **50,** 2003-2004.

Newkome, G.R., Young, J.K., Baker, G.R., Potter, R.L., Audoly, L., Cooper, D., Weis, C.D., Morris, K.F., Johnson, C.S. Jr. (1993) Cascade polymers: pH dependence of hydrodynamic radii of acid terminated dendrimers. *Macromolecules*, **26**, 2394-2396.

Nolan, L.M.A., Corish, J., Corrigan, O.I., Fitzpatrick, D. (2003) Iontophoretic and chemical enhancement of drug delivery Part I: Across artificial membranes. *Int. J. Pharm.*, **257**, 41-55.

Ottaviani, M.F., Matteini, P., Brustolon, M., Turro, N.J., Jockusch, S., Tomalia, D.A. (1998) Characterization of starburst dendrimers and vesicle solutions and their interactions by cw- and pulsed-EPR, TEM, and dynamic light scattering. *J. Phys. Chem. B*, **102**, 6029-6039.

Patri, A.K., Majoros, I.J., Baker Jr, J.R. (2002) Dendritic polymer macromolecular carriers for drug delivery. *Curr. Opinion Chem. Biol.*, **6**, 466–471.

Patri, A.K., Thomas, T., Baker, J.R. Jr, Bander, N.H. (2002) Antibody-dendrimer conjugates for targeted prostate cancer therapy. *Polym. Mater. Sci. Eng.*, **86**, 130.

Pavlov, G.M., Errington, N., Harding, S.E., Korneeva, E.V., Roy, R. (2001) Dilute solution properties of lactosylated polyamidoamine dendrimers and their structural characteristics. *Polymer*, **42**, 3671-3678.

Pavlov, G.M., Korneeva, E.V., Meijer, E.W. (2002) Molecular characteristics of poly(propylene imine) dendrimers as studied with translational diffusion and viscometry. *Colloid Polym. Sci.*, **280**, 416-423.

Peters, T.J. (1996) In: *All about Albumin, Biochemistry, Genetics and Medical Applications.* San Diego, Academic Press, 20-32.

Prosa, T.J., Bauer, B.J., Amis, E.J., Tomalia, D.A., Scherrenberg, R. (1997) A SAXS study of the internal structure of dendritic polymer systems. *J. Polym. Sci. Part B: Polym. Phys.*, **35**, 2913-2924.

Pujar, N.S., Zydney, A.L. (1994) Electrostatic and electrokinetic interactions during protein transport through narrow pore membranes. *Ind. Eng. Chem. Res.*, **33**, 2473-2482.

Ramaswamy, C., Sakthivel, T., Wilderspin, A.F., Florence, A.T. (2003) Dendriplexes and their characterisation. *Int. J. Pharm.*, **254**, 17-21.

Reek, J.N.H., de Groot, D., Oosterom, G.E., Kamer, P.C.J., van Leeuwen, P.W.N.M. (2002) Core and periphery functionalized dendrimers for transition metal catalysis; a covalent and a non-covalent approach. *Rev. Mol. Biotechnology*, **90**, 159-181.

Rietveld, I.B., Bedeaux, D. (2001) The viscosity of solutions of poly (propylene imine) dendrimers in methanol. *J. Colloid Interface Sci.*, **235**, 89-92.

Roberts, J.C, Adams, Y.E., Tomalia, D., Mercer-Smith, J.A., Lavallee, D.K. (1990) Using starburst dendrimers as linker molecules to radiolabel antibodies. *Bioconjugate Chem.*, **1**, 305-308.

Roessler, B.J., Bielinska, A.U., Janczak, K., Lee, I., Baker, J.R. (2001) Substituted β-cyclodextrins interact with PAMAM dendrimer-DNA complexes and modify transfection efficiency. *Biochem. Biophys. Res. Commun.*, **283**, 124-129.

Rolland, A.P. (1998) From genes to gene medicines: Recent advances in nonviral gene delivery. *Crit. Rev. Ther. Drug Carrier Sys.*, **15**, 143-198.

Roovers, J., Comanita, B. (1999) Dendrimers and dendrimer-polymer hybrids. *Adv. Polym. Sci.*, **142**, 179-228.

Sadamoto, R., Tomioka, N., Aida, T. (1996) Photoinduced electron transfer reactions through dendrimer architecture. *J. Am. Chem. Soc.*, **118**, 3978–3979.

Sadler, K., Tam, J.P. (2002) Peptide dendrimers: Applications and synthesis. *Rev. Mol. Biotechnology*, **90**, 195-229.

Sakai, K. (1994) Determination of pore size and pore size distribution. 2. Dialysis membranes. *J. Membr. Sci.*, **96**, 91-130.

Sakakibara, S. (1971) In: *Chemistry and Biochemistry of Amino Acids, Peptides and Proteins*, Vol. 1. Weinstein, B., ed. New York, Marcel Dekker, 51-85.

Sakthivel, T., Toth, I., Florence, A.T. (1998) Synthesis and physicochemical properties of lipophilic polyamide dendrimers. *Pharm. Res.*, **15**, 776-782.

Salamat-Miller, N., Chittchang, M., Mitra, A.K., Johnston, T.P. (2002) Shape imposed by secondary structure of a polypeptide affects its free diffusion through liquid-filled pores. *Int. J. Pharm.*, **244**, 1-8.

Salamończyk, G.M., Kuźnikowski, M., Poniatowska, E. (2002) Dendrimers bearing three types of branching functions. *Tetrahedron Lett.*, **43**, 1747–1749.

Sanders, L.M. (1991) Controlled delivery systems for peptides. In: *Peptide and Protein Drug Delivery.* Lee, V.H.L., ed. New York, Marcel Dekker, 785-806.

Sato, N., Kobayashi, H., Saga, T., Nakamoto, Y., Ishimori, T., Togashi, K., Fujibayashi, Y., Konishi, J., Brechbiel, M.W. (2001) Tumor targeting and imaging of intraperitoneal tumors by use of antisense oligo-DNA complexed with dendrimers and/or avidin in mice. *Clin. Cancer Res.*, **7**, 3606-3612.

Saville, P.M., Reynolds, P.A., White, J.W., Hawker, C.J., Fréchet, J.M.J., Wooley, K.L., Penfold, J., Webster, J.R.P. (1995) Neutron reflectivity and structure of polyether dendrimers as Langmuir films. *J. Phys. Chem.*, **99**, 8283-8289.

Sheehan, J.C., Hess, G.P. (1955) A new method of forming peptide bonds. *J. Am. Chem. Soc.*, **77**, 1067.

Shukla, S., Wu, G., Chatterjee, M., Yang, W., Sekido, M., Diop, L.A., Műller, R., Sudimack, J.J., Lee, R.J., Barth, R.F., Tjarks, W. (2003) Synthesis and biological evaluation of folate receptor-targeted boronated PAMAM dendrimers as potential agents for neutron capture therapy. *Bioconjugate Chem.*, **14**, 158-167.

Sideratou, A., Tsiourvas, D., Paleos, C.M. (2000) Quaternized poly(propylene imine) dendrimers as novel pH-sensitive controlled-release systems. *Langmuir*, **16**, 1766-1769.

Singer, S.J., Nicolson, G.L. (1972) The fluid mosaic model of the structure of cell membranes. *Science*, **175**, 720-731.

Singh, P., Moll, F. 3rd, Lin, S.H., Ferzli, C., Yu, K.S., Koski, R.K., Saul, R.G., Cronin, P. (1994) Starburst dendrimers: enhanced performance and flexibility for immunoassays. *Clin. Chem.*, **40**, 1845-1849.

Sommer, A.P., Ben-Moshe, M., Magdassi, S. (2004) Size-discriminative self-assembly of nanospheres in evaporating drops. *J. Phys. Chem. B*, **108**, 8-10.

Stebani, U., Lattermann, G., Wittenberg, M., Wendorff, H. (1996) Metallomesogens with branched, dendrimeric amino ligands. *Angew. Chem. Int. Ed. Engl.*, **35**, 1858-1861.

Stechemesser, S., Eimer, W. (1997) Solvent-dependent swelling of poly(amido-amine) starburst dendrimers. *Macromolecules*, **30**, 2204-2206.

Stewart, J.M., Young, J.D. (1984) In: *Solid Phase Peptide Synthesis* (2nd edn.). Pierce Chemical Co., Rockford III, 42.

Sui, G., Micic, M., Huo, O., Leblanc, R.M. (2000) Synthesis and surface chemistry study of a new amphiphilic PAMAM dendrimer. *Langmuir*, **16**, 7847-7851.

Tajarobi, F., El-Sayed, M., Rege, B.D., Polli, J.E., Ghandehari, H. (2001) Transport of poly amidoamine dendrimers across Madin–Darby canine kidney cells. *Int. J. Pharm.*, **215**, 263-267.

Tam, J.P. (1988) Synthetic peptide vaccine design-synthesis and properties of a high-density multiple antigenic peptide system. *Proc. Natl. Acad. Sci. USA*, **85**, 5409–5413.

Tam, J.P., Heath, W.F., Merrifield, R.B. (1983) Deprotection of synthetic peptides with a low concentration of HF. *J. Am. Chem. Soc.*, **105**, 6442-6455.

Tam, J.P., Wong, T.W., Riemen, M.W., Tjeong, F.S., Merrifield, R.B. (1979) Cyclohexyl ester as a new protecting group for aspartyl peptides to minimize aspartamide formation in acidic and basic treatments. *Tetrahedron Letters*, **42**, 4033-4036.

Tande, B.M., Wagner, N.J., Mackay, M.E., Hawker, C.J., Jeong, M. (2001) Viscosimetric, hydrodynamic, and conformational properties of dendrimers and dendrons. *Macromolecules*, **34**, 8580-8585.

Tanford, C (1961) In: *Physical Chemistry of Macromolecules*. New York, Wiley, 324 and 396.

Tang, M.X., Redemann, C.T., Szoka, F.C. Jr (1996) In vitro gene delivery by degraded polyamidoamine dendrimers. *Bioconjugate Chem.*, **7**, 703–714.

Terabe, S., Otsuka, K., Ando, T. (1985) Electrokinetic chromatography with micellar solution and open-tubular capillary. *Anal. Chem.*, **57**, 834-841.

Thompson, D. (1987) *On Growth and Form*, Cambridge University Press, London, 16-21.

Tomalia, D.A., Baker, H., Dewald, J.R., Hall, M., Kallos, G., Martin, S., Roeck, J., Ryder, J., Smith, P. (1985) A new class of polymers: starburst-dendritic macromolecules. *Polym. J.*, **17,** 117-132.

Tomalia, D.A., Durst, H.D. (1993) Genealogically Directed Synthesis: Starbust/Cascade Dendrimers and Hyperbranched Structures. *Top. Curr. Chem.*, **165,** 193-313.

Tomalia, D.A., Naylor, A.M., Goddard, W.A. (1990) Starburst dendrimers: molecular level control of size, shape, surface chemistry, topology and flexibility from atoms to macroscopic matter. *Angew. Chem. Int. Ed. Engl.*, **29,** 138-175.

Tomalia, D.A., Uppuluri, S., Swanson, D.R., Li, J. (2000) Dendrimers as reactive modules for the synthesis of new structure-controlled, higher-complexity megamers. *Pure Appl. Chem.*, **72,** 2343–2358.

Toth, I., Sakthivel, T., Wilderspin, A.F., Bayele, H., O'Donnell, M., Perry, D.J., Pasi, K.J., Lee, C.A., Florence, A.T. (1999) Novel cationic lipidic peptide dendrimer vectors: In vitro gene delivery. *S.T.P. Pharma. Sci.*, **9,** 93-99.

Turnbull, W.B., Stoddart, J.F. (2002) Design and synthesis of glycodendrimers. *Rev. Mol. Biotechnology*, **90,** 231-255.

Uppuluri, S., Keinath, S.E., Tomalia, D.A., Dvornic, P.R. (1998) Rheology of dendrimers I: Newtonian flow behaviour of medium and highly concentrated solutions of polyamidoamine (PAMAM) dendrimers in ethylenediamine (EDA) solvent. *Macromolecules*, **31**, 4498-4510.

Uppuluri, S., Morrison, F.A., Dvornic, P.R. (2000) Rheology of dendrimers II: Bulk polyamidoamine dendrimers under steady shear, creep, and dynamic oscillatory shear. *Macromolecules*, **33**, 2551-2560.

Uppuluri, S., Swanson, D.R., Piehler, L.T., Li, J., Hagnauer, G.L., Tomalia, D.A. (2000) Core-shell tecto(dendrimers) I. Synthesis and characterization of saturated shell models. *Adv. Mater.*, **12**, 796-800.

Wang, P.W., Liu, Y.J., Devadoss, C., Bharati, P., Moore, J.S. (1996) Electroluminescent diodes from a single-component emitting layer of dendritic macromolecules. *Adv. Mater.*, **8**, 237–241.

Wang, Y., Bai, Y., Price, C., Boros, P., Qin, L., Bielinska, A.U., Kukowska- Latallo, J.F., Baker, J.R., Bromberg, J.S. (2001) Combination of electroporation and DNA/dendrimer complexes enhances gene transfer into murine cardiac transplants. *Am. J. Transplant*, **1**, 334-338.

Watanabe, S., Iwamura, M. (2003) Dendritic caged compounds. *J. Photochem. Photobiol., A: Chem.*, **155**, 57-62.

Watanabe, S., Regen, S.L. (1994) Dendrimers as building blocks for multilayer construction. *J. Am. Chem. Soc.*, **116**, 8855-8856.

Wiwattanapatapee, R., Carreño-Gómez, B., Malik, N., Duncan, R. (2000) Anionic PAMAM dendrimers rapidly cross adult rat intestine *in vitro*: a potential oral delivery system? *Pharm. Res.*, **17**, 991-998.

Wooley, K.L., Hawker, C.J., Fréchet, J.M.J. (1993) Unsymmetrical three-dimensional marcomolecules: Preparation and characterization of strongly dipolar dendritic macromolecules *J. Am. Chem. Soc.*, **115**, 11496–11505.

Yajima, H., Fujii, N., Funakoshi, S., Murayama, E., Watanabe, T., Otaka, A. (1988) New strategy for the chemical synthesis of proteins. *Tetrahedron*, **44**, 805-819.

Yu, K., Russo, P.S. (1996) Light scattering and fluorescence photobleaching recovery study of poly(amidoamine) cascade polymers in aqueous solution. *J. Polym. Sci. B Polym. Phys.*, **34**, 1467–1475.

Zanini, D., Roy, R. (1997) Synthesis of new α-thiosialodendrimers and their binding properties to the sialic acid specific lectin from Limax flavus. *J. Am. Chem. Soc.*, **119**, 2088-2095.

Zeng, F., Zimmerman, S.C. (1997) Dendrimers in Supramolecular Chemistry: From Molecular Recognition to Self-Assembly, *Chem. Rev.*, **97**, 1681-1712.

Zhang, J., Moore, J.S., Xu, Z., Aquirre, R.A. (1992) Nanoarchitectures I. Controlled synthesis of phenylacetylene sequences. *J. Am. Chem. Soc.*, **114**, 2273-2274.

Zhang, Z., Smith, B.D. (2000) High-generation polycationic dendrimers are unusually effective at disrupting anionic vesicles: Membrane bending model. *Bioconjugate Chem.*, **11**, 805-814.

Zhuo, R.X., Du, B., Lu, Z.R. (1999) In vitro release of 5-fluorouracil with cyclic core dendritic polymer. *J. Control. Rel.*, **57**, 249–257.

RE: Correction of Thesis; Design and Characterisation of Dendritic Molecules

I have corrected the thesis as advised and discussed the corrections with Prof. Florence. The corrected version has 14 pages more than the original. The following is the summary of corrections.

1. Introductory chapter and sections have been rewritten as discussed.

2. The rationale for the studies has been incorporated into the end of Chapter 1 (p35). The statement regarding the physico-chemical properties of dendrimers has been amended.

3. In Chapter 1, the section discussing biocompatibility of dendrimers has been revised, including 2003 literature (p 34).

4. Additional information regarding the purification and characterisation of the synthesised compounds has been added (Appendices 2 and 3 for dendrons [p156-162]; Appendix 4 for didendrons [p163]). The reader has been directed accordingly.

5. Known solubility data for the compounds has been added (Appendix 6). The reader has been directed accordingly (p165).

6. A scheme outlining the synthetic route leading to compounds 1a-c has been included (Fig 2.5, p52).

7. Sample preparation for microscopy has been incorporated into Appendix 6, including preparation methods for each picture accordingly. The reader has been directed accordingly (p164).

8. Explanation of data points and error bars has been included at the beginning of each 'Results and Discussion' section.

9. Chapter 4 has been corrected regarding Fick's laws of diffusion. Based on the experimental set-up (Meyer and Guttman, 1968), sink conditions are maintained and diffusion obeys Fick's second law and not the first law. The correct assumptions have been applied to the data and all results and figures have been appropriately amended. An explanation of the diffusion profiles has been added and an explanation of why there is no lag-time in the system used (with additional references – p100). Appendix 7 (p167) relates to this chapter and the reader is directed accordingly.

10. The differences in the diffusion data for the 8-amino dendron, on p101, p112, and p116 has been explained. The figure on p101 represents diffusion in the absence of NaCl. Information regarding stirring during experiments has been added (p95, p96)

11. The reference for the viscometer has been included (Ref. 1, p168).

07958 377 337
gaurang.purohit@ulsop.ac.uk.

12. An introduction to the viscosity of dendrimers has been added to Chapter 5 (p122). Existing viscosity literature has been discussed in relation to the results (p141).

13. The didendron structure on p130 has been corrected.

14. The results regarding the dendron aggregates, in Chapter 5, has been discussed further (p146).

15. The contents pages, list of figures, list of tables and references have all been amended accordingly.